MASTERARBEIT | MASTER'S THESIS

Titel | Title

Variation of Crown Morphology in Great Ape Upper Premolars

verfasst von | submitted by

Nina Oberklammer BSc

angestrebter akademischer Grad | in partial fulfilment of the requirements for the degree of

Master of Science (MSc)

Wien | Vienna, 2025

Studienkennzahl lt. Studienblatt | Degree programme code as it appears on the student record sheet:	UA 066 827
Studienrichtung lt. Studienblatt | Degree programme as it appears on the student record sheet:	Masterstudium Evolutionäre Anthropologie
Betreut von | Supervisor:	Univ.-Prof. Dr. Gerhard Weber
Mitbetreut von | Co-Supervisor:	Cinzia Fornai PhD

猿も木から落ちる[1]

[1] Japanese proverb

ABSTRACT

Teeth have been long studied in the field of evolutionary anthropology and are important for taxonomic classification. In particular, the human and great ape dentitions have been studied well in 2D-approaches. But traditional methods with 2D-measurements are not able to capture tooth shape comprehensively. The number of studies published using geometric morphometrics has been increasing for the past two decades, but their focus is mainly molars, especially when it comes to great apes.

Great apes are separated on a genus-level, which gives us the opportunity to study various evolutionary traits and morphological differences. In this small pilot study the focus lies on the upper third (P^3) and fourth premolars (P^4) of *Pan troglodytes*, *Pongo pygmaeus*, and *Gorilla gorilla* investigating the dental crowns using geometric morphometric methods in order to quantify their 3D-morphology and variation.

Nonmetric variation of premolar dentition in great apes is also underrepresented in the literature to this date and we were able to demonstrate at least trends of their variability in the three taxa.

Keywords: maxillary dentition, *Pan troglodytes, Pongo pygmaeus, Gorilla gorilla,* geometric morphometrics

ZUSAMMENFASSUNG

Zähne werden seit langem im Feld der evolutionären Anthropologie untersucht und sind für die taxonomische Klassifizierung wichtig. Insbesondere das menschliche Gebiss und das der Menschenaffen wurden mit 2D-Ansätzen gut untersucht. Traditionelle Methoden mit 2D-Messungen können die Zahnform jedoch nicht ganzheitlich erfassen. Die Anzahl veröffentlichter Studien mit Methoden der geometrischen Morphometrie nahm in den letzten zwei Jahrzehnten zwar zu; diese Arbeiten konzentrieren sich jedoch hauptsächlich auf Mahlzähne und nicht Vormahlzähne, ein Gebiet, das insbesondere bei Menschenaffen unterrepräsentiert ist.

Menschenaffen werden auf Gattungsebene unterschieden, was uns die Möglichkeit gibt, verschiedene evolutionäre Merkmale und die entsprechenden morphologischen Unterschiede zu untersuchen. In dieser kleinen Pilotstudie liegt der Fokus auf den oberen dritten (P^3) und vierten Prämolar (P^4) von *Pan troglodytes, Pongo pygmaeus* und *Gorilla gorilla*. Wir untersuchen die Zahnkronen mit geometrisch-morphometrischen Methoden, um ihre 3D-Morphologie zu quantifizieren und ihre Variation zu untersuchen.

Die nicht-metrische Variation der Prämolarenbezahnung bei Menschenaffen ist bis heute in der Literatur ebenfalls unterrepräsentiert und wir konnten zumindest Trends ihrer Variabilität in den drei Taxa nachweisen.

Schlüsselwörter: Maxilläres Gebiss, *Pan troglodytes*, *Pongo pygmaeus*, *Gorilla gorilla*, geometrische Morphometrie

CONTENTS

1 INTRODUCTION

1.1 Great ape upper premolars

Numerous studies on the dental morphology of hominids including great apes have been published covering a variety of research questions: Enamel thickness (Kono, 2004; Smith et al., 2008; 2012), how and to what extent the Enamel Dentine Junction (EDJ) influences the Outer Enamel Surface (OES) (Guy et al., 2015), nonmetric dental traits (Hardin & Legge, 2013), root morphology (Moore et al., 2013), and phylogeographic patterns/subspecies analyses assessed by measurements from 2D-images (Uchida, 1998; Pilbrow, 2006; 2010), to exemplify just a few.

Great apes, like all *Catarrhini*, possess two premolars per dental quadrant. In anthropology, they are referred to as the third and fourth premolars (P^3 and P^4 for upper premolars P_3 and P_4 for lower premolars respectively) because the first and second premolars were reduced over the course of evolution with respect to the primitive *Eutherian* mammals.

Despite the basic Bauplan for teeth in primates being rather consistent across species, various taxa are characterized by their specific dental morphologies, also in relation to their respective dietary requirements. The great ape genera have differing dietary habits being able to incorporate all kinds of foods into their diet but having different kinds of preferences and fallback foods. In the classic literature, *Pongo pygmaeus* is, for the most part, described as being mainly frugivorous (Galdikas, 1988, Fox et al., 2004) and *Pan troglodytes* as a basically plant-based omnivore (Sugiyama & Koman, 1987), whereas *Gorilla gorilla* is described as mainly folivorous (Fox et al., 2004; Yamagiwa & Mwanza, 1994). If their fallback foods are considered or a closer look is taken at eating habits at a subspecies level, however, it becomes apparent that these general categories do not apply in all circumstances.

P. t. troglodytes incorporates several different kinds of foods from fruits and leaves to meat into its diet, but is mainly frugivorous, preferring ripe fruits (Sugiyama & Koman, 1987; Berthaume, 2014). *P. pygmaeus* has been reported feeding on leaves and seeds and in some populations on insects to a relatively great extent (12%) while maintaining a clear preference

for fruits whenever available (Fox et al., 2004). Though most *Gorilla* subspecies have been described in the past as mainly folivorous Fox et al., 2004; Yamagiwa & Mwanza, 1994), *Gorilla g. gorilla* is described as almost exclusively frugivorous (Rogers et al., 1990 In Berthaume 2014; Williamson 1988), with fallback foods such as barks and leaves (Yamagiwa et al., 2009).

Evolutionary signals may also play a role in the morphological variation across the three studied genera. Since *Pongo pygmaeus* branched off relatively early (16-17 Mya) from the phylogenetic tree leading to the African *Hominidae* (Fig. 1.2), one can expect a different dental morphology compared to *Pan troglodytes* and *Gorilla gorilla*, which separated from one another at a much later point (8-9 Mya) (Perelman et al., 2011).

1.2 Gross morphology of upper premolars

Upper premolars in great apes are generally bicuspid teeth. In most individuals, the paracone is larger and distinctly higher than the protocone, except for the fourth premolar P^4 in *Pongo*, where both cusps are approximately the same size (Fig. 1.1) (Swindler, 2002).

The paracone and the protocone are separated through a mesiodistal developmental groove which is especially wide and deep in *Gorilla*. The occlusal surface is outlined by marginal ridges both mesially and distally. In most individuals there are two crests present; the first one originates from the paracone or mesially to the mesial marginal ridge, and the second crest runs distally from the protocone to the paracone, separating the occlusal area into three parts (Swindler, 2002).

In all great apes the premolar has a larger bucco-lingual (BL) width than mesio-distal (MD) length (Hooijer, 1948), with the paracone's tip oriented centrally and the tip of the protocone positioned more mesially, especially in P4 (Hillson, 1996). The mesio-buccal surface of the P3 is more prominent compared to P4, especially in Pongo (Hooijer, 1948). Unworn Pongo premolars express crenulations on the occlusal surface of the enamel which can mask underlying dental structures (Swindler, 2002).

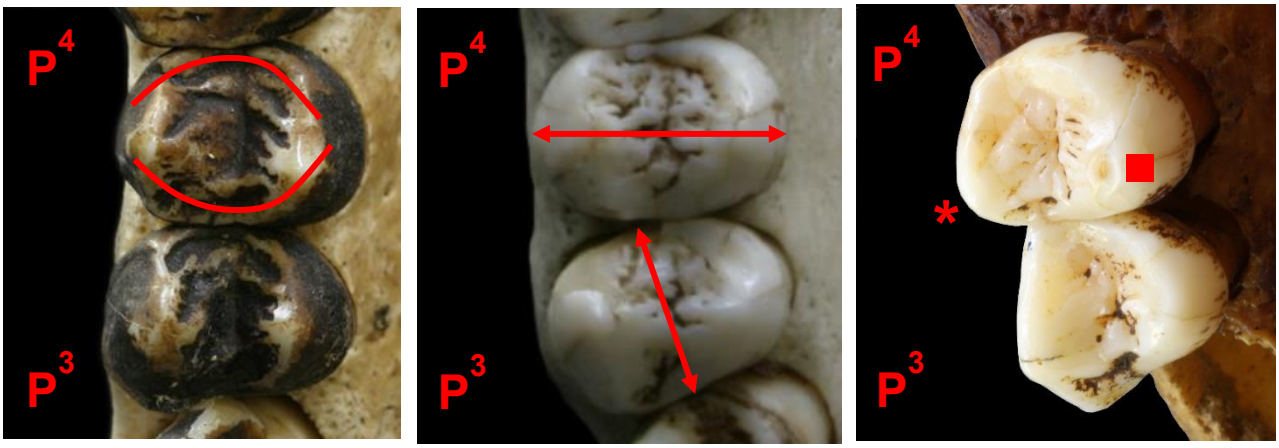

Fig. 1.1: Upper left premolars of great apes. From left to right: *Gorilla gorilla gorilla* NMW_3116, *Pongo pygmaeus* 21497, marked MD length on P3, marked BL width on P4, visible crenulations on both teeth, and *Pan troglodytes verus* FF_106. P^4s at the top, P^3s at the bottom half of each picture. Note that the paracone tips are oriented more centrally on *Gorilla* and *Pongo*, but in this example both * paracone and ■ protocone are oriented more mesially in *Pan* (to some degree due to the photographys angle).

1.3 Phylogenetic tree of extant *Hominidae*

Great apes form a taxonomical unit, (family *Hominidae*, Fig. 1.2), which consists of two extant subfamilies: *Homininae* and *Ponginae* (Swindler, 2002; Groves, 2018). The subfamily of the *Homininae* is further divided into the extant tribes of *Gorillini*, *Panini* and *Hominini*.

The subfamily of the *Ponginae* consists of only one extant genus, *Pongo* which further branches into the three species *Pongo pygmaeus, Pongo abelii* (Groves 2001; 2018) and *Pongo tapanuliensis* with the last one first described in 2017 (Nater et al., 2017). *Pongo pygmaeus* further branches into three subspecies; *P. p. pygmaeus*, *P. p. wurmbii*, *P. p. morio* (Groves, 2001), although there is discussion regarding the validity of these subspecies mentioned and population groups in general (Brandon-Jones et al., 2016) as there is about all non-human great ape taxa.

Traditionally, *Pongo* was regarded as consisting of two subspecies – *Pongo pygmaeus pygmaeus* (the Bornean *Pongo*) and *Pongo pygmaeus abelli* (the Sumatran *Pongo*) based on morphological differences (e.g. Nowak, 1991; Groves 2001). However, analyses of their DNA at the end of the 20th century suggested greater differences between those two just like in other recognized species such as *Pan troglodytes* and *Pan paniscus*. The two *Pongo* species,

as they since have been accepted as distinct species (Groves, 2001), most probably separated 2.3± 0.5 million years ago (Zhang et al., 2001; Zhi et al., 1996: 1.5-1.7 Mio years ago).

Additionally, the *Pongo* species found and described in 2017, *P. tapanuliensis* (Nater et al., 2017) seems to have split from the Bornean orangutan – although it habituates Sumatra – around 2.41 million years ago. The earliest divergence in the *Pongo* genus probably happened much earlier at about 3.97 million years ago (Scally et al., 2012).

The *Pongo pygmaeus* branch is divided into the following subspecies (although debated by Fischer et al., 2006): *Pongo pygmaeus morio* (East Bornean Pongo) (Mendoca et al., 2017), *Pongo pygmaeus pygmaeus* (Bornean Pongo) (Delgado & van Schaik, 2000) and *Pongo pygmaeus wurmbii* (Groves, 2001).

The *Panini* with the genus *Pan* is commonly divided into the two species *Pan troglodytes*, the common chimpanzee, and *Pan paniscus*, the pygmy chimpanzee or bonobo chimpanzee (Pilbrow, 2006). *P. troglodytes* further branches into different subspecies, although the distinction for those is still debated (Fischer et al., 2006). To date, four subspecies are mostly recognized; *P. t. troglodytes, P. t. verus*, *Pan t. schweinfurthii* and *Pan t. vellorosus* (Gonder et al., 2006) now known as *Pan t. ellioti* (Oates et al., 2009). Since this study's aim is not to discuss the classification of *Pan* subspecies and deals with two broadly recognized and rather distinct subspecies (*P. t. troglodytes* and *P. t. verus*), there will be no further expansion on the different views in subspecies classification.

The *Gorillini* taxon is represented only by the genus *Gorilla* to date. Two extant *Gorilla* species exist; *Gorilla gorilla* and *Gorilla beringei* (Groves, 2002). *Gorilla gorilla gorilla,* also called the Western Lowland Gorilla, is one of two subspecies of the Western Gorillas (*Gorilla gorilla*) and also the one examined in this study ,the other is *Gorilla gorilla diehli* (Groves, 2002). Just as with the above-mentioned *P. pygmaeus* subspecies and *P. troglodytes* subspecies, there is also still debate on whether these *G. gorilla* subspecies should be considered as such (Fischer et al., 2006).

The *Hominini* tribe further leads to the subtribe *Hominina* which is only represented by the genus *Homo* that only consists of one extant species, *Homo sapiens*. *Hominini* will not be part of our study, as it focuses on dental shape variation in non-human great apes.

The separation of the three taxa described in this study (*Pan*, *Pongo*, *Gorilla*) took place during the last 20 million years, with *Ponginae* forming a separate branch about 16-17 million years ago, *Gorillini* branching off the hominin tree about 8-10 million BP and *Panini* and *Hominini* separating about 6-7 million years ago (Perelman et al., 2011), although the dates are still debated as there are different approaches on speciation estimation – molecular findings, immunological analyses, anatomical comparison – and different approaches and findings within those (see Bradley, 2008 for a more comprehensive summary) with molecular models pointing to a much later separation of about 6 million years for *Gorillini* and 3.7 million years for the separation of *Panini* and *Hominini,* there is consensus that *Panini* and *Hominini* are the most closely related ones (Scally et al., 2012).

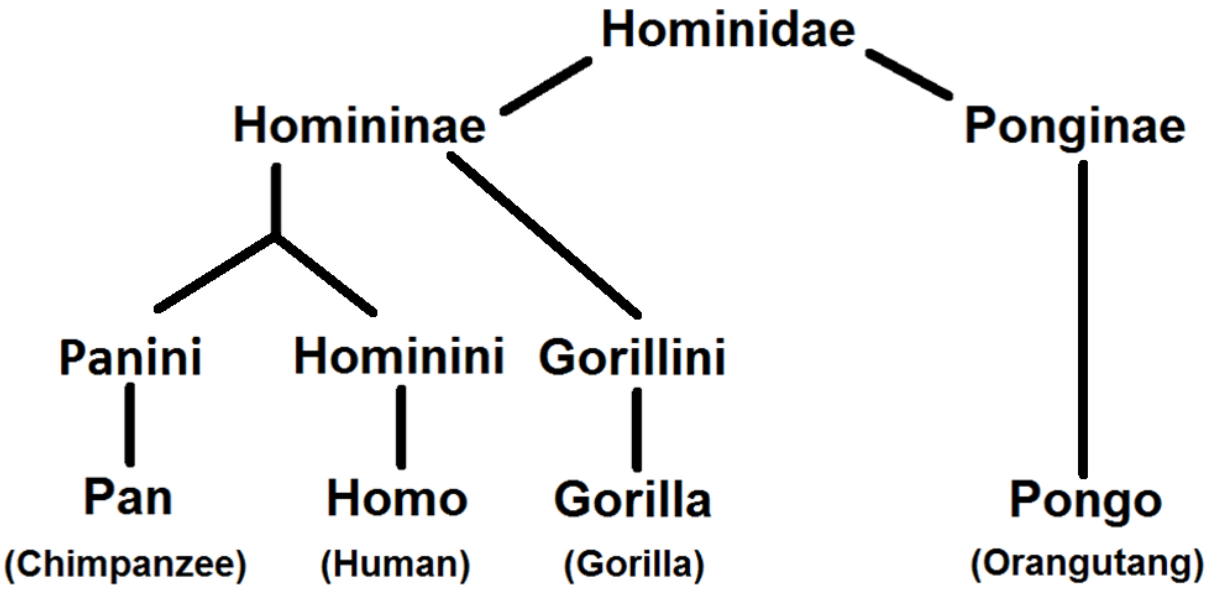

Fig. 1.2: Phylogenetic tree of the *Hominidae.*

1.4 Advantages of tooth investigation

Tooth morphology is often used for hominoid taxonomic classification. One reason for this is that dental morphology can be very characteristic for a species. Not only are teeth evolutionarily conservative (Slavkin & Diekwisch, 1997), but dental tissues are very hard and stiff with enamel being the strongest material in the mammal body. It consists of hydroxyl apatite and is up to 99% inorganic, with a melting point at 1650°C. Dentine is also very strong with a fraction of approximately 70% inorganic material (Meyer, 1995; Elliot, 1997).

Because teeth are the strongest material in the mammal body, they are often the only material preserved in the fossil record. Additionally, other molecules, for instance groundwater fluorine, can replace the hydroxyl in the hydroxylapatite. This altered fluorine hydroxyl apatite has a much lower solubility and therefore preserves even better and longer in the fossil record.

Bones, being larger and less resistant than teeth, have a higher risk of being altered by taphonomic factors, including chemical or mechanical strains (for example destruction by carnivores, scavengers, tectonic shift, and soil pressure). Therefore, teeth are especially important for primate paleontology (Ulhaas et al., 2004) and thus for evolutionary anthropology.

Unlike bones, dental crowns are not renewed constantly, replaced only once during the lifetime of an individual (deciduous to permanent dentition with different morphology), and already formed crowns are less prone to alteration by physiological stress (e.g. activity level), disease, and other forces in comparison to bones.

Teeth do not change after odontogenesis other than by wear and stress-induced mechanical damage. The dental crown does not remodel, however dental alterations may occur, such as secondary dentine and tooth cement growth into the pulp chamber as a consequence to dental wear. Wear (abrasion, attrition), however, does alter the shape of teeth which hampers the study of their original shape (Hillson, 2005).

Changes occur on the occlusal surfaces as effects of mastication and usage of teeth as tools (para-masticatory use), as well as on interproximal aspects as pressure is constantly applied from adjacent teeth, making it harder to examine structures on the Outer Enamel Surface (OES). The underlying dentine, however, or rather the Enamel Dentine Junction (EDJ), can be studied instead as it correlates highly with the OES morphology without being so prone to wear and tear (Fornai et al., 2015; Guy et al., 2013; 2015; Ortiz et al., 2012). Although it is not immune to alterations, the enamel wears more quickly on account of encountering abrasive materials and chemicals first.

There are different approaches to dental paleontology; in this study we will focus on dental morphology of the upper premolars of extant great apes. Size and shape of premolars in most extant primates are distinct but also vary within species and between sexes. We will shed some light on those differences, focusing on the inter-genera differences.

1.5 Nonmetric traits

Nonmetric traits have been studied for human dentition extensively (e.g. Pilbrow 2006, 2010; Hlusko, 2004; Van Reenen, 1995) and the dental guideline for those traits, ASUDAS (Turner et al., 1991; Scott & Turner, 1997) is well known. Studies on hominin dental nonmetric variation are constantly published as well (e. g. Martin et al., 2017; Braga et al., 2016; Hardin & Legge, 2013; Ortiz et al., 2012) but few on dental traits in *Pan* and *Gorilla*, and of those most investigating molars (Scott & Turner, 1997; Broom, 1937; Bailey, 2002; Bailey, 2008) and not premolar dentition.

When studying nonmetric traits, it is important to realize that most traits visible on the enamel surface have corresponding structures on the dentine. The OES formation is a result of and highly constrained by the underlying EDJ morphology (Guy et al., 2013; 2015; Ortiz et al., 2012). This allows studying nonmetric variation in moderately worn teeth where the OES has already been altered due to exposure to abrasive materials and chemicals.

Since the EDJ morphology is considered more conservative, and OES structures originate at the interface between the OES and EDJ, some researchers believe that differences in traits regarding OES and EDJ should only vary in grade of expression (Ortiz et al., 2012; Skinner et al. 2009). Due to differences in enamel deposition, which occurs at a later stage in tooth development, originally formed nonmetric traits might be expressed at a weaker grade or possibly even concealed when already expressed weakly at the EDJ (Butler, 1956). The only known trait with a real lack of correspondence, according to Skinner et al. (2010), is the enamel crenulation in *Chiropotes*, a pithecin monkey where these “wrinklings” seems to be formed solely by enamel deposition without contribution of the underlying EDJ. But Skinner et al. (2010) goes on to describe the same trait – crenulations on the enamel – in *Pan* and *Pongo* as originating at the EDJ and only being more prominently visible on the OES.

Some studies pointed out that the classification system for human dental variation does not fully apply and cover especially the degree of traits for non-human tooth variation (Van Reenen, 1995; Van Reenen & Reid, 1995; Johanson, 1974; Robinson, 1956) and established new systems. Since there is no established classification system for all great ape dental features yet, the ASUDAS classification system for human dentition will be used (Turner et al.,

1991) with some modifications and additions where needed, as other researchers have done in the past in the face of a lack of an established system (e.g. Ortiz et al., 2012).

1.6 Geometric morphometrics

„*Geometric morphometrics* – the suite of methods for the acquisition, processing, and analysis of shape variables that retain *all* of the geometric information contained within the data.“ (Slice, 2005).

Crown morphology is not easily represented by traditional 2D-measurements. These measurements do not capture dental morphology adequately because of its complex and irregular three-dimensional shape. Although in the past, researchers have tried to capture and compare form and shape of anatomical features with linear distances, angles, and other two-dimensional measurements, linear measurements especially cannot effectively describe form or shape. Angles and distances as ratios to one another are more suitable, but due to differences in values (angles cannot be converted to distances), they are of limited use in further statistical analyses.

Only after Geometric morphometrics (GM) was developed in the ’80s and ’90s, an adequate solution was found (Bookstein, 1991; Mitteröcker & Gunz, 2009; Weber & Bookstein, 2011). Virtual methods ensure the integrity of the material using a landmark-based approach to overcome the limitations of 2D-measurements non-invasively. The advent of computed tomography in combination with the statistical tools of Geometric Morphometrics have allowed investigation of the outer and inner 3D-morphology of teeth in detail. Data can be obtained by taking X-ray images, CT- and µCT-scans, and reconstructing the desired structures using dedicated software programs.

Landmark-based data is collected in a two- or three-dimensional coordinate system to represent the form of an object. Landmarks are anatomical points. The unambiguity of these points/structures are described by Bookstein (1991) and Weber & Bookstein (2011) who define six different types of landmark data (chapter 3.3 “Geometric morphometrics”).

To be able to explore shape variation in great ape premolars non-invasively on the OES and EDJ these virtual GM methods were used.

1.7 Aims

The main aim of this study is to explore shape variation of the upper premolar morphology within and between the main great ape taxa (*Gorilla*, *Pan*, and *Pongo*).

Although there is a multitude of studies on great ape dental morphology (e.g. Kono, 2004; Smith et al., 2008; 2012; Guy et al., 2013; Hardin & Legge, 2013; Moore et al., 2013; Uchida, 1998; Pilbrow, 2006; 2010) only a few focus on hominin premolars (e.g. Gómez-Robles, 2011, Krenn et al. 2019), some on great ape crown morphology with GM methods (e.g. Guy et al., 2013; Olejniczak et al., 2004; 2007; Braga et al., 2016; Skinner et al., 2009), but so far none of them has yet addressed the 3D shape and size of great ape premolars.

Therefore we want to shed light on the 3D shape variation of great ape upper premolars including nonmetric traits of both the EDJ and the OES, comprising specimens featuring unworn or only moderately worn teeth.

In this study we will analyse different aspects of the tooth crown with GM methods; the EDJ morphology and the cervical and enamel crown outlines, as well as a combination of those datasets. For the EDJ we collected landmarks and semi-landmarks (as well as pseudo-landmarks) on the occlusal area which offer many advantages to capture shape (Olejniczak et al., 2004) but have the huge disadvantage of being mostly applicable to unworn or slightly worn teeth. To be able to collect the same/similar landmark data on the OES, our sample size would have been stunted drastically as only very few teeth that had reached the dental plane were unworn or only worn to an extent where we would have been able to reconstruct and include them when investigating shape on the occlusal surface.

Therefore, to increase sample size as well as establish possibilities to capture and distinguish shape from different genera based on more easily accessible data and data from even heavily worn teeth as well, the dental outlines (crown outline on the OES, cervical outline on the EDJ) were introduced.

Most surface structures on the enamel have corresponding dentine structures, however some of the dentine structures have no visible correspondence on the enamel structures and very rarely vice versa. Since the underlying dentine is less worn for obvious reasons and thus better

preserved in most cases we decided to focus on the dentine, especially the area where the enamel touches the dentine, the EDJ. For nonmetric traits however we compare the traits on the OES to the ones of the EDJ wherever possible with the goal to not only capture the nonmetric variation within and between species but also within a single tooth.

For most of the premolar nonmetric traits in great apes there is neither a comprehensive classification system nor adequate scoring systems that capture all variations. Although studies have been published on great ape nonmetric dental morphology (e.g. Hardin, 2012; Ortiz et al., 2012) we will rely on the ASUDAS classification system (Turner et al., 1991) and will describe new additional traits we were able to observe in our specimens.

2 MATERIALS

For this study we focused on great apes permanent upper third premolars (P^3s) and upper fourth premolars (P^4s). For practical reasons, we included primarily left-sided premolars whenever present and fitting criteria (both P^3 and P^4 present, minimal wear, etc.). If they were not present or not usable (worn, broken, anomalies), the right-side antimeres were considered after mirroring. Therefore any kind of (fluctuating or directional), was not taken into account as asymmetries were not a topic of this thesis, especially due to limitation of material availability.

Our dental dataset (Table 2.1) comprises 42 individuals, thus 84 teeth (P^3 and P^4 for each individual). It consists of 24 *Pan t. verus*, two *Pan t. troglodytes*, ten *Pongo pygmaeus* and six *Gorilla gorilla gorilla* (Fig 2.1). Both wild and captive specimens were included. Twenty-four of the *Pan*-specimen were made available by the Frankfurt Senckenberg Museum and are part of their *P. t. verus* collection. All the other 18 specimens are part of the great ape collection of the Natural History Museum of Vienna (NHM Vienna). Specimens of both collections were visually pre-selected for usability, of which a third of the specimens had to be further excluded from this study after µCT-imaging (12 of the originally selected 36 individuals of the Senckenberg Museums specimens and 9 of the pre-selected 27 specimens from the NHM Vienna).

The subspecies attribution of the *Pongo* specimens included in this study is unknown to us. In fact, all specimens were labelled as '*Pongo pygmaeus*' with no further specification. The exact provenience of the specimens might have helped the classification of these specimens, but this information, too, was not available for all the individuals included in this study. Additionally, the fact that a new *Pongo* species, *Pongo tapanuliensis* (Nater et al., 2017) was only recently described made it even more difficult for us to determine the correct species affiliation of our *Pongo* sample. It is likely that our sample is composed mainly of *Pongo pygmaeus*; however, a definite taxonomic attribution of the specimens is uncertain and an attribution to a subspecies (i.e., *Pongo p. pygmaeus*, *P. p. morio* and *P. p. wurmbii*) impossible within the framework of this study. We therefore decided to remain with the original labeling,

comparing the great apes on the genus level, for which classification and verification on the subspecies level is not of great importance.

For our study we included only specimens featuring unworn to moderately worn teeth, for which the EDJ was preserved completely or worn at maximum to a stage that allowed virtual reconstruction. Therefore, only young adults and juveniles with at least completely formed permanent tooth crowns were included in this study. Some of the premolars we used had not yet erupted fully but with the completion of tooth crown formation, this should not have lead to any greater bias in analyzing its metric and nonmetric features.

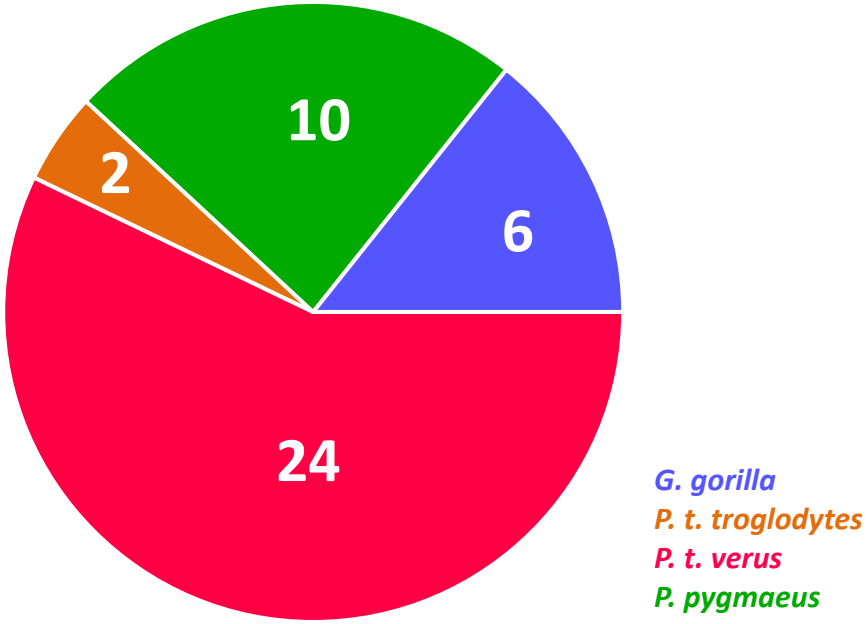

Fig. 2.1: Sample distribution for the three great ape genera. Additional subspecies specification for *Pan*.

We included only teeth without pathologies that showed no or only little damage and wear up to stage 3 on the Molnar wear stage (Molnar, 1971).

Molnar wear stages (Molnar, 1971):

- 1 – unworn
- 2 – wear facets without exposure of dentine (see f. ex. Fig. 2.2)
- 3 – small dentine patches in less than three cusps (see f. ex. Fig. 2.2)

An anomaly detected in our sample concerned an additional premolar in one of the *Gorilla* specimens. Since it was not safe to assume (although highly likely) that the additional premolar was a P^2, we could not determine with certainty which of the three premolars to use for analyses and therefore excluded that specimen.

Males and females were both included although sex was not known for all the specimens (Tab. 2.1). Sex for 17 adult specimens (10 males, 7 females) and two juveniles (both males) was determined at the time of collection/from collectors/lenders, which we kept as given.

Since sexual dimorphism is well known for canines (Swindler, 2002; Anemone & Swindler, 1999) we wanted to explore sex-related variation in premolars too. Therefore we performed sex determination for the remaining 13 adult *P. t. verus* individuals (Tab. 4.1).

As mentioned above (Chapter 1.5 Nonmetric traits), most surface structures on the enamel have corresponding dentine structures, however some of the dentine structures have no visible correspondence on the enamel structures or vice versa. Since the underlying dentine is less worn for not being exposed as much and therefore usually better preserved than the OES, we decided to focus mainly on the dentine, especially the area where enamel and dentine touch, the enamel dentine junction (EDJ). For nonmetric traits, however, we compare those found on the OES to those detectable on the EDJ wherever it was possible.

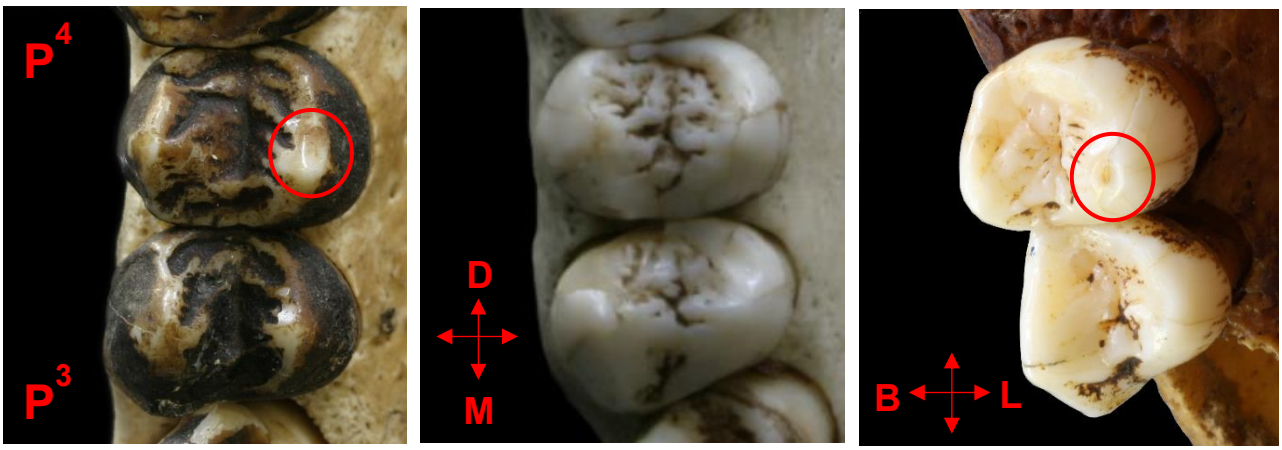

Fig. 2.2: Upper left premolars of great apes. From left to right: *Gorilla gorilla gorilla* NMW_3116, *Pongo pygmaeus* 21497 and *Pan troglodytes verus* FF_106. *Gorilla* with Molnar wear stage 2, *Pan* with Molnar wear stage 3 on the lingual cusp of P^4. P^4s at the top, P^3s at the bottom half of each picture. D = distal, M= mesial, B = buccal, L = lingual.

Table 2.1 – Great Apes' Sample

Species	Specimen	Collection	Age	Sex	Origin
Pan t. verus*	**SMF/PA/PC 311***	**FF**	adult	**ukn**	**w (Liberia)**
Pan t. verus	SMF/PA/PC 28	FF	adult	f	w (Liberia)
Pan t. verus	SMF/PA/PC 11	FF	juv	ukn	w (Liberia)
Pan t. verus	SMF/PA/PC 46	FF	juv	ukn	w (Liberia)
Pan t. verus	SMF/PA/PC 48	FF	juv	ukn	w (Liberia)
Pan t. verus	SMF/PA/PC 54	FF	juv	ukn	w (Liberia)
Pan t. verus	SMF/PA/PC 106	FF	adult	m	w (Liberia)
Pan t. verus	SMF/PA/PC 119	FF	juv	ukn	w (Liberia)
Pan t. verus	SMF/PA/PC 121	FF	adult	ukn	w (Liberia)
Pan t. verus	SMF/PA/PC 125	FF	juv	ukn	w (Liberia)
Pan t. verus	SMF/PA/PC 185	FF	juv	ukn	w (Liberia)
Pan t. verus	SMF/PA/PC 196	FF	adult	ukn	w (Liberia)
Pan t. verus	SMF/PA/PC 201	FF	adult	ukn	w (Liberia)
Pan t. verus	SMF/PA/PC 211	FF	juv	ukn	w (Liberia)
Pan t. verus	SMF/PA/PC 214	FF	juv	ukn	w (Liberia)
Pan t. verus	SMF/PA/PC 218	FF	adult	ukn	w (Liberia)
Pan t. verus	SMF/PA/PC 233	FF	adult	ukn	w (Liberia)
Pan t. verus	SMF/PA/PC 248	FF	adult	ukn	w (Liberia)
Pan t. verus	SMF/PA/PC 255	FF	juv	ukn	w (Liberia)
Pan t. verus	SMF/PA/PC 259	FF	adult	ukn	w (Liberia)
Pan t. verus	SMF/PA/PC 273	FF	juv	ukn	w (Liberia)
Pan t. verus	SMF/PA/PC 281	FF	adult	ukn	w (Liberia)
Pan t. verus	SMF/PA/PC 313	FF	adult	ukn	w (Liberia)
Pan t. verus	SMF/PA/PC 316	FF	adult	ukn	w (Liberia)
Gorilla g. gorilla	NMW/Gorilla_3113	NHM	adult	m	w (Congo)
Gorilla g. gorilla	NMW/Gorilla_3115	NHM	adult	m	w (Congo)

Gorilla g. gorilla	NMW/Gorilla_3116	NHM	adult	m	w (Congo)
Gorilla g. gorilla	NMW/Gorilla_3117	NHM	adult	m	w (Congo)
Gorilla g. gorilla	NMW/Gorilla 3118	NHM	adult	m	w (Congo)
Gorilla g. gorilla	NMW/Gorilla 41460	NHM	adult	m	w (Cameroon)
Pan t. troglodytes	NMW/Pan_13528	NHM	adult	m	z (Sierra Leone)
Pan t. troglodytes	NMW/Pan_28536	NHM	juv	m	z (Schönbrunn)
Pongo pygmaeus	NMW/Pongo_654	NHM	juv	ukn	z
Pongo pygmaeus	NMW/Pongo_657	NHM	juv	ukn	z
Pongo pygmaeus	NMW/Pongo_658	NHM	adult	f	w (Borneo)
Pongo pygmaeus	NMW/Pongo_800	NHM	adult	f	z (Schönbrunn)
Pongo pygmaeus	NMW/Pongo_3108	NHM	adult	f	w (Sumatra[1])
Pongo pygmaeus	NMW/Pongo_3047B	NHM	juv	m	z (Schönbrunn)
Pongo pygmaeus	NMW/Pongo_28801	NHM	adult	f	z (Schönbrunn)
Pongo pygmaeus	NMW/Pongo_31054	NHM	adult	f	z (Schönbrunn)
Pongo pygmaeus	NMW/Pongo_55206	NHM	adult	m	z (Schönbrunn)
Pongo pygmaeus	Pongo_anthro_21497	NHM	adult	f	ukn

Tab. 2.1: FF= Frankfurt Senckenberg Museum, Frankfurt am Main. NHM= Vienna Natural History Museum, Vienna. Age: juv= juvenile. If not declared as "juvenile", specimen is adult. Sex: m= male, f=female, ukn= unknown. Origin: w= wild individual, z= zoo animal. [1]indonesian Sumatra. ***Pan FF_SMF/PA/PC 311= template individual**.

3 METHODS

3.1 Sex determination of unclassified *Pan troglodytes verus*

All adult great ape specimens from the Natural History Museum of Vienna came with sex labels which we kept as given (the two unknown specimens were juveniles).

Since several *Pan troglodytes verus* specimens from the Senckenberg Museum in Frankfurt had not been sexed yet, determination of sex was carried out for all unsexed adult chimpanzee skulls we included in our dataset to increase the sample size with known sex which was already small due to numerous juveniles whose sex is not easily/at all determinable. Sex determination was done by four different persons at the Department for Evolutionary Anthropology, Vienna including the candidate and her supervisors, Univ.-Prof. Dr. Gerhard Weber, Dr. Cinzia Fornai, and Dr. Nicole Grunstra. The juvenile specimens remained unsexed.

The *P. t. verus* specimens were sexed based on well-known and established sex differences. Such differences include the canines, which are larger in all dimensions and have bigger roots in males than in females. They also appear to be rounder or rhomboid in males, whereas their shape is more oval in females (Swindler et al., 2002). We were able to observe that with the bigger sized canines, the overall shape of the dental arch changes too. Although canines were mostly missing within our dataset, we were able to apply the canine-induced shape change of the alveolar socket. With canines projecting outside of the dental arch when present, the male individuals show a less curved, more squared arch whereas the females show a more U-shaped, rounded one.

Further known sex differences are the nuchal and sagittal crests, which are more pronounced and robust in male individuals, mostly due to dimorphism in body size and ontogenetic scaling (Anemone & Swindler, 1999). The sagittal crest which, when strongly developed, suggests a male individual. We found that this trait was very variable in our dataset and should only be considered if the crest is really close to or touching in the posterior region to then be classified as male. In any other case the individual variation, at least in comparison with the specimens with known sex of this collection, was greater than the sex-dependent variation.

The nuchal crest can also be an indicator for sex, being more pronounced in male chimpanzees than females (Anemone & Swindler 1999). Additionally, we found that the temporal processes along the nuchal crest show more robustness and anterior-posterior elongation in male specimens.

3.2 Image acquisition & processing

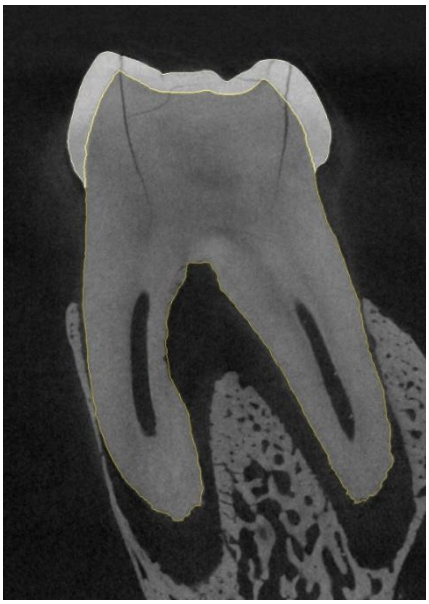

Fig. 3.1: Single slide of a µ-CT-scan of a great ape upper premolar.

µ-CT-scans (Fig. 3.1) of the great apes' maxillae were obtained at the Vienna µCT-Lab, Department of Evolutionary Anthropology, University of Vienna, using a V*iscom X8060 NDT µ-CT* scanner. The image resolution for all scans performed for this study ranged from 20 to 60 µm. Differences in image resolutions were owed to different sizes of the object to scan. In addition, a few scans acquired prior to working on this study, possessed lower resolution of approximately 80µm.

After the scanning process, 3D reconstructions with the obtained µCT-slides were done using XVR-CT. Then, a virtual segmentation of the two dentinal materials, enamel and dentine, was performed in *Amira 6.7* using Half-Maximum-Height (HMH) protocol (Spoor et al., 1993) and two surface models of the EDJ and the OES respectively were generated (Fig 3.2 & Fig. 3.6).

After manual reconstruction of minor missing dentine horn tips where necessary, the tooth crowns were oriented at a best-fit plane along the cervical outline. This outline was identified by placing landmarks along the enamel-dentine junction at the tooth cervix and computing the best-fit plane through these landmark points. The teeth were then cropped away below the plane (Benazzi et al., 2012; 2014) thereby removing its roots. The 3D models representing the OES and the EDJ of the cropped crowns were then exported for further data acquisition.

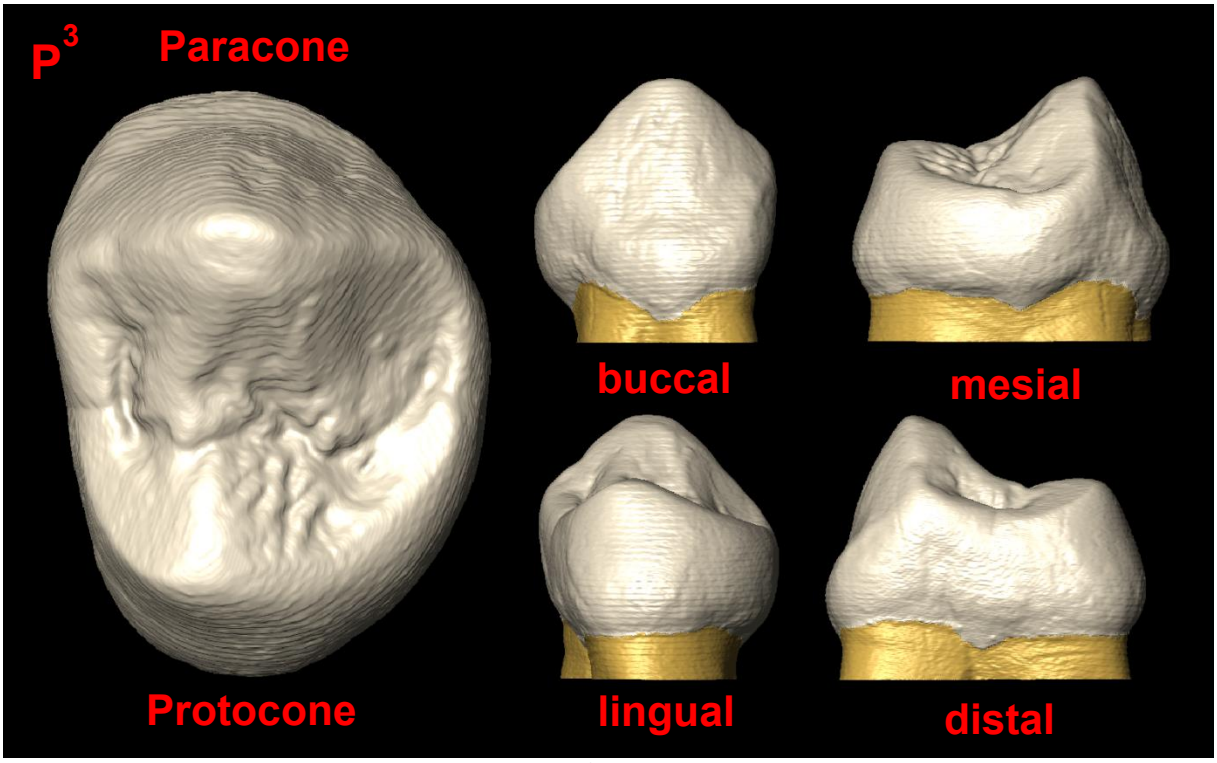

Fig. 3.2: Virtually segmented and reconstructed Pan P^3. Left: occlusal view, right upper row: buccal & distal view, right lower row: lingual & mesial view. Enamel cap in white, dentine in yellow.

3.3 Geometric morphometrics

Crown morphology is not easily represented by 2D-measurements as they do not capture dental morphology adequately. We therefore introduced non-invasive, virtual 3D methods using a landmark-based approach with the use of Geometric Morphometrics (GM) (see also Chapter 1.6 “Geometric morphometrics).

Landmarks are anatomical points; Bookstein (1991) and Weber & Bookstein (2011) defined six different types of landmark data:

The first type of landmarks (Type one) is located on structures with clear boundaries and are biologically homologous points (e.g. Bregma, Lambda).

Type two landmarks are geometrically chosen points and represent for instance (local) extremes of curvatures (highest and deepest points).

Type three landmarks are points chosen without any real homology (neither biological nor geometrical) but are midpoints (points marking symmetry etc).

Type four and five landmarks are better known as semi-landmarks, where the former represents landmarks on curves and the latter landmarks representing surfaces.

Type six landmarks are semi-landmarks, which are geometrically constructed.

In Geometric morphometrics, factors such as rotation, size, and orientation in space are removed when comparing landmark configurations to analyse shape variation. Mathematically speaking, GM uses the method of the sum of least squared distances; the sum of squared distances between corresponding landmarks is minimized. This procedure is called *Procrustes superimposition* and

- Translates the landmark dataset to the same centroid
- Scales to the same size and
- Rotates the sum of squared distances of corresponding landmarks to minimize them.

With more than two datasets to compare, a *Generalized Procrustes Analysis* (GPA) is performed. The main difference to the *Procrustes superimposition* is the successive approximation of the rotation to adjust the distances for each new dataset to minimize the sum of squared distances of all the data points. This process starts with a so-called template specimen/dataset, which is selected in the beginning and to which the next dataset is superimposed. All following landmark configurations of the other specimens are then fitted to a calculated mean of all the datasets, which is calculated every time another specimen is added to the analysis.

The results of the superimpositions are the *Procrustes distances*, which are the minimized sums of squared distances between all the landmark configurations and describe the differences in shape of these specimens (Slice, 2005; Pellegrini, 2009).

3.4 Crown and cervical outlines

For capturing shape differences in dental crown areas less affected by wear, two outlines – the cervical and the crown outline – were collected. To obtain the pseudo-landmark data for these outlines, the surface models of the EDJ and OES were imported into *Geomagic Design*

X64Bit (https://www.3dsystems.com) and re-oriented so that the buccal ridge of the dentine was parallel to the X-axis and the cervical plane orthogonal to it.

The cervical outline was not obtained by using the contour of the tooth crown at the height of the best-fit plane, as described in other studies (e.g. Benazzi et al., 2012; Fornai, 2015; Weber et al., 2016; Sarig et al., 2019), but rather as the EDJ contour at the height of this very plane (Fig 3.3). The reason for choosing this approach was a practical one; in many specimens in our dataset the enamel was damaged, and big parts were missing at the tooth cervix which would not have been easily reconstructed with high accuracy. Because of this as well as not yet erupted crowns with intact dentine and often heavily damaged enamel, we chose to use the cervical outline at the EDJ. This outline was obtained using a spline function tracing the outline on the cervical plane.

For the crown outline, its silhouette was projected and traced on the cervical plane using another spline function, correcting for minor damages and interproximal wear facets where necessary[2] (see also Fig. 3.6).

Both cervical and crown outlines were afterwards imported as *.igs files into the *Rhinoceros 4.0* software where the actual 24 equiangular pseudo-landmarks were collected (Benazzi et al., 2012). These pseudo-landmarks are constructed points which are not anatomically defined but made geometrically homologous by the reorientation prior to the landmark collection as described above.

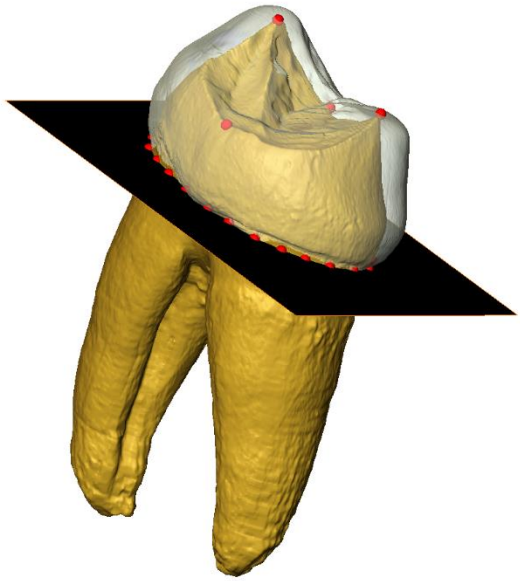

Fig. 3.3: Obtaining outlines. Reconstructed tooth with separated enamel cap, landmarks & cervical plane where the tooth crown was separated from its roots to obtain the cervical and the crown outline.

In *Rhinoceros 4.0,* a radial fan was created with its midpoint as the centroid of the outline shape area, dividing that area into 24 equiangular parts. The pseudo-landmarks were the points of

[2] These facets occur due to attrition and masticatory forces. Teeth are constantly moving mesially in the dental arcade and with time, facets at the contact points appear (see Introduction), for which we corrected.

intersection of this fan with the respective outline. The starting point (the first pseudo-landmark) was chosen to be orthogonal to the X-axis; 2nd-24th were the following intersections counted counterclockwise (Fig. 3.4).

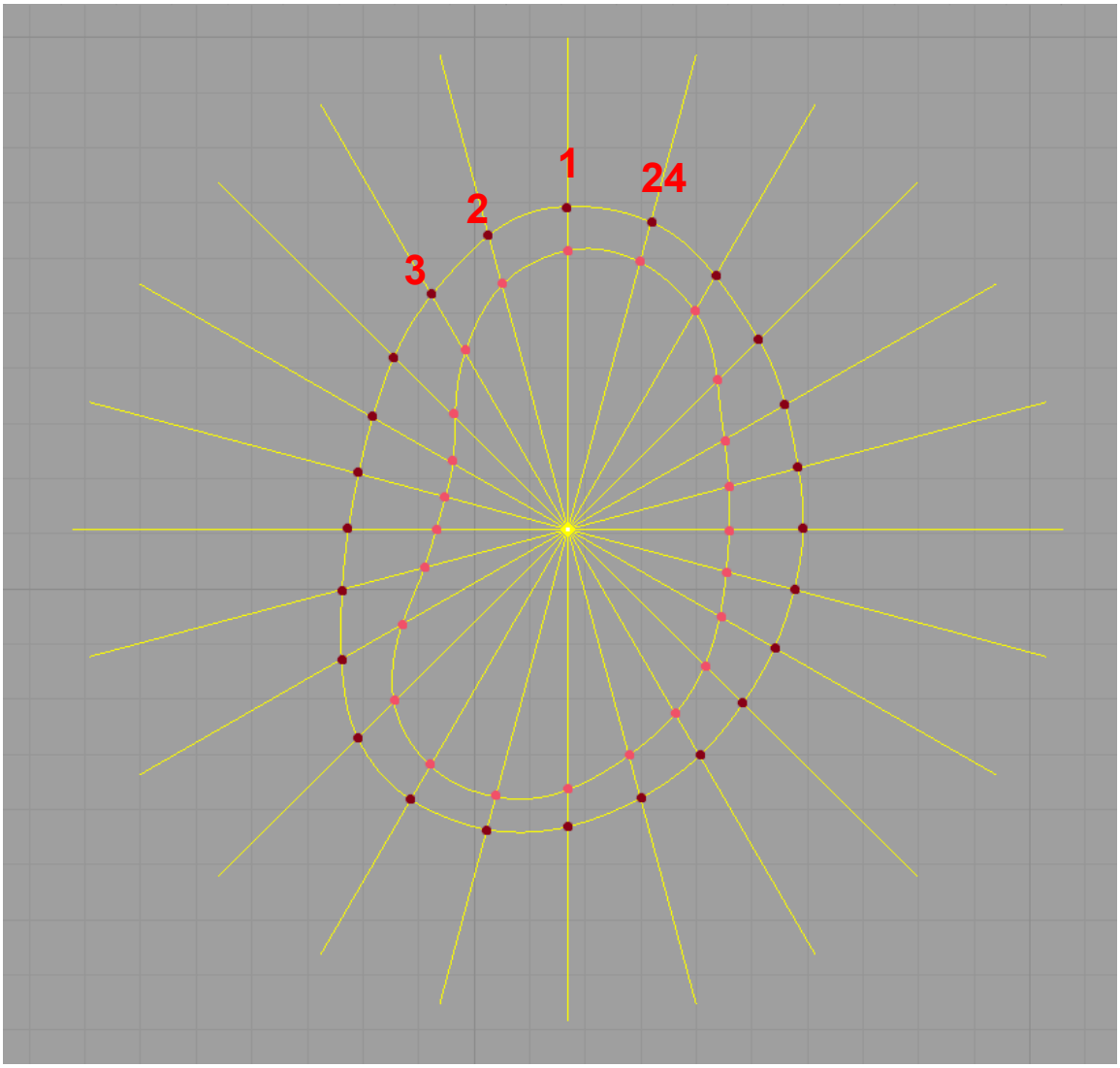

Fig. 3.4: Obtaining pseudo-landmarks on Pan P4. Dark red: 24 equiangular pseudo-landmarks for enamel crown outline; light red: 24 equiangular pseudo-landmarks for cervical outline – both counterclockwise; yellow point: area centroid.

3.5 Analysis of the EDJ

For the analysis of the EDJ, the dentine surface model was reduced to 150,000 triangular faces in *Amira 5.6*, converted into an *.obj file and imported into *Evan Toolbox 1.75 (https://www.evan-society.org)*, where the landmark and semi-landmark data were collected (Benazzi et al., 2012, 2014).

After a standardized re-orientation in *Geomagic Design X64Bit* (the buccal ridge of the dentine was rotated until parallel to x-axis), we collected landmarks of the EDJ in *EVAN Toolbox 1.75* as well as landmarks on the the cervical and enamel crown outlines in *Rhinocerus*.

The landmarks on the EDJ (Fig. 3.5):

- 1 – horn tip of paracone (highest tip)[3]
- 2 – horn tip of protocone (highest tip)
- 3 – deepest midpoint on distal marginal ridge
- 4 – deepest midpoint on mesial marginal ridge

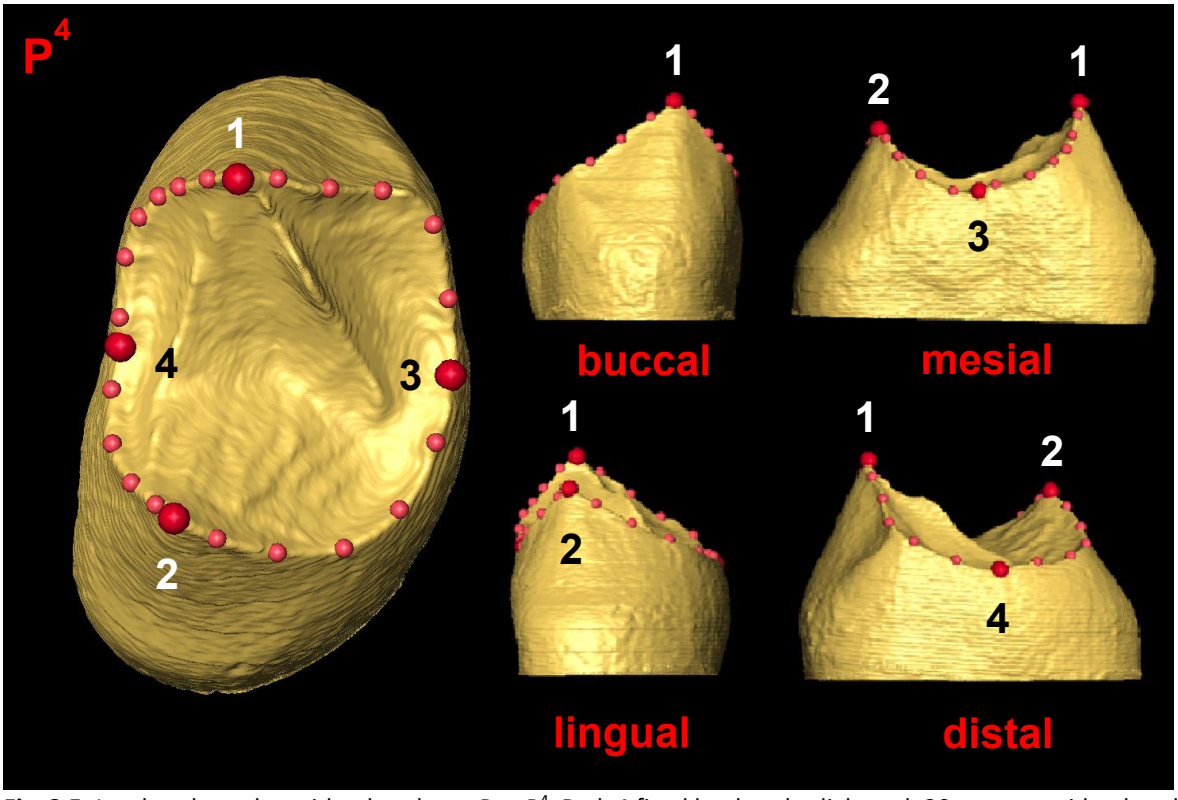

Fig. 3.5: Landmarks and semi-landmarks on Pan P^4. Red: 4 fixed landmarks; light red: 20 curve semi-landmarks.

For obtaining the curve semi-landmarks, a curve on the occlusal marginal ridge of each premolar was created by first collecting landmarks (approximately 200-350) along the ridge starting and ending at the paracone horn tip. Then, a template specimen was chosen to place the semi-landmarks on. For the EDJ 20 curve semi-landmarks (Benazzi, 2012; 2014) were placed equidistantly on the chosen template individual (FF Pan 311), for P^3 and P^4 respectively. The semi-landmarks were placed equidistantly along the created curve; ten on the mesial side

[2] Note: the highest horn tips might not always be anatomical homologous points, f. ex. on the paracone of FF Pan 281 it probably is not.

and ten on the distal side between landmarks 1 and 2 (paracone and protocone horn tips). These created semi-landmarks were then projected onto all other target specimens and slid on their curves of each individual. The process of projecting and sliding went on, until the bending energy was minimized (Bookstein, 1991; Gunz & Mitteröcker, 2009). All analyses for the occlusal EDJ morphology were performed with *EVAN toolbox 1.75*.

Landmark data for cervical outline and EDJ-morphology were combined to achieve a more comprehensive dataset, which better captures the whole dental crown shape.

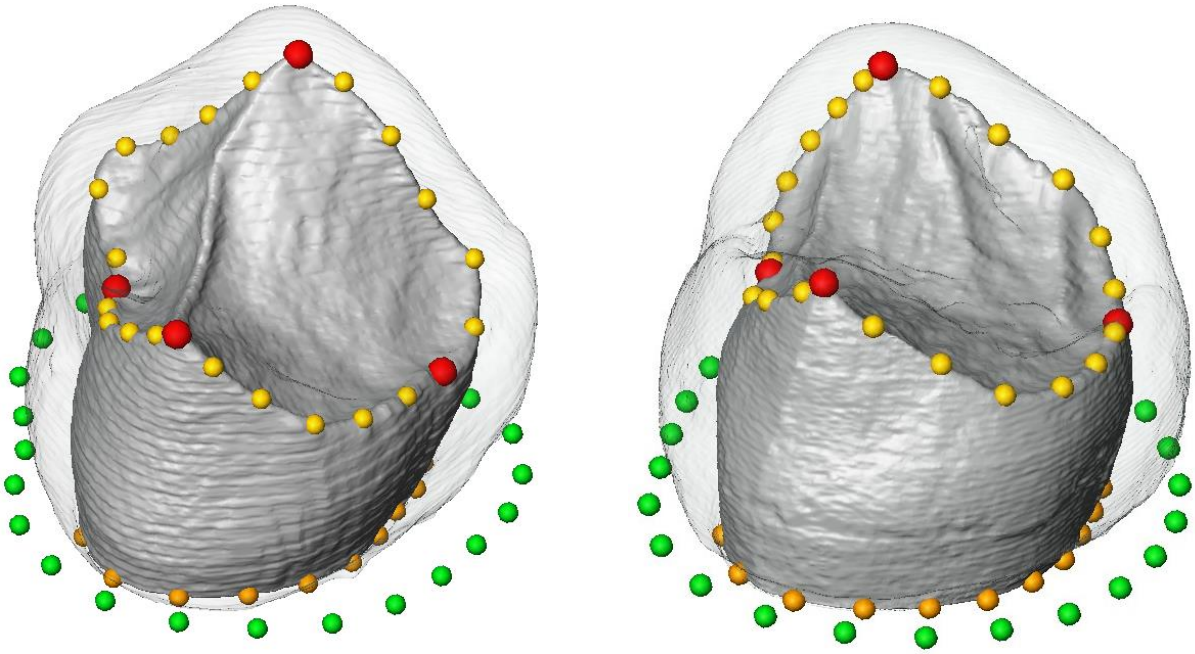

Fig. 3.6: Visualization of all landmark types used. red: 4 Landmarks on the EDJ, yellow: curve semi-landmarks on the occlusal marginal ridge on the EDJ, orange: Pseudo-landmarks on EDJ (cervical outline) & green: pseudo-landmarks of projected OES (crown outline) of P^3 (left) and P^4 (right) in *Pan*.

A *Generalized Procrustes Analysis* (GPA) was performed prior to all other statistical analyses for the metric traits. The GPA is an analysis where the landmark configurations are scaled, oriented and rotated until the sum of squared distances is minimized. This was done in order to remove non-shape related information to be able to compare shape variation on its own. The residuals of this analysis are the real differences in shape (invariant to size, orientation, and location) (see chapter 1.6 “Geometric morphometrics”).

A Principal Component Analysis (PCA) was then performed, investigating variance within the sample in cervical outline, crown outline, occlusal EDJ morphology and the combined datasets of occlusal EDJ morphology and cervical outlines.

A Two-Block Partial Least Squares Analysis (2B-PLS) was performed, investigating covariation between all combinations of cervical outlines, crown outlines, occlusal EDJ morphology and between the combined datasets (cervical outline & occlusal EDJ morphology) for third and fourth premolars.

3.6 Nonmetric traits

Nonmetric traits have been studied for human dentition (see also chapter 1.5 "Nonmetric traits") but studies on dental traits in *Pan*, *Pongo* and *Gorilla* especially in premolars remain scarce. For this study, we defined traits previously described for great ape premolar dentition (Swindler, 2002), as well as using ASUDAS guidelines (Turner et al., 1991; 1997) for human dentition (mostly traits found on human molars), and our own observations in the present dataset to establish a preliminary catalogue for nonmetric traits in great ape premolars.

Previously described traits in the literature include mesial and distal crests in *Pongo*, lingual cingula in *Gorilla* (Swindler, 2002), small crenulations, buccal cingula, hypocones and metacones in some cases in *Pongo* OES (Hooijer, 1948). Buccal cingula have been described in *Pongo* premolars "(…) as a slight swelling along the anterior edge (…)" by Hooijer (1948). Swindler (2002) was able to find few hypocones in *Gorilla*. Buccal and lingual cingula, as well as transverse crests, a crista obliqua, cusp 5 and anterior and posterior fovea have been described in deciduous premolars in *Pan* and *Gorilla* by Hardin (2012). Regarding cingula, Ortiz et al. (2012) described shelf-like structures in *Pan* molars, visible as "small depressions" in teeth with a weaker expression of the trait and huge "shelf-like" structures in molars with a strong expression of this trait.

Altogether we included fourteen different nonmetric dental traits in our analysis, both for the OES – and with one exception – as well as the EDJ. For all traits in which orientation is a factor, teeth were oriented the same way as for the GM analysis of the EDJ (the buccal ridge of the dentine was rotated until parallel to x-axis). The traits were categorized as following:

1. Crenulations

Crenulation, also known as “wrinklings” on the occlusal surface, that are not ridges/additional cusps or other nonmetric traits (Fig. 3.7).

➔ present/ absent

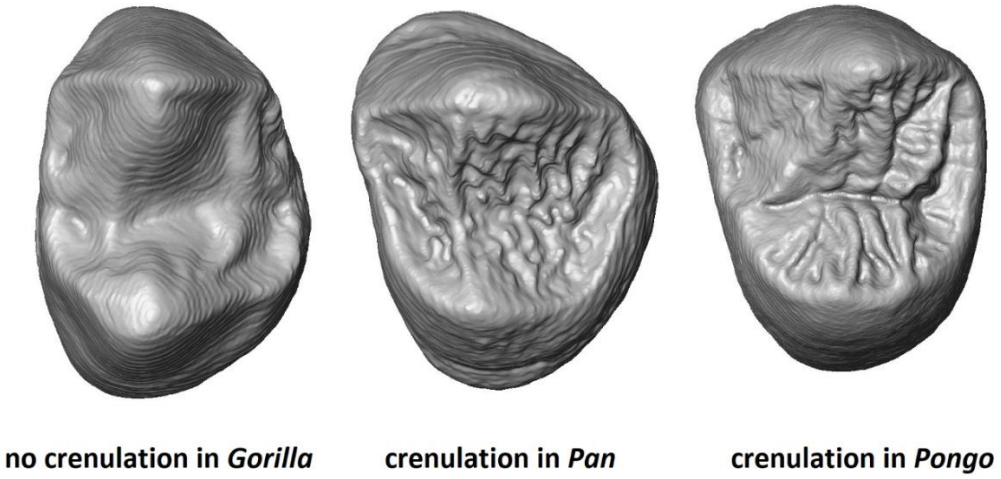

Fig. 3.7: Crenulations on the OES: *Gorilla* 3117, P^4; *Pan* 28536, P3; *Pongo* 654; P^3.

2. Mesial crest

The mesial crest (Fig.3.8) is one of the two main ridges on great ape premolars (the second one being the distal crest), which begins at the paracone cusp/horn tip or mesially to it and ends at the protocone tip or mesially to it at the marginal ridge (Swindler, 202029).

➔ present/ absent

➔ grades of expression 1-4

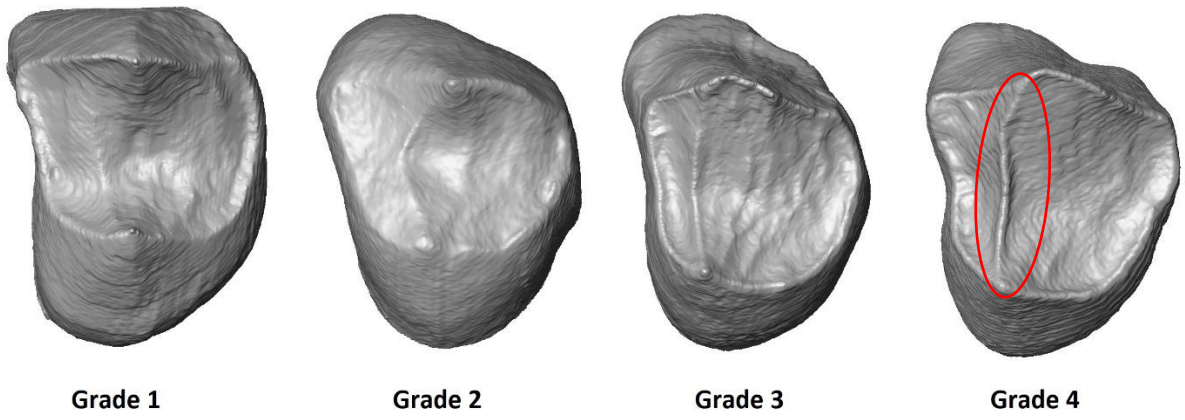

Fig. 3.8: Mesial Crests: All P3: *Gorilla* 3116, *Pongo* 31054, *Pan* 214, Pan 211. no crest, 1 = faint, 2 = weak, 3 = intermediate, 4 = strong.

3. Distal crest

The distal crest (Fig. 3.9) is the second main crests and extends distally to the mesial crest between protocone and paracone (Swindler, 2002).

➔ present/ absent

➔ grades of expression 0-4

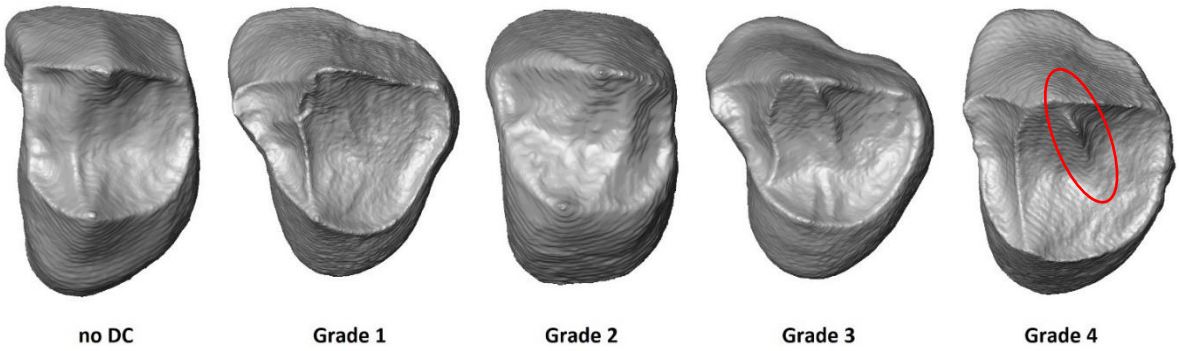

Fig. 3.9: Distal Crests: All P3: *Gorilla* 3113, *Pan* 248, *Pongo* 55206, Pan 106, *Pan* 196. 0 = no crest, 1 = faint, 2 = weak, 3 = intermediate, 4 = strong.

4. Metacone

The metacone is also known as the third cusps on upper molars, cusp 3 and the distobuccal cusp (Scott & Irish, 2017) and can be found on premolars at the corresponding area (Fig. 3.10). It represents a form of molarization.

➔ present/ absent

➔ grades of expression 1-4

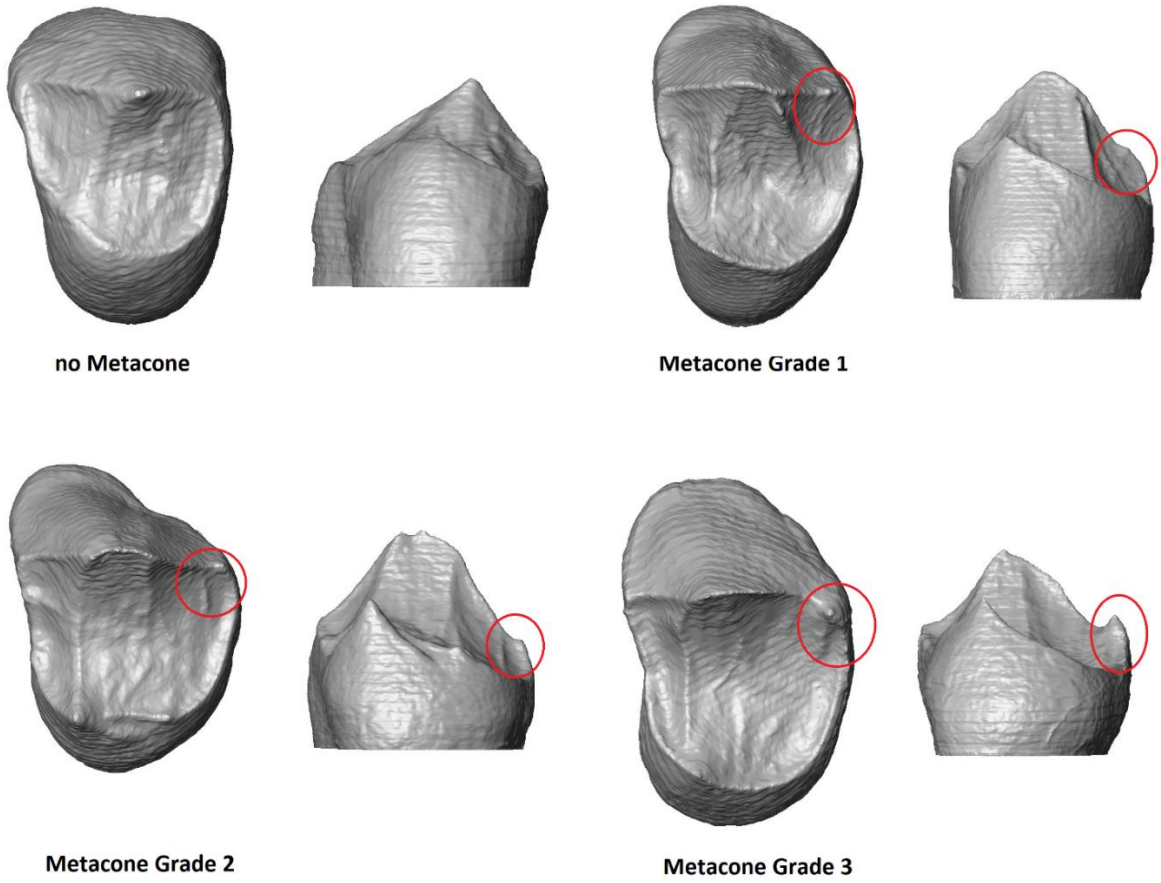

Fig. 3.10: Metacones, all P3: occlusal and lingual views. 1 = miniscule tubercle, or crest, 2 = small tubercle 3 = distinct protrusion/tip.

5. Hypocone

The hypocone is also known as the fourth and last cusp on the upper molar, cusp 4 and distolingual cusp (Scott & Irish, 2017) and can be found on premolars (Fig. 3.11) on the corresponding area and represents a form of molarization.

➔ present/ absent

➔ grades of expression 1-4

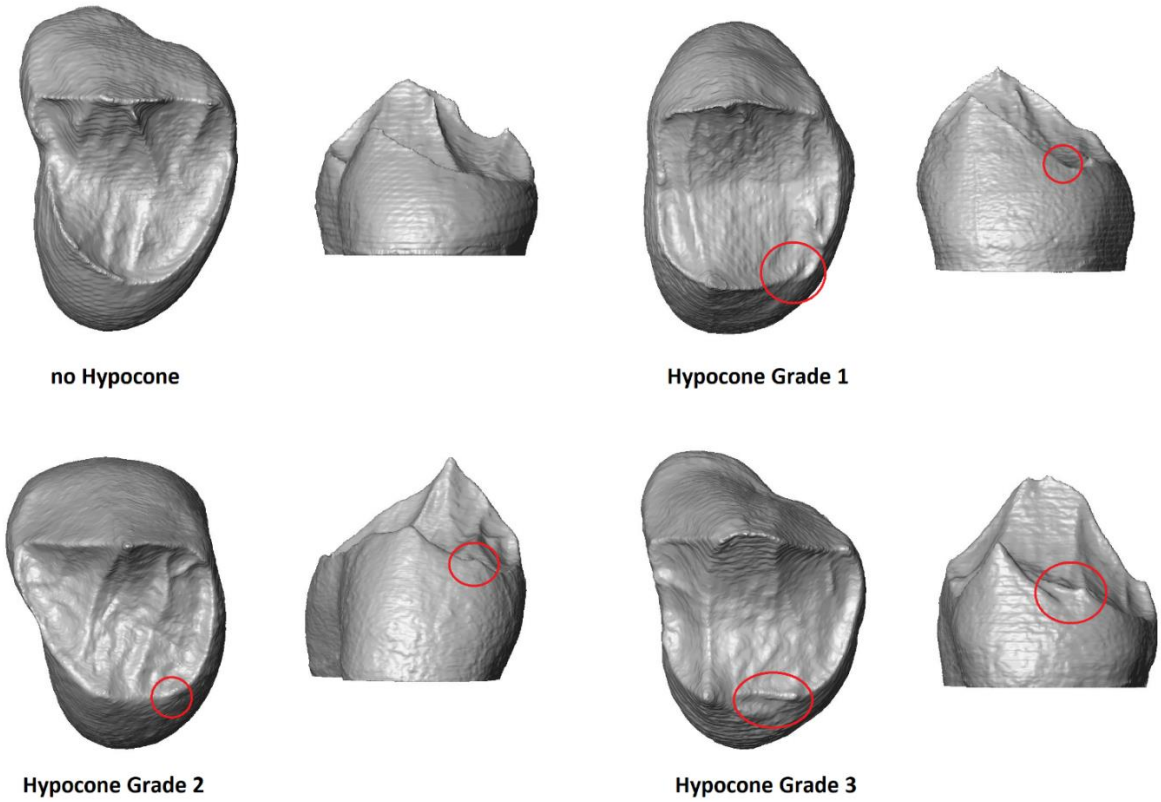

Fig. 3.11: Hypocones: occlusal and lingual views. 1 = miniscule tubercle, or crest, 2 = small tubercle 3 = distinct protrusion/tip with or without crest.

6. Additional cusps

Additional cusps, which have not been defined as crenulations, metacones or hypocones (See Fig. 3.12).

➔ present/ absent

➔ location: mesial, distal, buccal, lingual

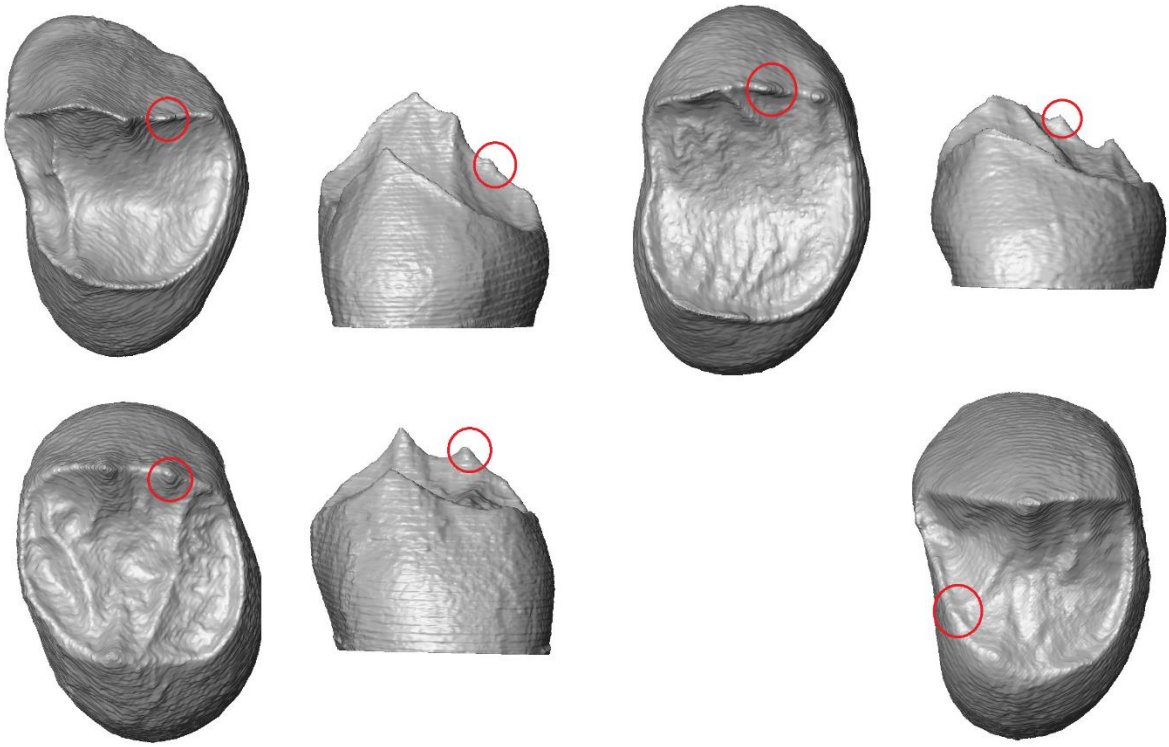

Fig. 3.12: Additional Cusps: all P3; upper row: bucco-distal cusps, occlusal and lingual view. Lower row: first two: occlusal and lingual view of big bucco-distal cusp, 3rd figure: occlusal view of mesio-lingual cusp.

7. Occlusal tubercles

A tubercle on the occlusal surface area rather (Fig. 3.13) than on the marginal ridge in contrast to other additional cusps (Fig. 3.12).

➔ present/ absent

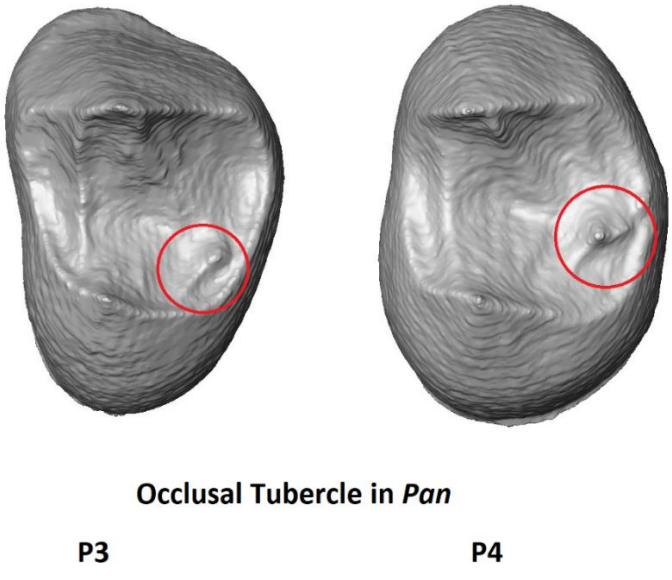

Fig. 3.13: Occlusal Tubercles. in P^3 and P^4: *Pan* 54.

8. Mesial transverse crests

A crest/ridge beginning mesially at the marginal ridge, transverse to the mesial crest (Fig. 3.14).

➔ present/ absent

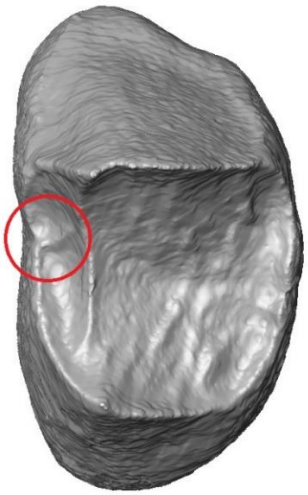

Fig. 3.14: Mesial transverse crest, *Pan* 125, P^3.

9. Distal transverse crests

A crest/ridge beginning at the distal aspect of the marginal ridge, transverse to the distal crest (Fig. 3.15).

➔ present/ absent

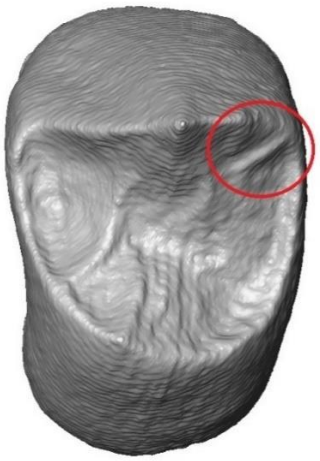

Fig. 3.15: Distal transverse crest, *Pan* 125, P^3.

10. Side "depressions"

Depressions on either the buccal and or lingual aspect of the tooth crown as a flattening of the cusp in that area, accompanied by crest-like boundaries mesially and/or distally to the flattened area (Fig. 3.16).

➔ present/ absent

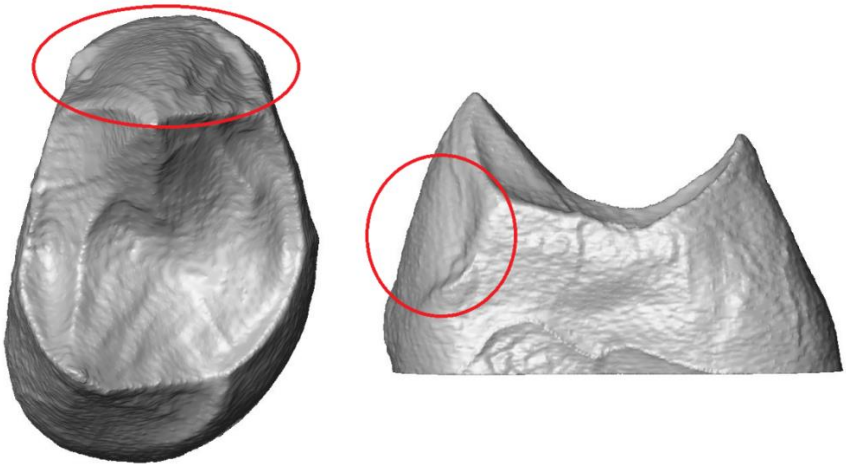

Fig. 3.16: side "depressions" in *Gorilla* 41460 P^4

11. Buccal "cingula" & lingual "cingula"

"Cingula" or shovelling of the buccal and/or lingual cusp near the tooth cervix (Fig. 3.17), visible on both the EDJ and OES, most often accompanied by side "depressions" (Fig. 3.16), but not always. More sloping near the cervix in *Pan*, then *Gorilla*, described in *Pongo* as "(…) slight swelling along the anterior edge." Hooijer (1948).

➔ present/ absent

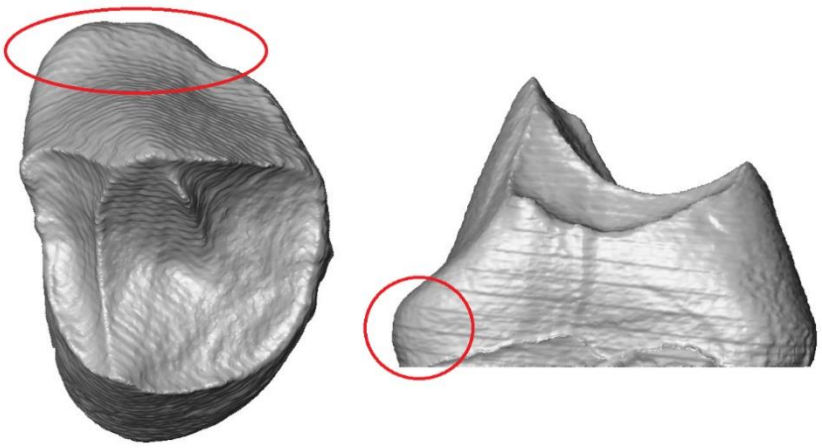

Fig. 3.17: buccal "cingulum"/shovelling in *Pan* 196 P3,

12. Rotation of lingual cusp/horn tip

The relative position of the lingual cusp/horn tip and therefore its rotation within the tooth can vary. We did not assess whether the absolute volume of the lingual cusp in regard to the BL-axis was found lingually to the BL-axis, but rather the position of the cusps tip, respectively horn tip in regard to the BL-axis (Fig. 3.18). For classification, the tooth was re-oriented (the same way as for obtaining pseudo-landmarks for the cervical and crown outlines); the buccal ridge of the dentine parallel to the X-axis (the BL-axis).

➔ present/ absent

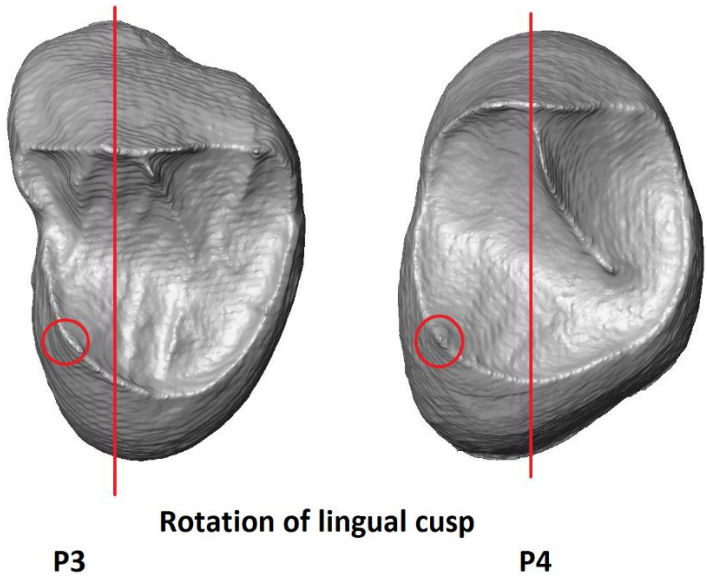

Fig. 3.18: Rotation of lingual cusp/horn tip. in *Pan* P^3 and P^4. Lingual horn tip marked with circle.

13. Bifurcated cusp/horn tip

Bifurcation of the paracone cups and/or horn tip, from elongation of the tip without true bifurcation to two distinct horn tips in close proximity to each other (Fig. 3.19) – not a metacone (cf. Fig. 3.10).

➔ present/ absent

➔ grades of expression 1-4

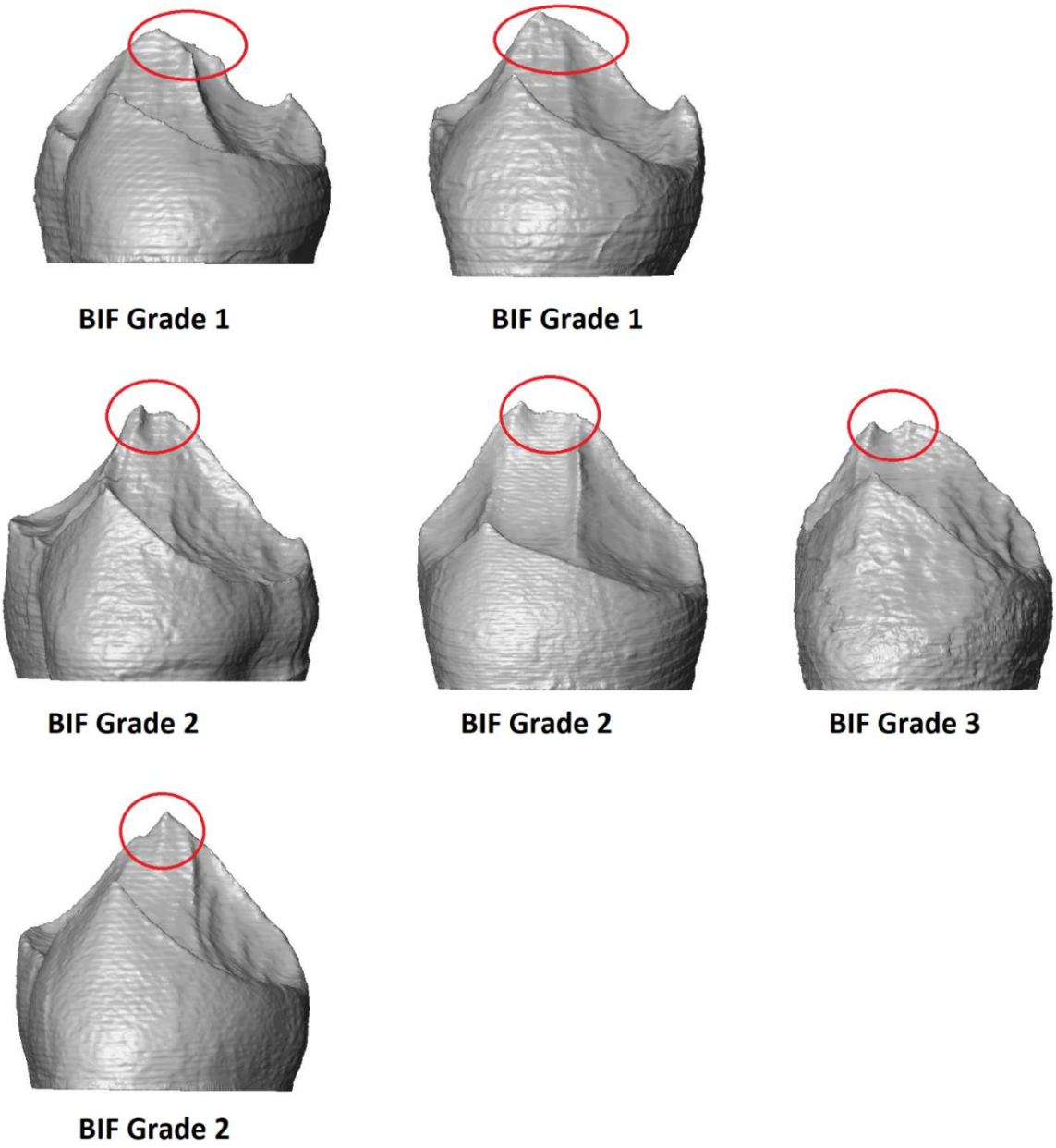

Fig. 3.19: Bifurcations of buccal horn tip: all P3, first two rows: bifurcations distally, 3rd row bifurcation mesially. Grade 1: no real bifurcation, flat elongated tip. Grade 2: one clearly distinguishable horn tip and flat elongated horn. Grade 3: two clearly visible horn tips. Grade 4: two distinct horn tips on EDJ and OES.

14. Circular marginal crest

A crest beginning and ending at the marginal ridge at a rather close distance, producing an optically circular crest (Fig. 3.20).

➔ present/ absent

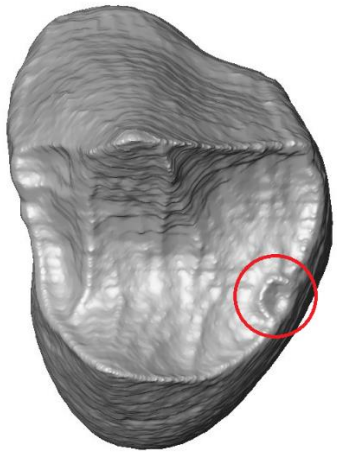

Fig. 3.20: Circular crest, *Pan* 46, P3.

4 RESULTS

4.1 Sex determination of unclassified *Pan troglodytes verus*

The results of the sex determination of the unclassified *P. t. verus* specimens from the *P. t. verus*-collection of the Frankfurt Senckenberg Museum are reported in Table 4.1. Of 13 individuals, 4 were classified as males, 6 as females, 3 as indeterminate.

Table 4.1 – Sex determination of *Pan troglodytes versus*

Individuals with unknown sex	**Sex Determination**			
Specimen	**Fornai**	**Weber**	**Grunstra**	**final**
SMF/PA/PC 201	F	IND	M	**IND**
SMF/PA/PC 169	IND	M	M?	**IND**
SMF/PA/PC 196	M	F?	F	**IND**
SMF/PA/PC 231	M?	M?	M	**M**
SMF/PA/PC 233	F	F	F	**F**
SMF/PA/PC 218	M?	M	M	**M**
SMF/PA/PC 311	F?	F?	F	**F**
SMF/PA/PC 259	F	F?	F	**F**
SMF/PA/PC 281	M?	M	M	**M**
SMF/PA/PC 248	F	F	F?	**F**
SMF/PA/PC 121	M	M	M	**M**
SMF/PA/PC 313	F	F	F	**F**
SMF/PA/PC 316	F	F	F	**F**

Tab. 4.1: Collection: *Pan t. verus* collection from the Frankfurt Senckenberg Museum. The three observers: Cinzia Fornai, Gerhard Weber, Nicole Grunstra. Final: final decision. F= female, M= male, IND= indeterminate, F?= female with uncertainty, M?= male with uncertainty.

4.2 Nonmetric traits

Nonmetric traits were examined on the OES and the EDJ of all 42 individuals. Not all traits have corresponding expressions on both structures since they can be present on the OES or EDJ only (Olejniczak et al., 2004; Ortiz et al., 2012; Guy et al. 2013; 2015).

A nonmetric trait that has been found on *Pongo* and *Pan* premolars, but not on *Gorilla* teeth are crenulations. In *Pongo* they are expressed more heavily, in *Pan* to a lesser degree. Bifurcations of the buccal cusp/horn tip were also a trait detected in *Pan* and *Pongo*, but not in *Gorilla*. It was a rather common trait in *Pan* (EDJ: 38% in P^3s, 46% in P4s) and less frequent in *Pongo* (EDJ: P^3: 20%, P4: 10%) and not found in any of the *Gorilla* specimen in this current study.

Crenulations were found more frequently on P^4 than P^3 in *Pan* and *Pongo* (EDJ: 96% & 100% in P^4s, 62% & 79% in P^3s), none in *Gorilla*.

Occlusal tubercles were only present in *Pan* both on P3 and P^4 (Pan 54), as well as circular crests, which was present in one *Pan* P^3 only (*Pan* SMF/PA/PC 46).

Additional cusps, such as metacones, hypocones and further additional, not classified cusps with varying frequencies, were more frequently detected on the EDJ. Metacones and hypocones were prevalent in all taxa, accessory transverse crests more seldom.

Mesial and distal crests were found in more than 2/3 of all teeth in all species and were more often detected on the EDJ than the OES. In addition, the mesial and distal crests (Swindler, 2002) show a range of variability in all three taxa, ranging from continuous strong crest to faint interrupted ones, sometimes only visible on the buccal or lingual aspect of the tooth and missing completely in others. In all taxa (20-33% in *Gorilla*, 23-63% in *Pan*) but especially in *Pongo* P^3 protocones (100% on the EDJ) respectively the horn tips of the lingual cusps were rotated heavily mesially.

Buccal or lingual “cingula” were only present in African great apes in our dataset. They were found in almost all *Pan* P^3, some in *Pan* P^4 and *Gorilla* (P^3 & P^4), none in *Pongo*.

In *Pan* the chance of a mesial rotation of the lingual cusp occurred twice as much in P4s than in P^3s (EDJ: 31% vs 62%), in *Pongo* it was the opposite (EDJ: 80% in P^3 vs 30% in P^4). In *Gorilla*, it was overall lesser common, with the trait being presented by 33% in both P3 and P4 (EDJ).

For analysis of frequencies of nonmetric traits (Tab. 4.2), teeth were excluded individually for each trait if they were too broken or worn too extensively to assure accuracy when identifying said trait. 100% therefore represents not necessarily that the trait was found in all premolars, but rather that it was present in all specimens that were able to be examined for said trait accurately.

Table 4.2 – Frequencies of nonmetric traits

Traits	*Pan*				*Pongo*				*Gorilla*			
	P^3		P^4		P^3		P^4		P^3		P^4	
	OES	EDJ	OES	EDJ	OES	EDJ	OES	EDJ	OES	EDJ	OES	EDJ
crenulation	62%	/	96%	/	70%	/	100%	/	0%	/	0%	/
mesial crest	100%	100%	96%	85%	100%	100%	86%	100%	100%	100%	100%	100%
distal crest	85%	96%	100%	100%	67%	90%	80%	90%	67%	83%	67%	83%
metacone	31%	50%	38%	46%	0%	20%	60%	50%	33%	83%	33%	67%
hypocone	19%	23%	38%	27%	30%	50%	40%	40%	0%	50%	33%	17%
additional cusps	17%	31%	0%	15%	30%	10%	17%	60%	0%	0%	0%	17%
occlusal tubercle	0%	4%	12%	27%	0%	0%	0%	0%	0%	0%	0%	0%
mesial trans. crest	16%	38%	23%	4%	0%	20%	0%	0%	20%	33%	20%	17%
distal trans. crest	8%	8%	23%	4%	20%	20%	0%	0%	0%	0%	0%	17%
„cingula“	92%	100%	12%	23%	0%	0%	0%	0%	0%	20%	50%	33%
Side „depressions“	73%	92%	73%	92%	50%	50%	50%	80%	100%	100%	100%	100%
cusp rotation	23%	31%	63%	62%	100%	80%	11%	30%	20%	33%	25%	33%
bifurcated horntip	13%	38%	25%	46%	25%	20%	0%	10%	0%	0%	0%	0%
circular crest	0%	4%*	0%	0%	0%	0%	0%	0%	0%	0%	0%	0%

Tab. 4.2: Percentage of traits per genus for all P^3 and P^4 preserved enough to determine the trait. mesial trans. crest = mesial transverse crest; distal trans. crest = distal transverse crest; cusp rotation = rotation of lingual cusp; circular crest = distal marginal circular crest. *found on *Pan t. verus* SMF/PA/PC 46, P^3 only.

4.3 Metric analyses

4.3.1 Shape P^3

4.3.1.1 P^3 cervical outline

The Principal Component Analysis (PCA) for the P^3 cervical outline shape reveals a grouping effect of the three studied genera *Pan*, *Pongo* and *Gorilla*, but with some overlap between those groups. The first three PCs explain 83.56% of the total variation (Tab. 4.3). PC1 (45.70%) in principle distinguishes between *Gorilla* versus *Pan* and *Pongo*, while both *Gorilla* and *Pongo* are somewhat separated from *Pan* along PC2 (23.15%) (Fig. 4.1). Along the first PC the most apparent shape variation of the cervical outline is on the distal aspect of P^3; from a distally straight cervical outline in *Gorilla* to a distally protruding outline in *Pan* and *Pongo*. The change of the cervical outline along PC2 is one on the distal tooth aspect again; from a protruding distal area in *Pan* to an indented distal area on the other end of the spectrum.

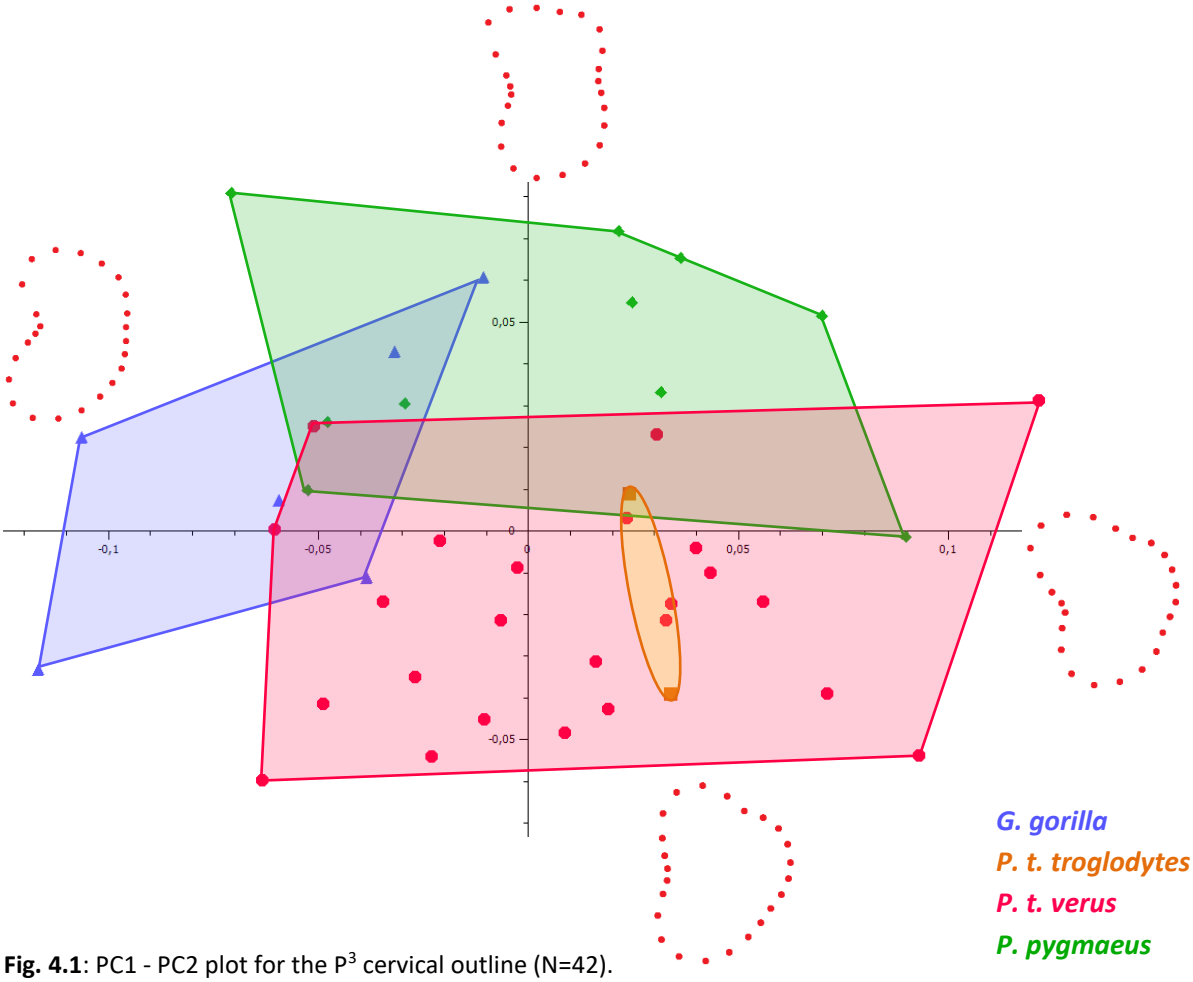

Fig. 4.1: PC1 - PC2 plot for the P^3 cervical outline (N=42).

4.3.1.2 P^3 crown outline

For the shape analysis of the enamel crown outline in P^3, one *Gorilla* (NMW 3118) was excluded due to its incomplete enamel cap, which was heavily chipped off and impossible to reconstruct with high accuracy.

The first three PCs explain 82.78% of the total variation (Tab. 4.3) with a PCA plot that shows quite an extensive overlap between *Pan* and *Pongo*. *Gorilla* separates quite well from the rest of the sample. The shape change of the crown outline along PC1 (47.83%) is similar to that of the cervical outline. On the one end, the lingual cusp is rotated more mesially with a straight distal outline aspect (*Gorilla*), on the other end the distal aspect is pronounced and protruding. Along PC2 (21.14%) the outline changes from a rounded triangular shape with distal protrusion to an oval rectangular shape with a straight distal aspect (Fig. 4.2).

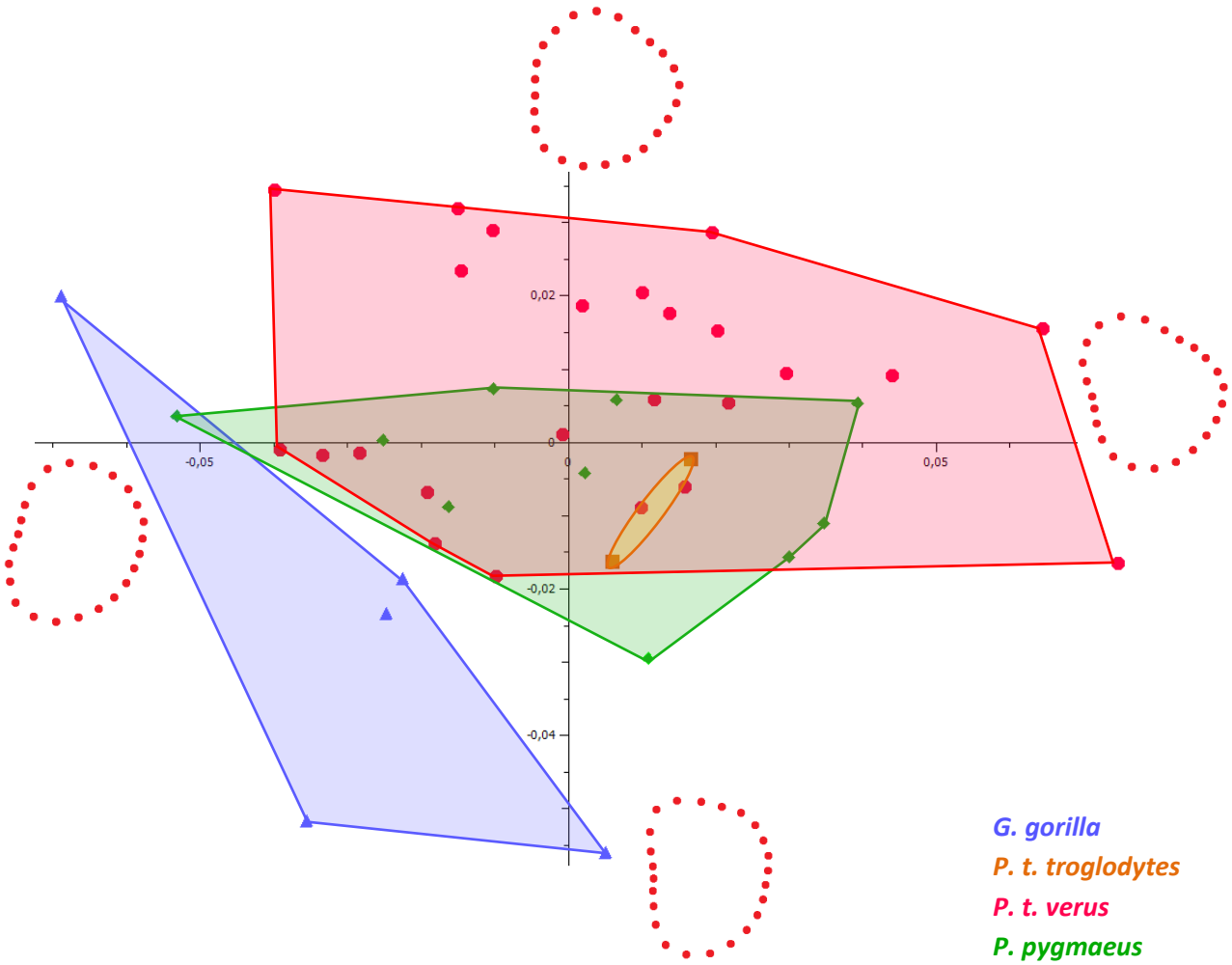

Fig. 4.2: PC1 - PC2 plot for P^3 crown outline. (N=41)

4.3.1.3 P^3 EDJ morphology

In P^3s 65.13% of total variance is explained by the first three PCs (Tab. 4.3). The morphology of the P^3 occlusal EDJ separates *Pongo* completely from the African apes very clearly along PC1 (39.34%), while *Pan* and *Gorilla* show a strong overlap. The shape variation ranges from a distally pronounced outline with horn tips oriented more centrally in *Pongo* to a more mesially pronounced outline and more distally oriented horn tips in African taxa (Fig. 4.3). Along PC2 (14.01%), specimens vary in the height of the horn tips in relation to the occlusal marginal ridge, which is not taxonomically diagnostic at all in our sample.

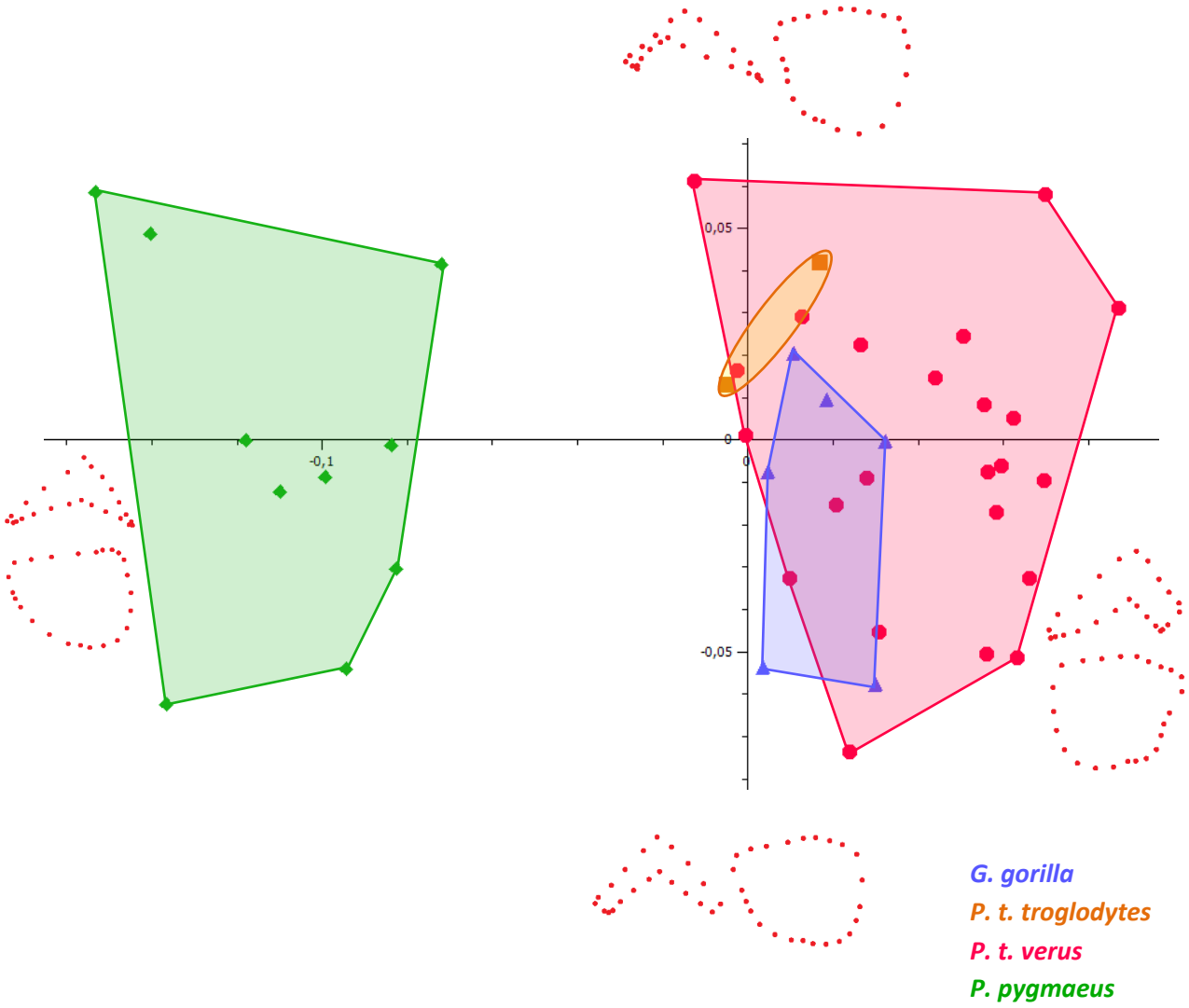

Fig. 4.3: PC1 - PC2 plot for the P^3 EDJ (N=42).

4.3.1.4 P^3 combined dataset

The PCA of the combined dataset (occlusal EDJ morphology plus cervical outline) of P^3 shows a good separation of the African hominids versus *Pongo* for the first two PCs (Fig. 4.4) but the combination of PC1/PC2 also separates well between the *Pan* and *Gorilla*. The first three PCs (Fig. 4.5) explain 57.21% of total variation, with PC1=21.85%, PC2=18.38%, PC3=16.98% (Tab. 4.3).

Along PC1, the relative position of the buccal and lingual horn tips changes. Additionally, the relative size of the mesial aspect to the distal aspect of the EDJ changes, with *Pan* having a relatively larger, protruding distal area compared to *Pongo* and *Gorilla* and both horn tips being oriented more distally.

Along PC2, the dentinal crown changes from a rectangular occlusal surface with kidney-shaped cervical aspect in *Pan* to triangular occlusal and oval cervical appearance in the other two genera. The depth of the occlusal ridge and, accordingly, the height of the horn tips change too. *Pan* shows high horn tips and a pronounced curvature in the occlusal marginal ridge and *Gorilla* and *Pongo* have higher tooth crowns with flatter occlusal ridges. Along PC3, *Gorilla* separates from the other two genera, with a relatively smaller occlusal to cervical area compared to the other two taxa.

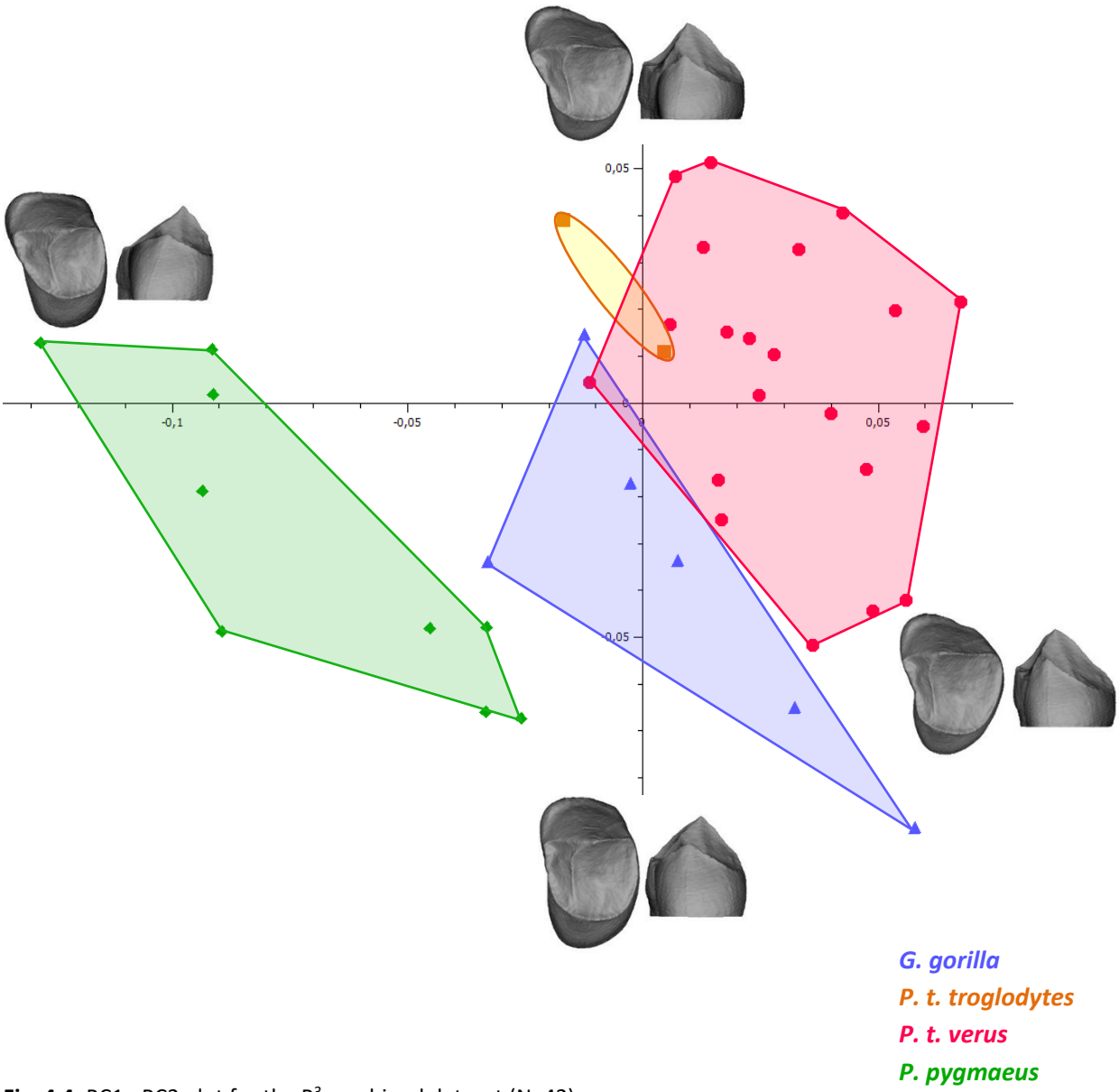

Fig. 4.4: PC1 - PC2 plot for the P^3 combined dataset (N=42)

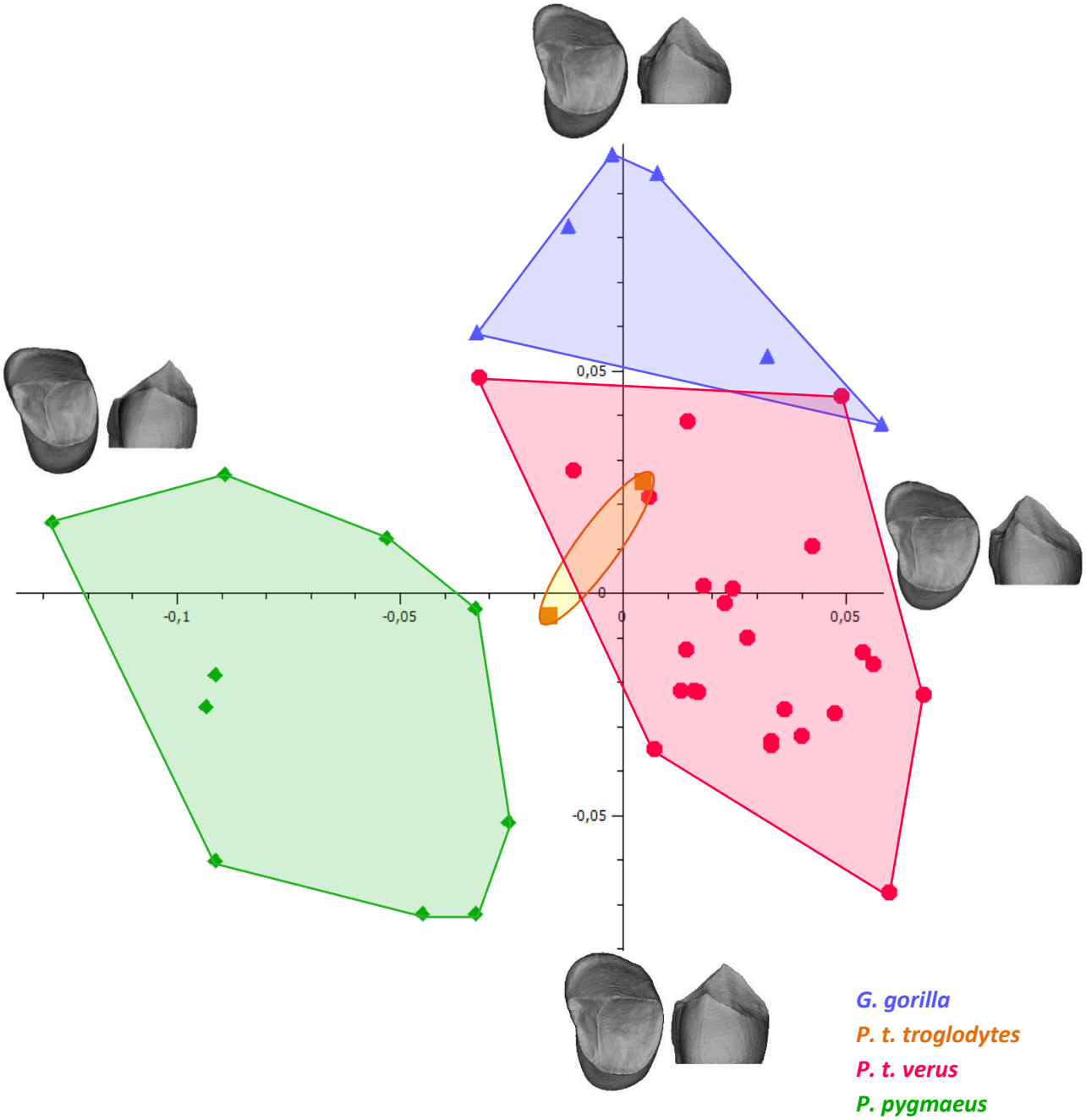

Fig. 4.5: PC1 - PC3 plot for the P^3 combined dataset (N=42)

4.3.2 Shape P^4

4.3.2.1 P^4 cervical outline

For the cervical outline of P^4 85.30% of variance is explained by the first three PCs (Tab. 4.3). The PCA shows some grouping effects with overlaps for all three genera. There is separation between *Pan* and *Pongo* on the first Principal Component with a small overlap and *Gorilla* being in the middle of the spectrum. Overall, the first principal component (58.29%) seems to depict the three genera forming groups gradually from *Pan* to *Gorilla* to *Pongo*. The shape of the cervical outline changes along PC1 from a bean-shaped one with a protruding distal tooth aspect, with a more mesially rotated lingual cusp in *Pan* to a more oval outline with a more distally rotated lingual cusp and a straight distal aspect in *Pongo*. Along PC2 (18.63%), the outline changes from an elongated outline bucco-lingually to a trapezoid and relatively wider shape bucco-lingually, especially of the lingual aspect (Fig. 4.6).

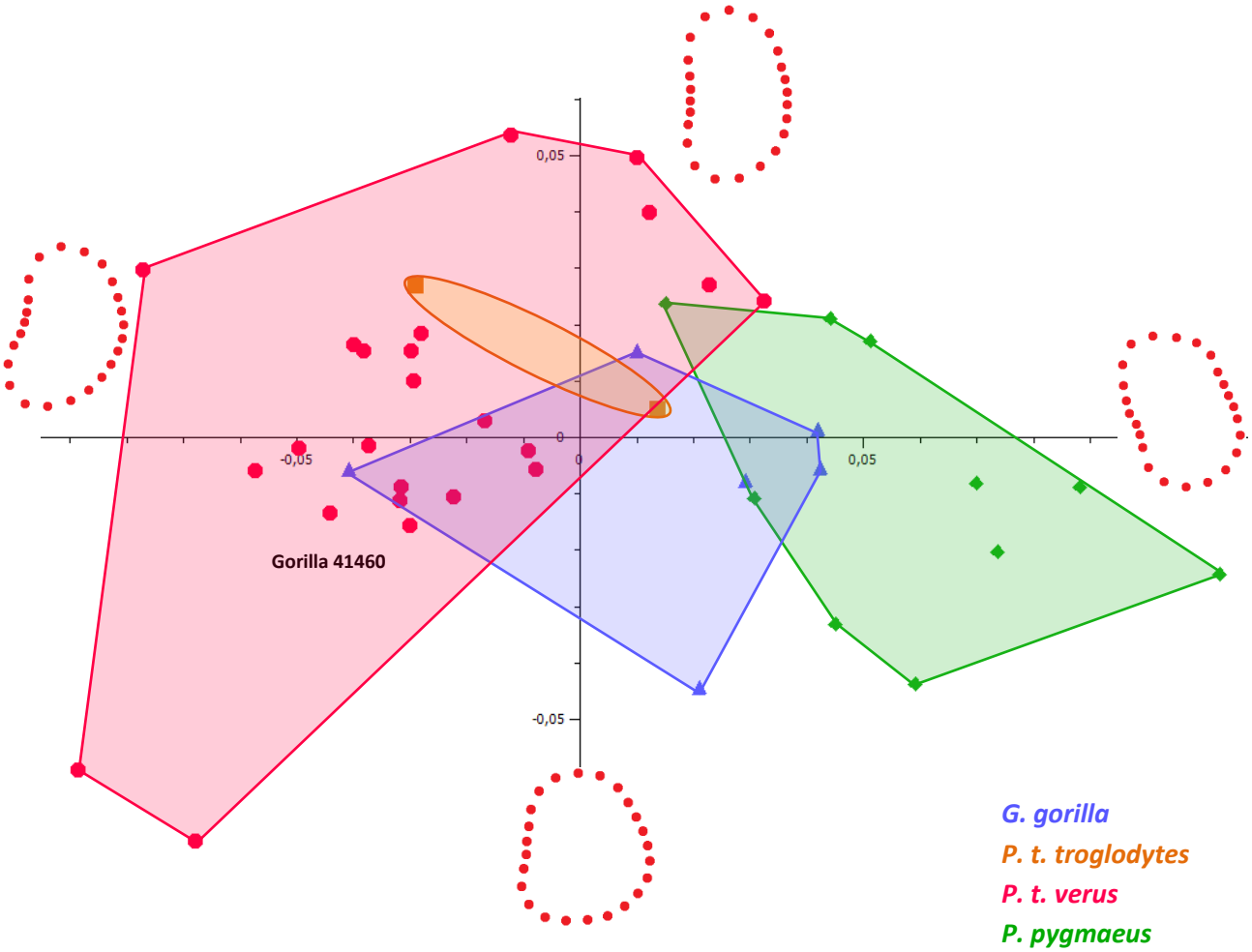

Fig. 4.6: PC1 - PC2 plot for the P^4 cervical outline (N=42)

4.3.2.2 P^4 crown outline

For the shape analysis of enamel crown outline in P^4, Gorilla NMW 3118 was excluded once again (as for P^3) due to the enamel being so heavily chipped that the structure could not be reconstructed without great uncertainty.

The first three PCs explain 85.20% of the total variance (Tab. 4.3). *Pongo* and *Pan* form clusters along PC1 (62.90%), *Gorilla* grouping amidst those two with overlaps between all three genera. The shape of the crown outline changes along the first PC from a more mesially rotated lingual cusp in *Pan* with a slight distal protrusion to a more distally tilted one in *Pongo*. Along the second PC (20.43%), the crown outline changes from a slightly more elongated oval (as for the cervical outline) in its bucco-lingual aspect to a wider, hence rounded one (Fig. 4.7).

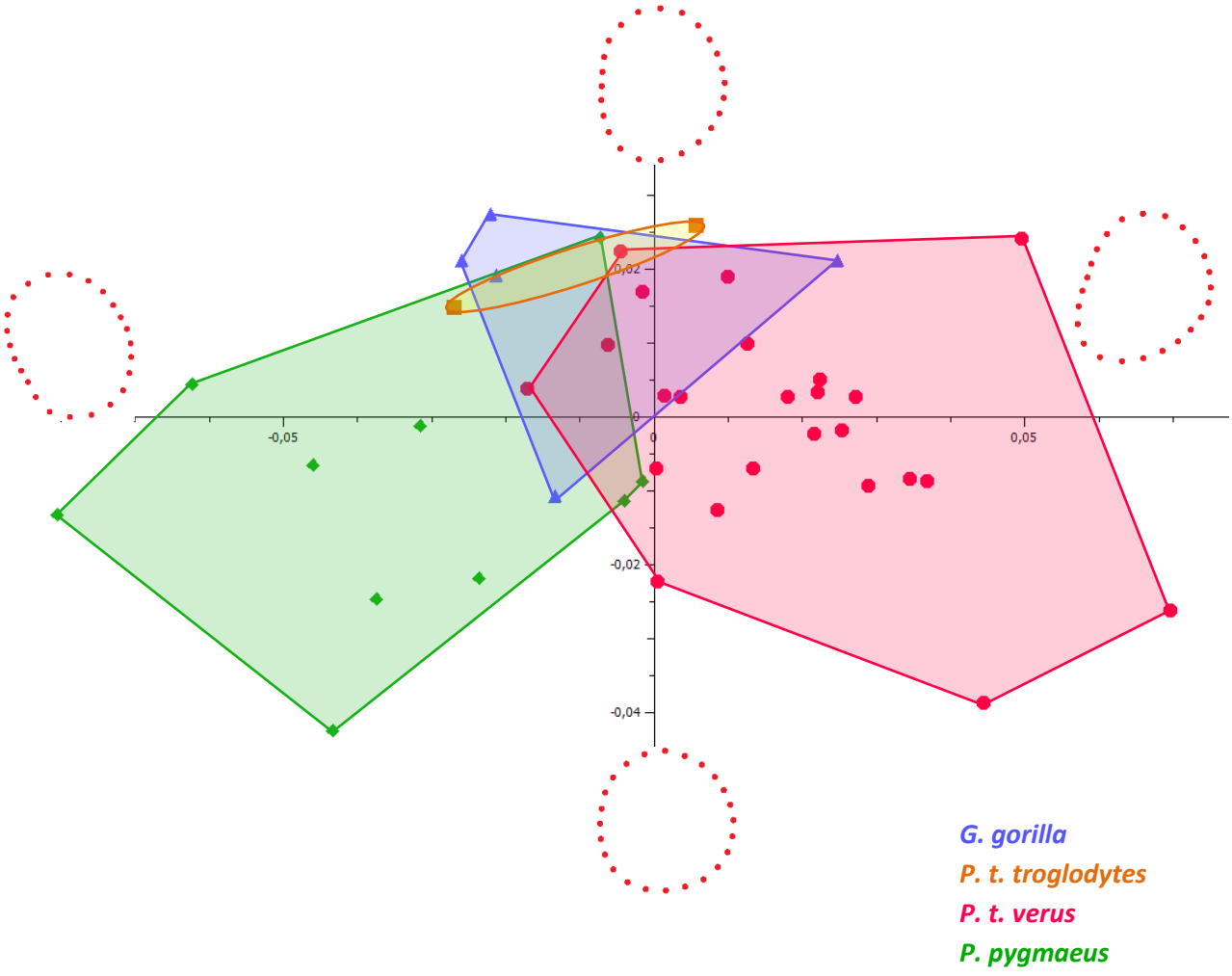

Fig. 4.7: PC1 - PC2 plot for the P^4 crown outline (N=41)

4.3.2.3 P^4 EDJ morphology

In P^4s 60.57% of total variance is explained by the first three PCs (Tab. 4.3). The analysis for shape differences in P^4 occlusal EDJ morphology shows a good separation of *Pongo* from the African great apes. *Pongo* separates from *Pan* mainly along the first Principal Component and from *Gorilla* on the second Principal Component. The shape of the EDJ changes along PC1 (31.67%) from a relatively symmetrical mesial to distal and buccal to lingual aspect in *Pongo* with horn tips positioned centrally to a shortened mesial margin with horn tips oriented more mesially and a more elongated bucco-lingual aspect in *Pan*. Along PC2 (16.39%) the shape changes from a flattened marginal ridge with lower horn tips in *Pongo*, to high horn tips in relation to the occlusal margin in *Gorilla* (Fig. 4.8).

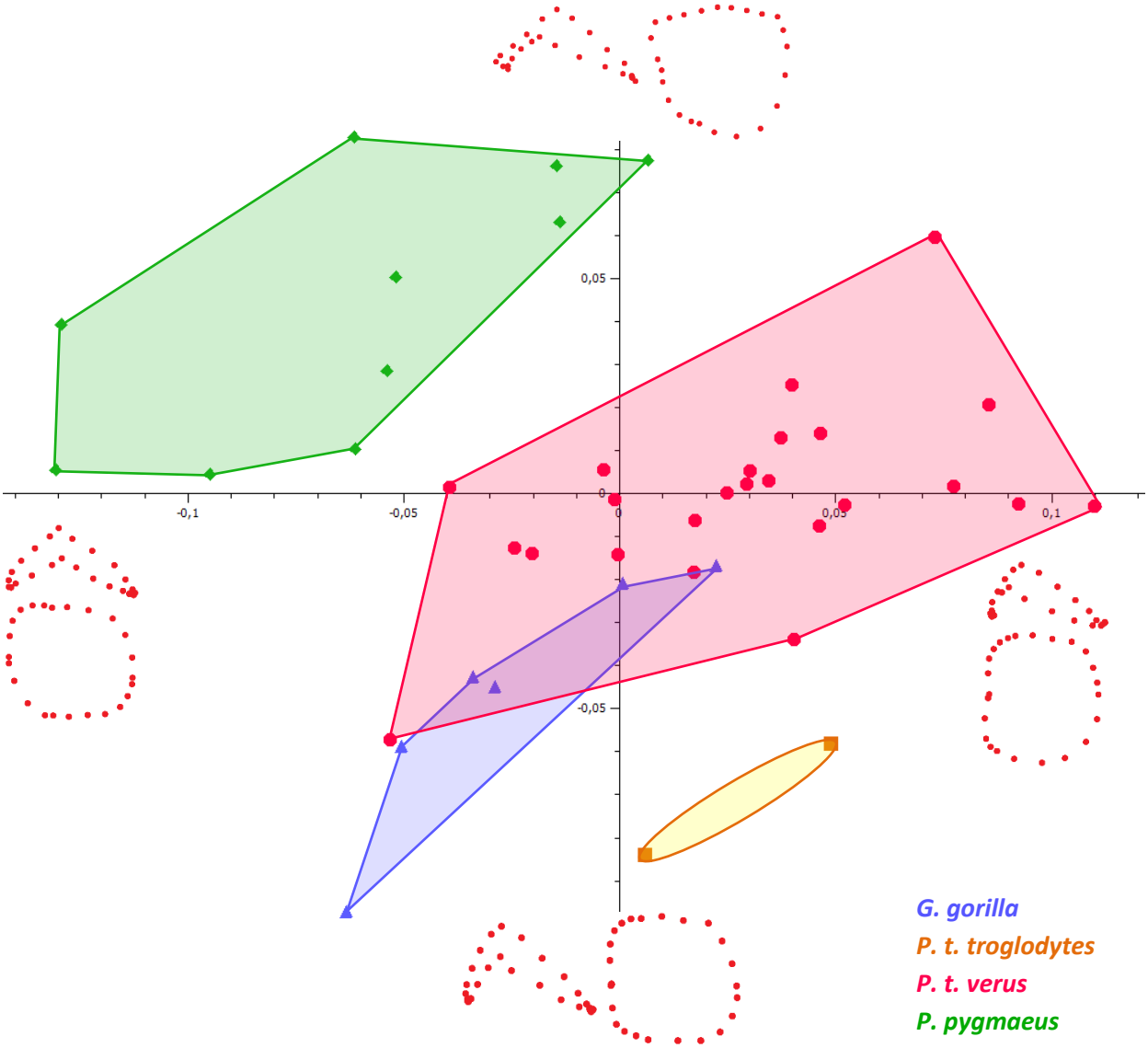

Fig. 4.8: PC1 - PC2 plot for the P^4 EDJ (N=42)

4.3.2.4 P^4 combined dataset

The PCA of the combined dataset (occlusal EDJ morphology plus cervical outline) of P^4 shows similar patterns to the P^3 results by separating well between Asian and African apes. One *Gorilla* (Gorilla 41460) is again far off in the *Pan* group (Fig. 4.9). The first three Principal Components explain 59.61% of variation with PC1=33.47%, PC2=15.97% and PC3=10.16% (Tab. 4.3).

The results are rather similar to the results in P^3. Along PC1, the relative size of the mesial to the distal aspect of the EDJ changes, with *Pan* having a relatively larger, protruding distal area compared to *Pongo* and *Gorilla* as well as the relative position of the horn tips, being more centrally oriented in Pongo and more mesially in the African apes (Fig. 4.9). Along PC2, the height of the horn tips and the height of the crown overall changes with *Gorilla* having high horn tips and pronounced curvature in the occlusal marginal ridge and *Pongo* having higher tooth crowns with a more flattened occlusal marginal ridge, thus lower horn tips. Along PC3, the ratio of occlusal surface to cervical area changes with more inwardly pointed horn tips and a relatively smaller occlusal area on one end of the spectrum to a relatively wider occlusal area on the other end (Fig. 4.10).

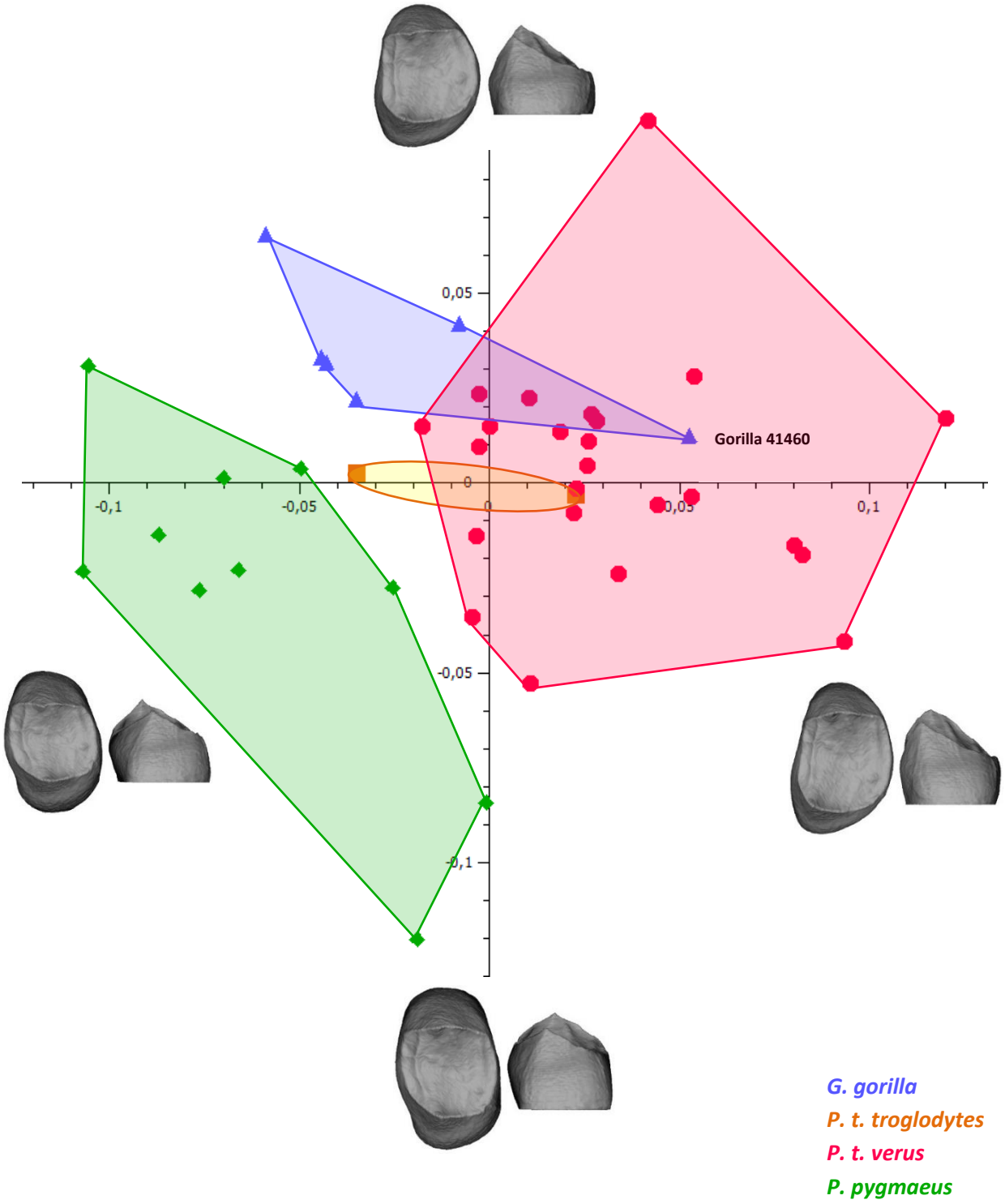

Fig. 4.9: PC1 - PC2 plot for the P^4 combined dataset (N=42)

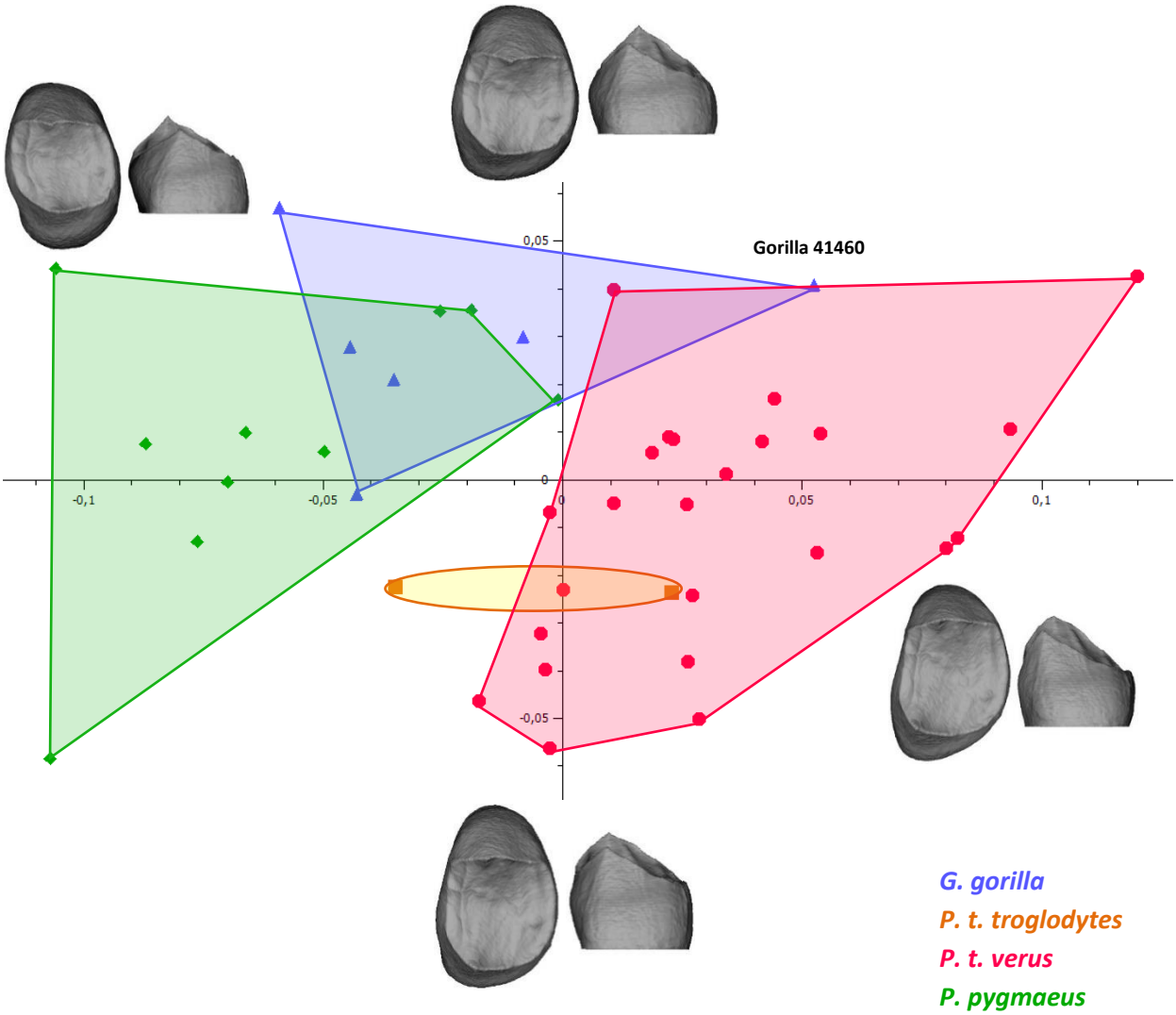

Fig. 4.10: PC1 – PC3 plot for the P^4 combined dataset (N=42).

Table 4.3 – Percentage of explained variance for PCs 1-3

	P^3				P^4			
PCs	**Cervical**	**Crown**	**EDJ**	**Combined**	**Cervical**	**Crown**	**EDJ**	**Combined**
1	45.70%	47.83%	39.34%	21.85%	58.29%	62.90%	31.67%	33.47%
2	23.15%	21.14%	14.01%	18.38%	18.63%	20.43%	16.39%	15.97%
3	14.72%	13.82%	11.77%	16.98%	8.27%	4.93%	12.61%	10.16%
1-3	83.56%	82.78%	65.13%	57.21%	85.20%	88.27%	60.57%	59.61%

Tab. 4.3: % of explained total variance for PCs 1-3 in shape space for P^3 and P^4 cervical outlines, crown outlines, EDJ morphology and the combined datasets (cervical outline + EDJ morphology). Principal Components (PCs) 1-3 listed, as well as the cumulative total explained variance of PCs 1-3.

4.3.3. Size of upper premolars

Size differs significantly, as macroscopically evident and described previously (Swindler, 2002), in both P^3 and P^4 on a 0.01-level (Kruskal-Wallis $p<0.01$) with *Pan* having the smallest and *Gorilla* the largest teeth (Fig 4.11 and Fig. 4.12). With no overlap in the distribution of centroid sizes for both P^3s and P^4s all three taxa can be separated with certainty by size only. Note that centroid size is a combination of several measurements (from all LM and sLM to the centroid) in 3D and thus quite different than the classic linear measurements used in dental morphology. There are some outliers in our sample; the P^3 of FF_Pan 54 is smaller (CV-interval 75%) than other *Pan* specimens which has no effect in assigning its tooth to the corresponding species (with *Pan* being the smallest of the three studied taxa anyways). Based on the observation of the skull, this individual is a juvenile of small size (its P^4 is an outlier on the smaller side as well). NMW_Pongo 55206 P^3 is on the other side of the spectrum and is an outlier for its large size, which comes rather close to but does not overlap with *Gorilla*s range of size distribution.

In P^3s *Gorilla* has the largest teeth, *Pongo* is intermediate, and *Pan* has the smallest teeth (Fig. 4.11). In P^4, the findings are very similar to those for P^3s (Fig. 4.12) and confirm previous findings of 2D-measurements (Swindler, 2002).

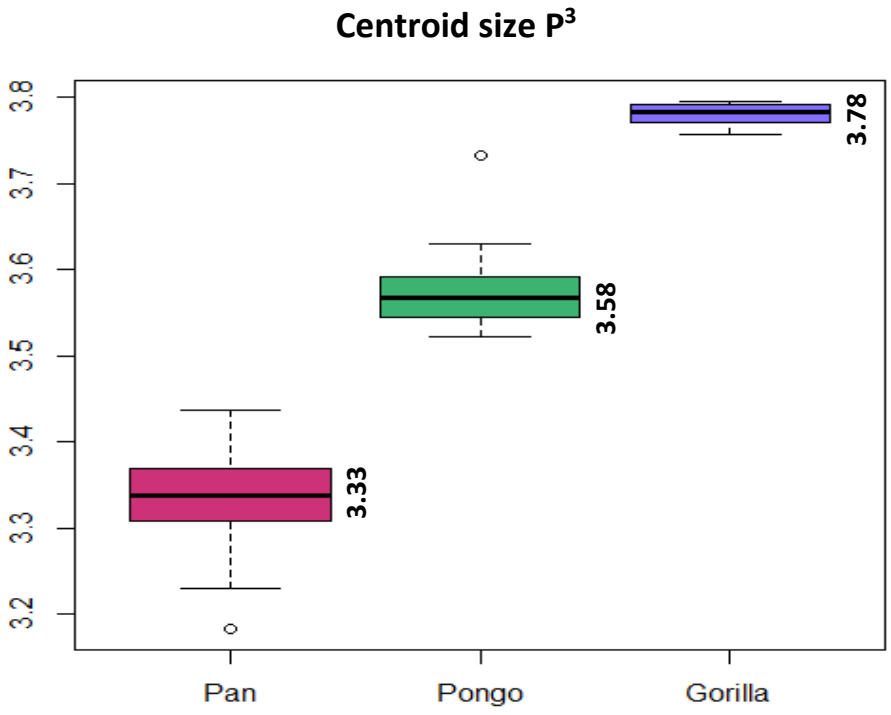

Fig. 4.11: Size for P^3 for combined dataset
○ Outlier (<75%>): *Pan*_54, *Pongo*_55206

G. gorilla
P. t. verus
P. pygmaeus

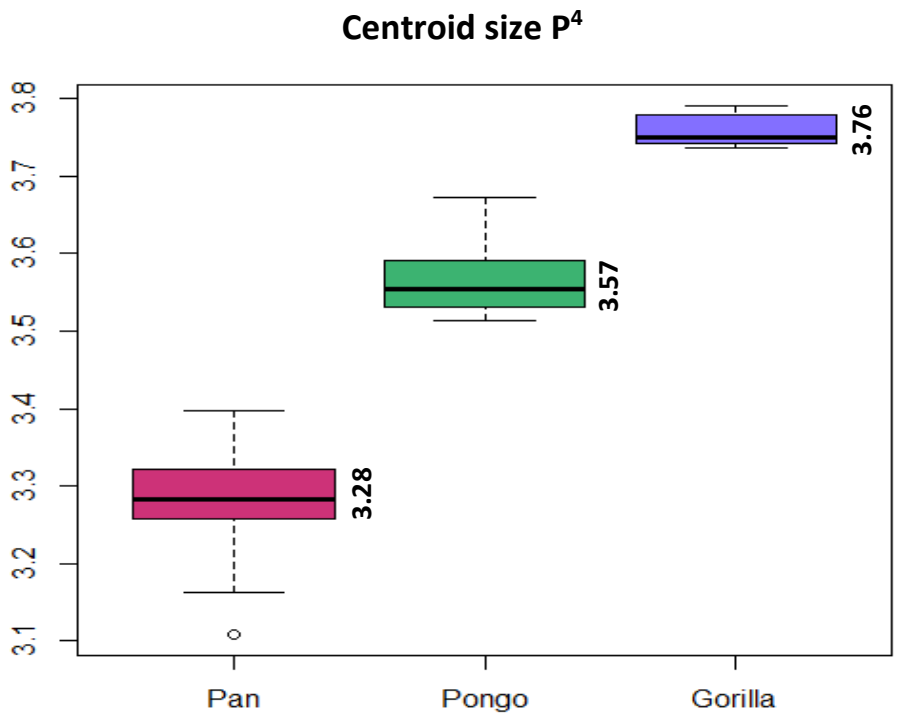

Fig. 4.12: Size for P^4 for combined dataset
○ Outlier (<75%>): *Pan*_54

G. gorilla
P. t. verus
P. pygmaeus

4.3.4 Analyses in form space

After evaluating the shape differences for different datasets we reintroduced size into our analyses, as size differences between the three genera has been documented in 2D-measurements (Swindler, 2002) and is also macroscopically apparent especially between *Pan* and *Gorilla*.

Principal Component Analyses of the combined datasets (occlusal EDJ morphology & cervical outline) in form space separate *Pan*, *Pongo*, and *Gorilla* perfectly (Fig. 4.13 & Fig. 4.14) along the first Principal Component (PC1 = 78.35% in P^3 and 84.63% in P^4). PC2 (5.09% in P^3 and 4.34% in P^4) separates between *Pongo* and *Gorilla*. This is evident for both P^3 and P^4. In both third and fourth premolar, changes along PC1 represent size differences, whereas changes along PC2 are more ambiguous.

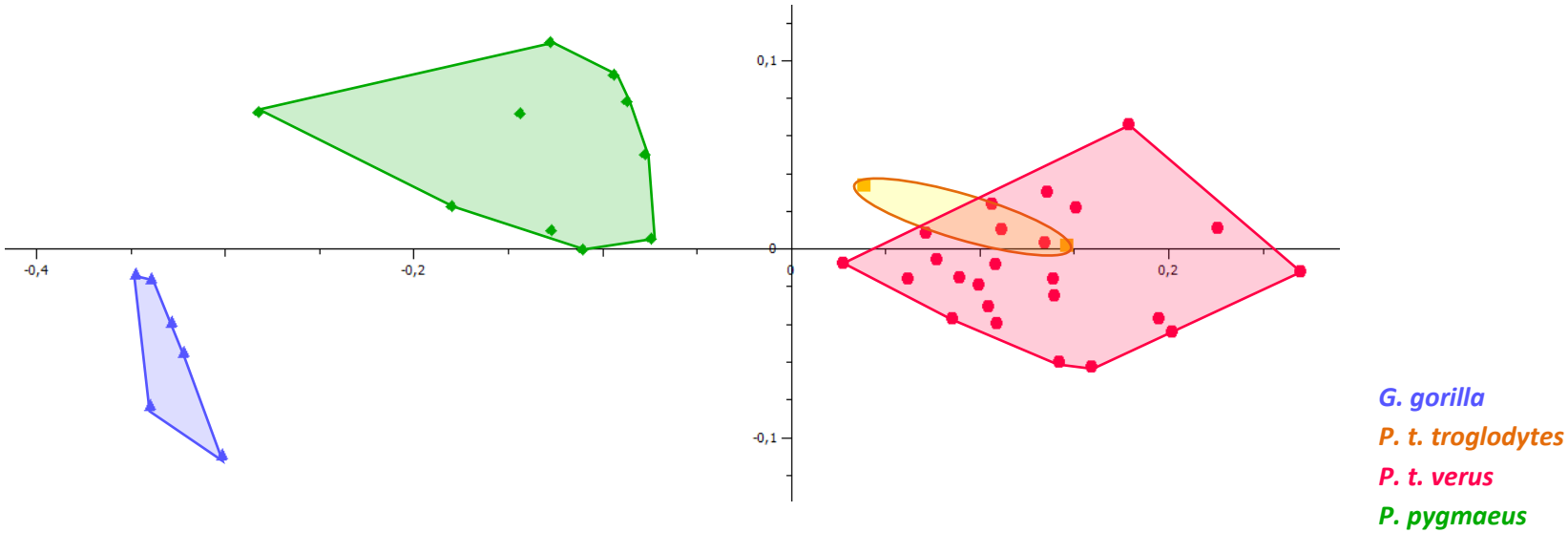

Fig. 4.13: PC1 - PC2 plot for the P^3 form (combined dataset of the EDJ & size) analysis (N=42)

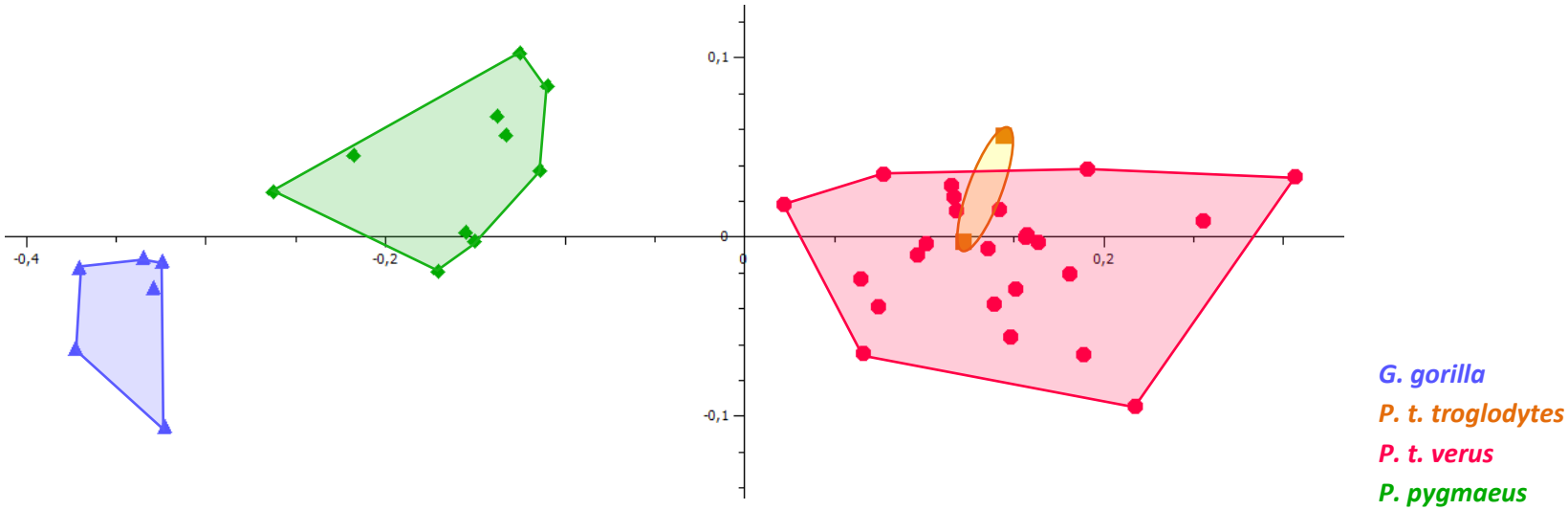

Fig. 4.14: PC1 - PC2 plot for the P^4 form (combined dataset of the EDJ & size) analysis (N=42)

4.3.5 Allometry

Table 4.4 – Regression for combined dataset

	Pan	Pongo	Gorilla
P^3	5.36%	9.26%	26.95%
P^4	5.08%	14.49%	13.11%

Tab. 4.4: Regression combined dataset (EDJ morphology & cervical outline) for *Pan*, *Pongo* and *Gorilla*.

The multiple multivariate regression analysis shows different magnitudes of size-dependant shape variation in the three great ape genera (Tab. 4.4). For *Pan*, the variance explained by size is about 5% (5.36% for P^3 and 5.08% for P^4) which is an allometry similar to that of humans (Buchegger, 2015, Krenn et al. 2019). In the two larger ape genera *Pongo* and *Gorilla,* however, it is significantly higher. With 9.26% for P^3, 14.49% for P^4 in *Pongo* and 13.11% in *Gorilla* P^4 and 26.95% in P^3 it exceeds allometry in *Pan* considerably. *Gorilla* P^3 hereby has the highest value for size dependant variation in shape. As stated earlier (Tab 2.1) for *Gorilla* only male individuals were available and included in this dataset. Therefore this result demonstrates male intrasexual allometry.

4.3.6 Partial Least Squares Analyses

To analyse how – and how much – the different datasets (crown outline, cervical outline, EDJ morphology, combined dataset for P^3 and P^4) and their shape traits vary together, a 2-Block Partial Least Squares Analysis was carried out comparing the cervical with the crown outlines, each of the outlines with the occlusal EDJ morphology and the combined datasets (cervical outline & EDJ morphology) of P^3s with P^4s with each other.

In some PLS-Analyses all three taxa had huge overlaps (e.g. P^3 crown outline vs cervical outline, Fig. 4.15) in others (e.g. P^3 cervical outline vs EDJ morphology, Fig. 4.17) a good distinction between *Pongo* and the African great apes was visible.

4.3.6.1 PLS P^3 crown outline versus cervical outline

The 2B-PLS of the P^3 crown and cervical outlines results in a pairwise correlation of r1= 0.95 (60.55% of the total squared covariance explained).

The crown outline and cervical outlines of P^3 covary in regard to their rotation and distal protrusion; more mesially rotated lingual cusp outlines are found on one with a slightly more mesially oriented buccal cups outline with distal protrusion and distally pronounced curvature, more centrally oriented lingual cup outlines with a straighter distal outline aspect was found on the other end with an overall only small grouping effect and huge overlaps (Fig. 4.15).

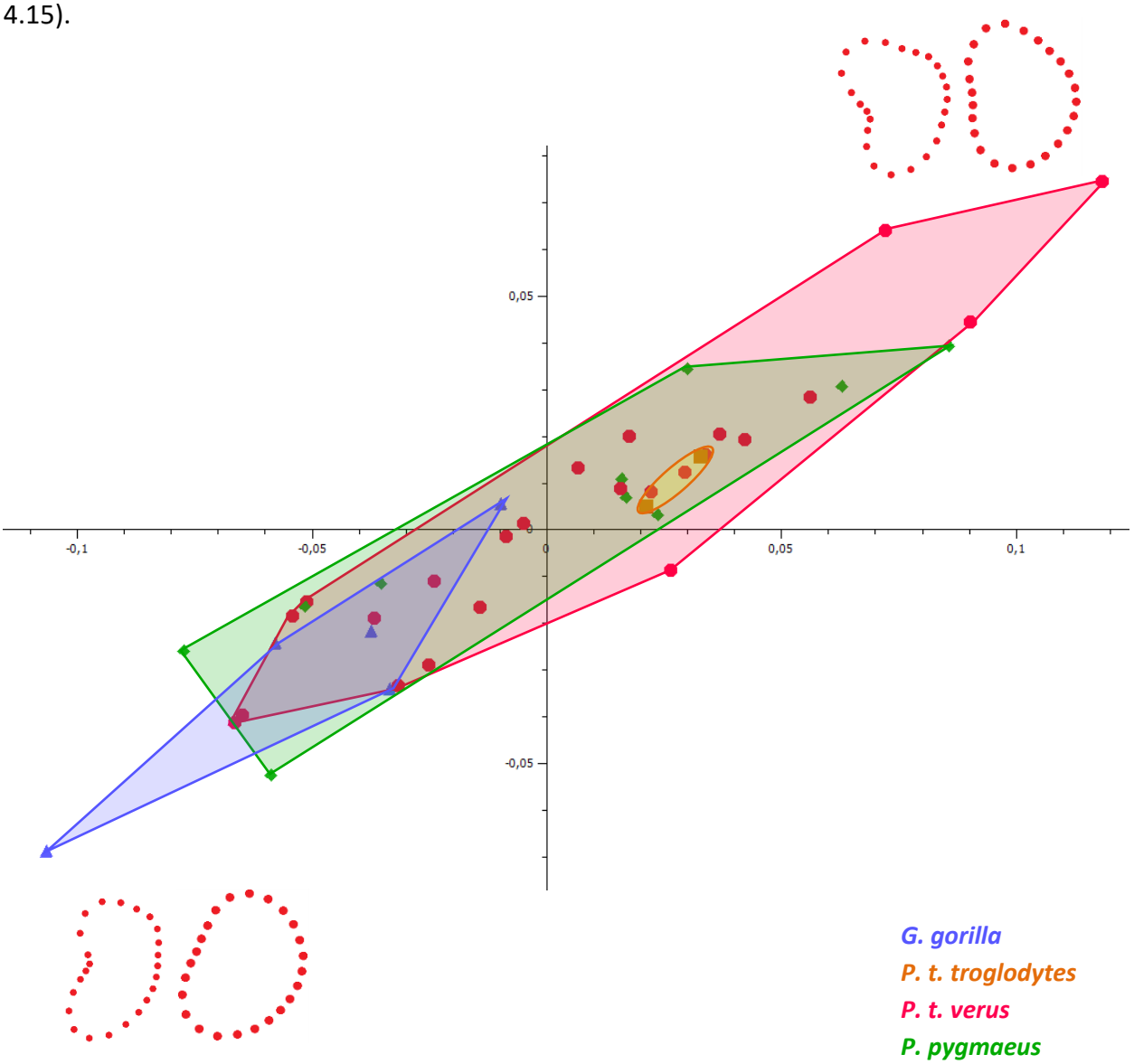

Fig. 4.15: PLS for P^3 crown outline vs. cervical outline (N=41).

4.3.6.2 PLS P^3 crown outline versus EDJ morphology

The 2B-PLS of the P^3 crown outline and the occlusal morphology of the EDJ (N=41) results in a pairwise correlation of r1=0.78 (30.66% of total squared covariance explained).

The crown outline and the EDJ morphology covary in regard to the orientation of the lingual cusps and distal protrusions; being rotated more mesially on one end with more mesially oriented horn tips to a more centrally oriented lingual cusp with more centraly oriented horn tips and more distally pronounced outline on the other end. Again, there were huge overlaps between all three taxa with no separation (Fig. 4.16).

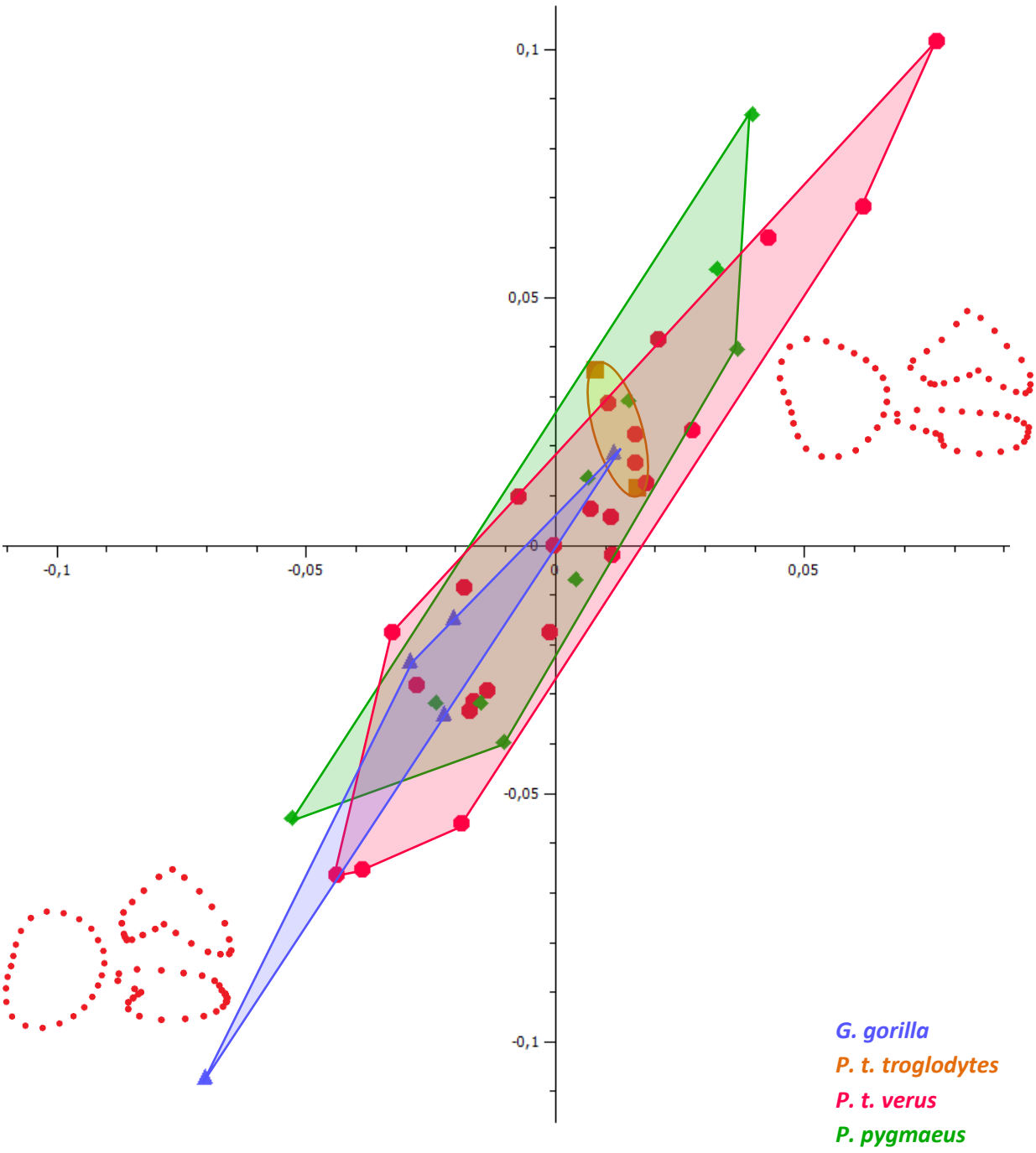

Fig. 4.16: PLS for P^3 crown outline vs. EDJ morphology (N=41).

4.3.6.3 PLS P^3 cervical outline versus EDJ morphology

The 2B-PLS of the P^3 cervical outline and the occlusal morphology of the EDJ results in a pairwise correlation of r1=0.65 (39.46% of total squared covariance explained). The cervical outline and the EDJ morphology covary in regard to the steepness of the lingual aspect of the marginal ridge, cusp orientation and orientation of the horn tips respectively; from the cervical

outline being distally protruding and curved with more mesially oriented horn tips among African great apes and a steeper marginal ridge on the lingual cusps to more centrally oriented horn tips and a flatter marginal ridge and particularly lower lingual horn tip and a distally slightly indented outline on the other end in *Pongo* (Fig. 4.17).

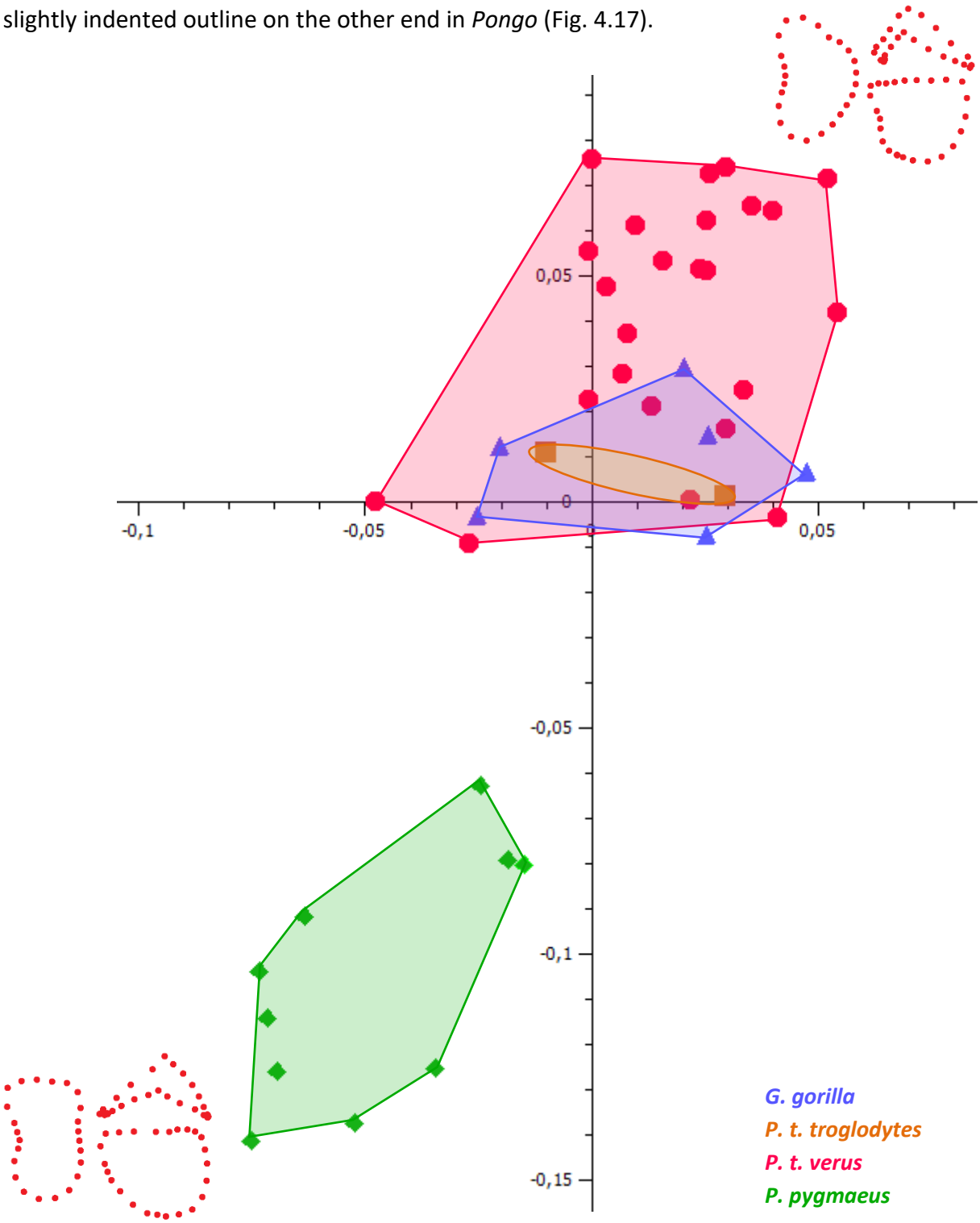

Fig. 4.17: PLS for P^3 cervical outline vs. EDJ morphology, (N=42).

4.3.6.4 PLS P^4 crown outline versus cervical outline

For the 2B-PLS of the P^4 crown outline and the cervical outline (with N=41, *Gorilla* NMW 3118 was excluded again due to the enamel crown being too broken) the correlation results in a pairwise correlation of r1=0.88 (84.96% of total squared covariance explained). Without the scattering of the Pongo dataset, it might have been even higher. Both outlines covary in their bucco-lingual and distal cusp outline aspect with more bucco-lingually elongated outlines and distally rather straight outlines on one end (*Pan*) to more condensed outlines buccally and lingually and more curvature and protrusion of the distal aspects on the other end (*Pongo*) (Fig. 4.18).

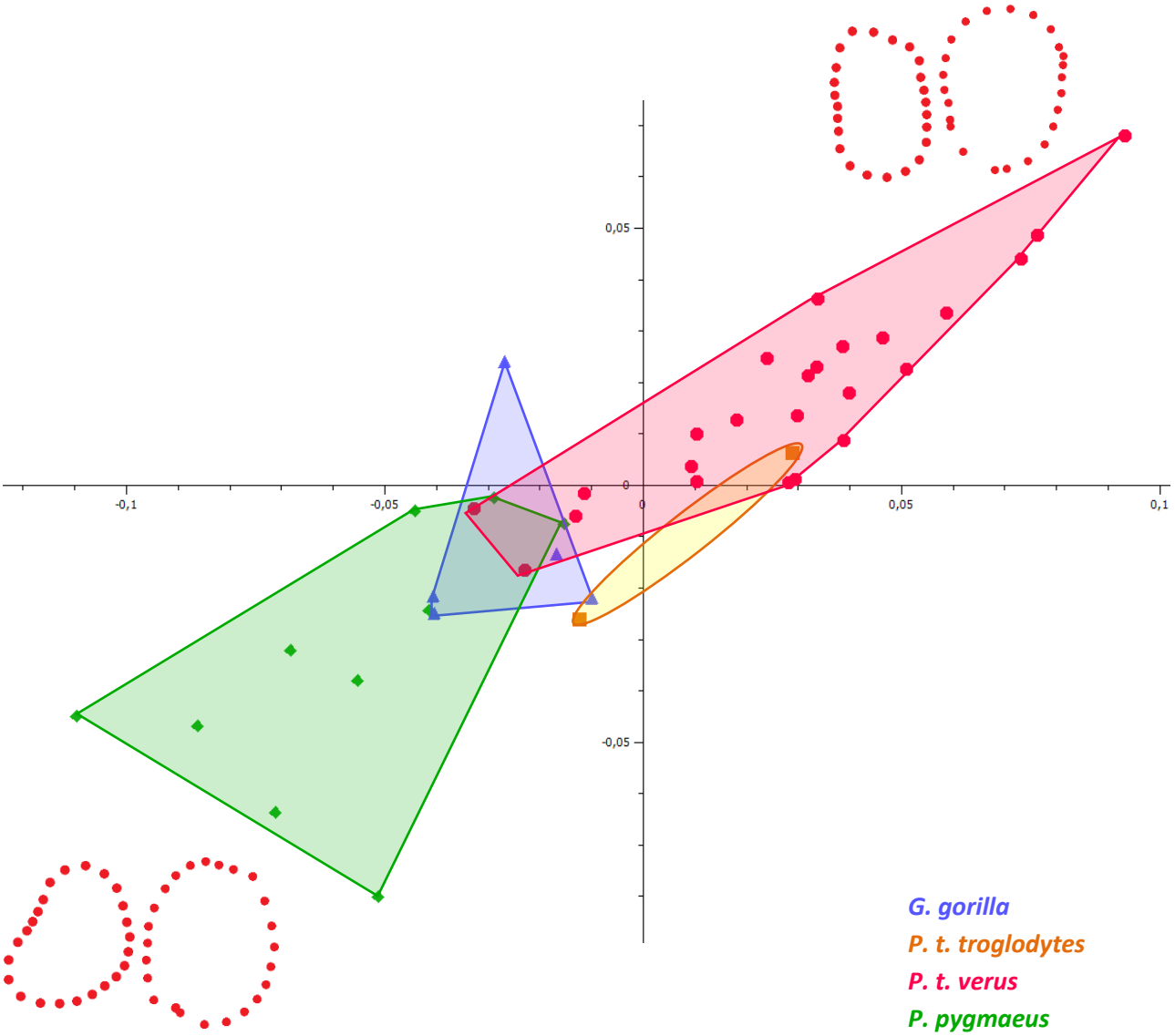

Fig. 4.18: PLS for P^4 crown outline vs. cervical outline, (N=41).

4.3.6.5 PLS P^4 crown outline versus EDJ morphology

The 2B-PLS of the P^4 crown outline and the occlusal morphology of the EDJ was done for 41 individuals (Gorilla NMW 3118 waws excluded) and results in a pairwise correlation of r1= 0.83 (81.58% of total squared covariance explained). The crown outline and the EDJ covary in regard to rotation and orientation of the cusps and horn tips respectively. From a slightly more mesially rotated lingual cusp and a distally curved protrusion of the outline, more mesially oriented horntips and a steeper marginal ridge on the lingual cusp on one side to a more centrally oriented lingual cusp and horn tips with a flatter marginal ridge of the lingual cusp on the other side (Fig. 4.19).

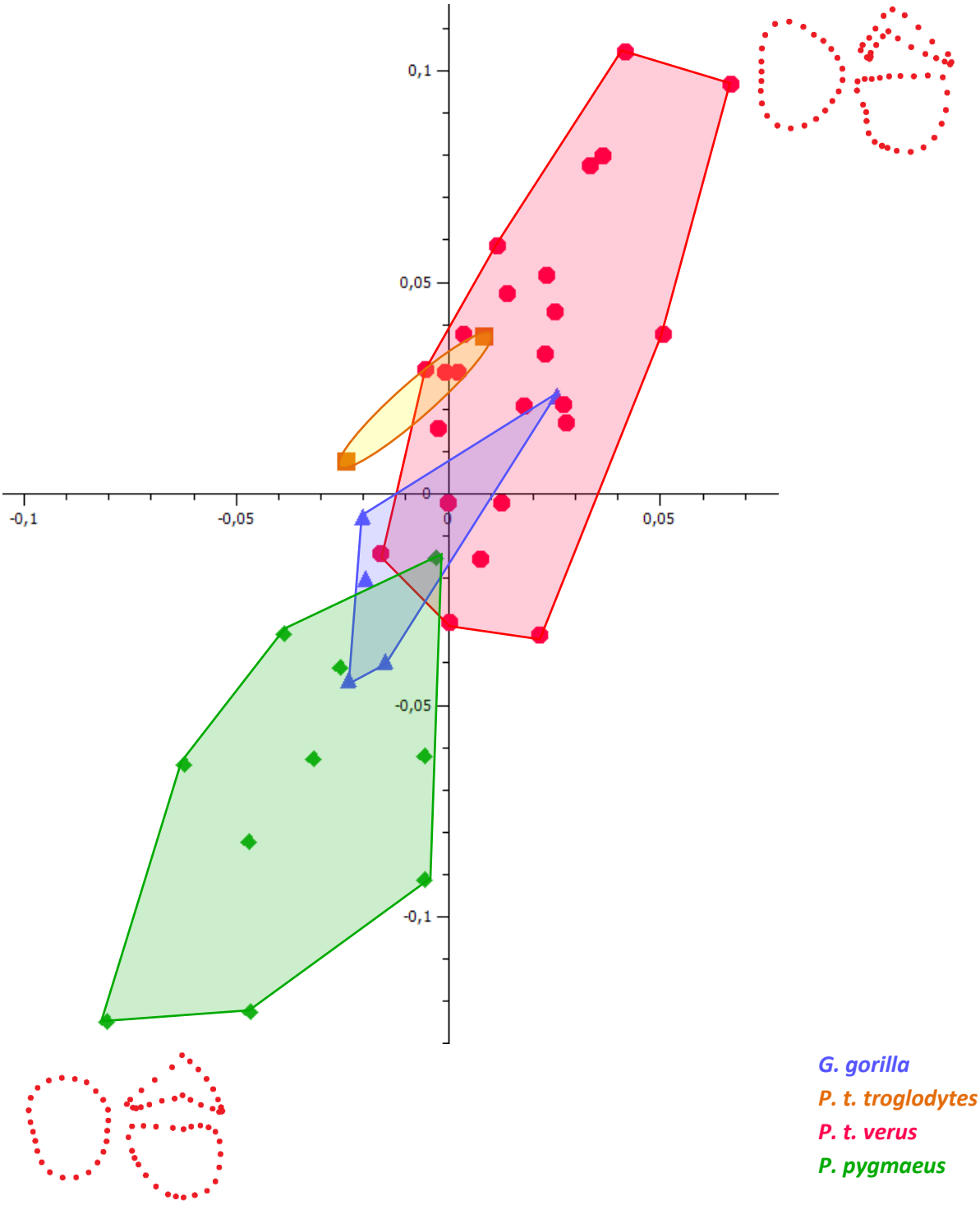

Fig. 4.19: PLS for P^4 enamel crown outline vs. EDJ morphology, (N=41).

4.3.6.6 PLS P^4 cervical outline versus EDJ morphology

The 2B-PLS of the P^4 cervical outline and the occlusal morphology of the EDJ results in a pairwise correlation of r1= 0.83 (80.34% of total squared covariance explained). The outline and the EDJ covary in regard to orientation of the cusps in its outline and the horn tips. On

one end horn tips are oriented more mesially with a steep marginal ridge and a curved distal protrusion on the cervical outline (*Pan* and *Gorilla*), on the other end horn tips are oriented more centrally on the tooth with a flatter marginal ridge and no curved protrusion of the distal tooth aspect (*Pongo*) There is a good distinction between the African great apes and Pongo with only minimal overlap (Fig. 4.20).

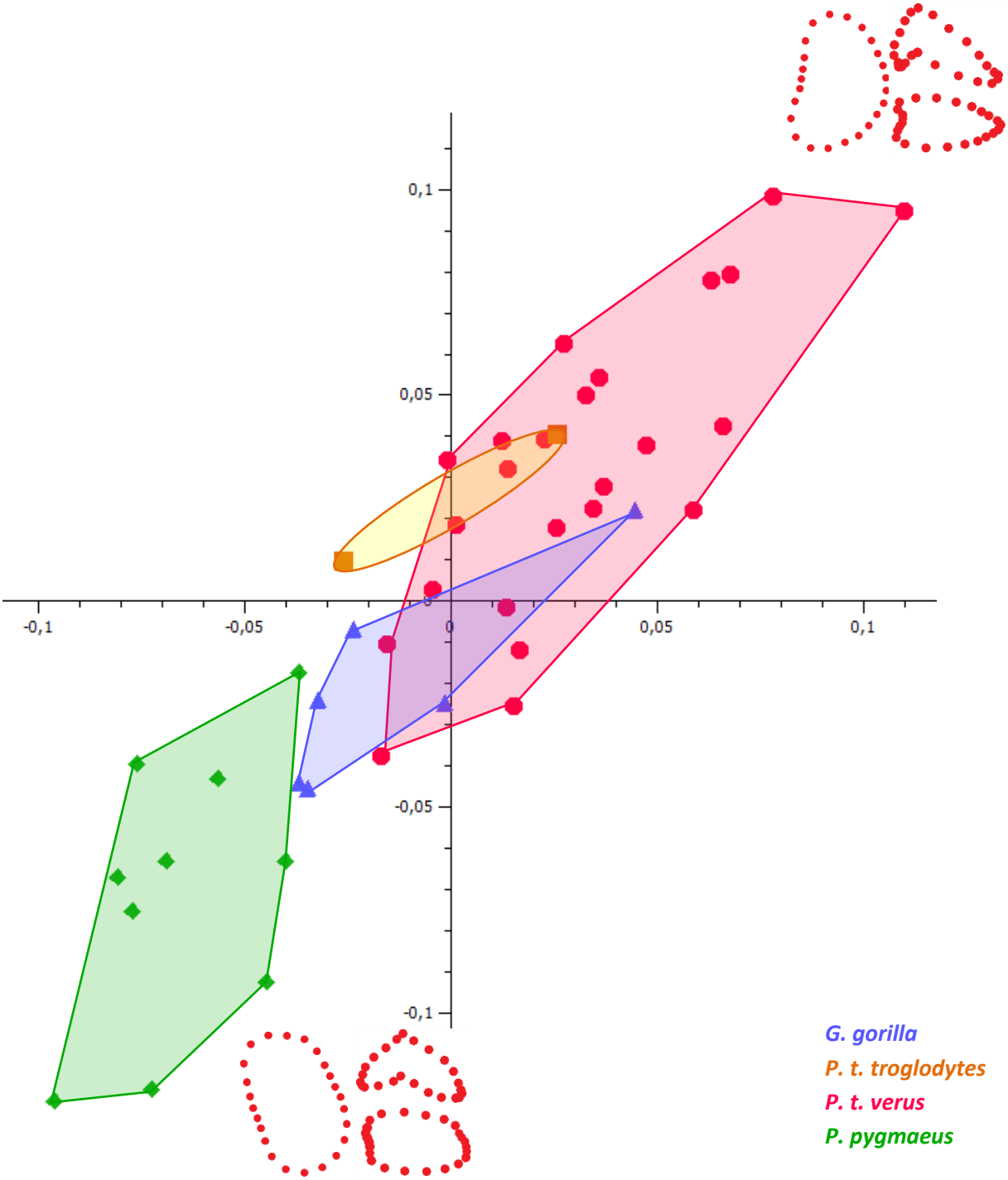

Fig. 4.20: PLS for P^4 cervical outline vs. EDJ morphology, (N=42).

4.3.6.7 PLS P^3 - P^4 combined dataset

The 2B-PLS of the combined datasets (EDJ morphology & cervical outline) of P^3 and P^4 results in a pairwise correlation of r1= 0.86 (41.14% of total squared covariance explained).

Both premolars vary together with regard to the relative location of the horn tips, the steepness of the marginal ridge and the relative size of mesial to distal occlusal area, as well as the more oval to kidney-shaped, distally protruding cervical outlines. This means, that if a P^3 is more kidney-shaped, so is the corresponding P^4. The kidney shaped outlines with steeper marginal ridged and more mesially oriented horn tips are typical for *Pan*, the other end with rather oval outlines without distal protrusion, more centrally oriented horn tips and flatter marginal ridges are typical for *Pongo*. Between those two groups, there is a perfect separation, *Gorilla* is intermediate and overlaps *Pan* and only minimally *Pongo* (Fig. 4.21).

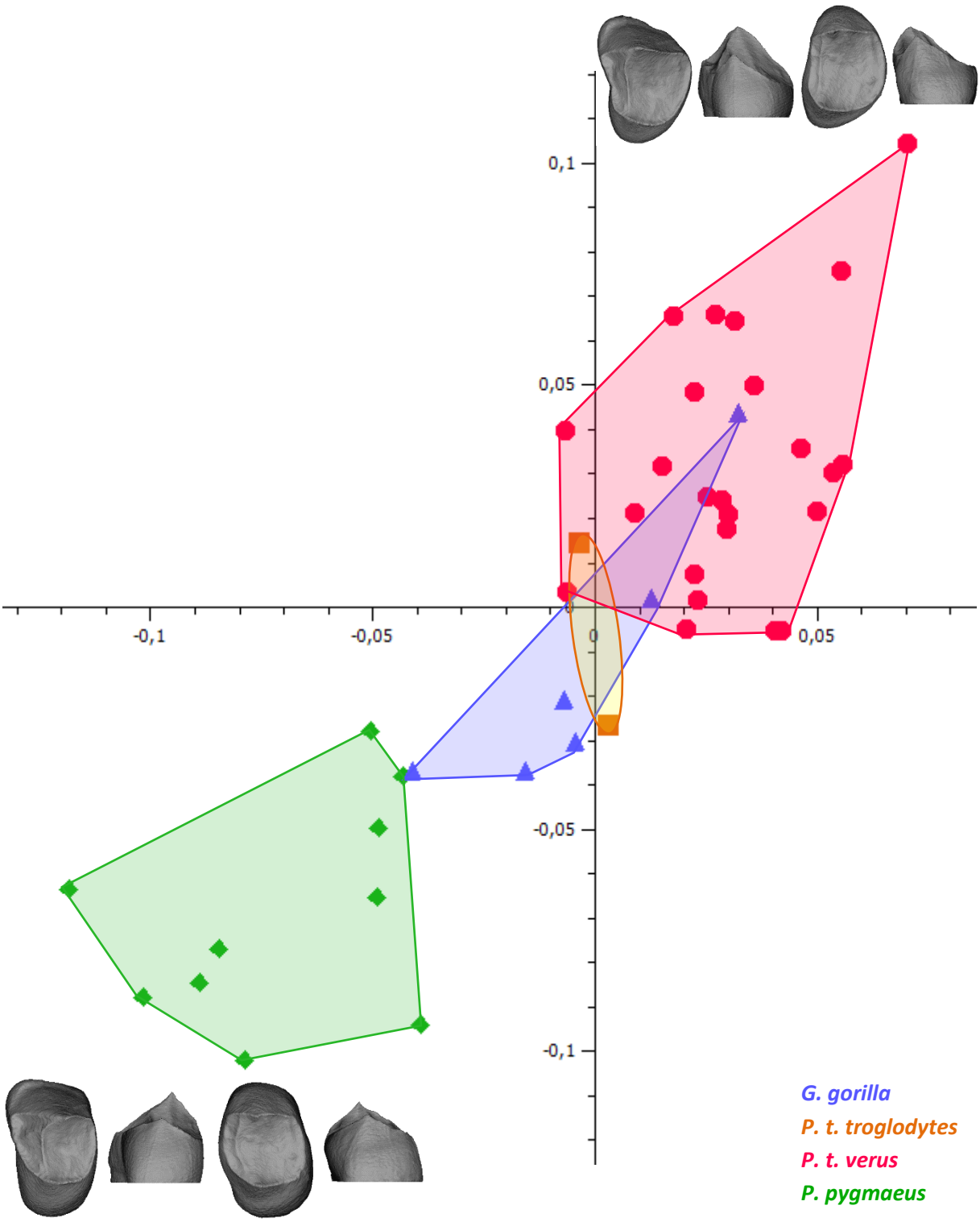

Fig. 4.21: PLS for P^3 vs. P^4 for combined dataset, (N=42).

5 DISCUSSION

The aim of this study was to explore the 3D shape variation of great ape upper premolars including nonmetric traits on both the EDJ and the OES.

5.1 Geometric morphometrics

Using a 3D approach to capture crown shape and size of upper premolars of the three great ape genera, we were able to demonstrate that shape alone can discriminate well between the Asian and African great apes, while form (thus including size) and even size alone distinguishes perfectly between all three taxa (Fig. 4.13 & Fig. 4.14).

With the present study we collected, amongst others, data for cervical and crown outlines which can be used to be compared to moderately (crown outline) and heavily (cervical outline) worn teeth. This approach has already been successfully applied in the past for discrimination between different species (Neanderthals and modern humans) (Benazzi et al., 2012). In this current study we were not able to separate the three taxa using this approach, though a grouping effect was seen, with large overlaps (Fig. 4.1, 4.2, 4.6, 4.7). This does not seem too surprising, since outlines of *Pongo* upper premolars seem to be quite similar to other hominids like those of humans: in a PCAs for cervical outlines and crown outlines in an earlier study done at the Department of Evolutionary Anthropology, University of Vienna by Buchegger (2015), *Pongo* P^3s overlapped partially with human P^3s and P^4s – although it was a small sample of only four *Pongo* teeth – could not be distinguished from human P^4s when size was excluded from the analysis.

In our study, in both P^3 and P^4 cervical and crown outlines on their own do not separate well between the three taxa; groups form but overlap to various degrees (Fig. 4.1, 4.2, 4.6, 4.7), whereas the occlusal EDJ morphology separates well between African and Asia great apes with overlaps between *Pan* and *Gorilla* (Fig. 4.3, 4.8). The combined dataset of the dentinal crown shape (occlusal EDJ morphology & cervical outline) separates best between the taxa; especially *Pan* from *Pongo*, with *Gorilla* being intermediate and overlapping with *Pan* but not

with *Pongo* (Fig. 4.4 & Fig. 4.9). The differences in premolar morphology can be described as distally protruding kidney-shaped P^3s and P^4s with steeper marginal ridges, resulting in higher horn tips in *Pan* and oval teeth with no distal protrusion and flatter marginal ridges, resulting in lower horn tips in *Pongo*.

This effect was also apparent in the 2B-PLS analyses, where *Pongo* and *Pan* were found on the opposing ends in most cases (especially in the combined datasets, see Fig. 4.21) with *Gorilla* being intermediate and often closer to the *Pan*-spectrum. This could likely be a result of evolutionary processes, as *Pongo* separated at a much earlier point in time (16-17 mya) from the lineage leading to African great apes than the two African representatives separated from each other (8-10 mya) (Perelman et al., 2011; Scally et al., 2012).

5.2 Nonmetric traits

Nonmetric traits can be recognized on both the EDJ and OES. Some traits on the enamel, however, do not have the same underlying dentinal structures and vice versa (Olejniczak et al., 2004; Guy et al. 2013; 2015). Ortiz et al. (2012) further found minor differences in correspondence between OES and EDJ in weakly expressed traits regarding *Pan* and *Homo* and suggested that this might be due to thicker enamel in humans, concealing underlying structures of the EDJ. *Pan* and *Pongo* have thinner enamel caps compared to *Homo*, the enamel thickness in *Gorilla* teeth is even thinner than in the other two great ape taxa (Hooijer, 1948). Nonetheless we were also able to demonstrate differences in correspondence between OES and EDJ for several nonmetric traits in our dataset (e.g. crenulations, occlusal tubercles, especially metacones and hypocones in *Gorilla* P^3, and bifurcated horn tips in *Pan*) – enamel thickness might therefore be just one factor in the different expressions or lack thereof.

Corrucini (1978) stated that EDJ morphology is phylogenetically more conservative and primitive than OES morphology, as it is formed earlier in ontogeny. This can lead to traits weakly expressed on the EDJ, being missing or not visible on the OES at all. Other researchers (Skinner, 2008; 2009; Bailey, 2001, Ortiz et al., 2012) in both minor and gross aspects doubt this lack of correspondence.

While the correspondence between OES and EDJ is not clear for some nonmetric traits such as the Carabelli's cusp and others on molars in the literature, we found ambiguous results in

several nonmetric traits in our dental sample. Most of the additional cusps, hypocones, metacones, as well as bifurcations of the paracone horn tips in our sample were better visible on the EDJ than on the OES. In some traits on the other hand, there was the exact opposite effect; mesial and distal transverse crest found on the OES seemed to not always correlate to findings on the EDJ and might even be considered artefacts or crenulations mistakenly identified as such crests. Especially in *Pan* P^4 the transverse crests were found a lot more frequently (both six times higher; one mesial and one distal transverse crest found on the EDJ vs. six of each on the OES).

Other nonmetric traits such as the "side depressions", which were clearly visible in *Gorilla*, but only expressed weakly in *Pan*, were hard to determine correctly on the OES in some cases, partly due to wear facets in several specimens, which can look quite similar. The only nonmetric trait found in this dataset that was not detectable on the EDJ but clearly visible on the OES were occlusal crenulations.

Buccal or lingual "cingula", at least in our premolar dataset, seem to only occur in African great apes, although they have been described in earlier studies in *Pongo* as well (Hooijer, 1948). The "cingula" were a common trait in in our *Pan* P^3s and were found in a few *Pan* P^4s and *Gorilla* (P^3s & P^4s), but not in *Pongo*.

Molarization or molariform premolars in terms of shape (inter alia metacones and hypocones) (Butler, 2007) were more frequently found in our dataset then described in earlier studies (Swindler, 2002). Metacones, in particular, were a rather frequent trait and present in all three taxa in both upper premolars to a varying degree. They were found in – from lowest to highest occurrence – 20% of *Pongo* P^3 (EDJ) and in 83% of *Gorilla* P^3 (EDJ). Hypocones were less prevalent but also present in all taxa, ranging from 17% in *Gorilla* P^3 to 50% in *Pongo* P^3.

To summarize: Apart from crenulations and some crests, nonmetric traits were better detectable on the EDJ than on the OES, because of wear, cracks, but also artefacts resulting in misinterpretations and being simply not detectable visually. The EDJ seems to be not only phylogenetically more conservative, but also the more robust and better suited anatomical unit for identifying weakly expressed traits. A taxonomic assessment based on nonmetric traits was not possible unfortunately, but some trends were detected; crenulations and bifurcated cups/horn tips were not present in our *Gorilla* specimens, "cingula" were only present in African great apes. Futures studies might investigate the prevalence of these

"cingula" in all great apes with a larger sample size to confirm or falsify our suggestion, that it might be an adaptative trait in African great apes (see next chapter "Tooth wear & function").

5.3 Tooth wear & function

"It seems that we observe an evolutionary compromise, and tooth evolution and dental biomechanics can only be understood, if we further investigate tooth function in respect to the dynamic changes of tooth structures during the lifespan of individuals." (Benazzi et al., 2013a).

With the exception of contemporary modern human populations – due to distinctly less mastication compared to the pre-modern era and consumption of increasingly less tough foods in favor of cooked, soft foods (Kaifu, 1999; Wrangham 1999) – all great apes and prehistoric modern human populations display moderate to heavy tooth wear.

With mastication being one of the core purposes of teeth and one of the main reasons for abrasion (Barrett, 1977) one could raise the question whether studying unworn teeth hinders important information on function which might be revealed by worn teeth instead. Heavy wear is not only inevitable but seems to be a necessity to withstand certain stresses throughout the lifespan and especially at later stages of life in all great apes, possibly all hominids including humans (Begg, 1954; Kaifu, 2000; Kaifu et al., 2003; Benazzi et al., 2013b). Local stresses have been demonstrated to being reduced by the emergence of larger surface areas in worn teeth. The stresses are distributed more equally to those surface areas rather than affecting small contact areas heavily (as in unworn teeth), leading to a decrease in tensile stresses in the entirety of the tooth crown (Benazzi et al., 2013a).

Nonmetric traits might also possess those functional advantages in worn teeth and could be part of adaptations to reduce and redistribute certain stresses. Benazzi et al. (2013a) demonstrated, that in *Gorilla* molars (lower second molars) the presence of a "shelf-like" protostylid reduced tensile stresses at the tooth cervix (which is more vulnerable due to the thin enamel in this area) protecting it and the entire tooth from margin cracks and tooth failure.

Although remaining highly speculative, one could presume that the shelf-like structures of the buccal and lingual "cingula" we identified in our *Pan* and *Gorilla* specimens (Fig 3.17) might have a similar effect and purpose. In our dataset in *Pan* more than 90% of P^3s have buccal or lingual "cingula" (OES 92%, EDJ 100%), in P^4s about one in five displays this trait (OES 12%, EDJ 23%). In *Gorilla,* "cingula" are found to a lesser extent in (P^3 EDJ 20%; P^4 EDJ 33%, OES 50%), whereas in our *Pongo* sample there are no "cingula" at all present. This might be an indication for "cingula" being an adaptation for consumption of tough foods in the African great apes; "cingula" might have similar properties as protostylids in *Gorilla* LM2 (Benazzi, et al., 2013a) protecting worn teeth from stresses occurring during consumption of tough fibrous foods. Although all (sub-)species examined in the current study are described as frugivores to varying extents (Berthaume, 2014; Carvalho, 2015), they rely on different fallback foods: for *P. troglodytes* they range from fibrous fruits and leaves to animal protein (Sugiyama & Koman, 1987; Berthaume, 2014), for *P. pygmaeus* these are mainly unripe fruits and seeds (Delgado & Van Schaik, 2000; Fox et al., 2004), and for *G. gorilla* leaves, bark and other tough parts of plants (Yamagiwa et al., 2009). Fallback foods might play a role in primate tooth morphology; as distribution and thickness of enamel seems to have adaptive advantages for the respective fallback foods with thicker occlusal enamel in *Pongo* for hard fallback foods (seeds and nuts) and *Gorilla* for tough fallback foods (leaves barks) (Constantino et al., 2009). This might – though highly speculative – explain why frugivorous *Pan* and *Gorilla*-(sub)species in our dataset might have "cingula" as an adaptation not for their primary food source but rather for their tough fallback foods and why *Pongo* does not display this trait.

Shape differences between the great ape taxa even in worn teeth do exist. For example, the angularity of the molar cusps differs; with high-crested teeth in *Gorilla* and rounded ones in *Pongo* indicating adaptation to efficiency with regard to breaking down specific foods (leaves in *Gorilla* vs. fruits in *Pongo*) (Ungar & M'Kirera, 2003; Cuozzo, 2016). As mentioned above, tough foods are part of *Gorilla*s fallback food; high crests help in breaking down tough foods. In our premolar sample we were able to detect similar findings with more angularly shaped cups in *Gorilla*, characterized on the one hand by the nonmetric trait "side depressions" with straight edges (Fig. 3.16), as well as in the PCAs, were both in P^3 and P^4 the curvature of the marginal ridge is more pronounced in *Pan* and to some extent in *Gorilla* with higher horn tips in regard to the deepest points on the occlusal margin curves (Fig. 4.21). In contrast, *Pongo* has particularly "flatter" premolars with a less pronounced curvature of the marginal ridge

leading to especially lower protocone horn tips. “Side depressions” if present are rounded and only expressed weakly.

Futures studies might explore the effects of “side depressions” and “cingula” regarding advantages in mastication of tough foods and reduction of local stresses in worn teeth to confirm or falsify our – highly speculative – suggestion, that these traits might be adaptations for consumption of tough fallback foods in African great apes.

5.4 Size

Although we used an entirely different size measurement (lnCS in 3D) than traditional studies (often distances in 2D such as M/D or B/L), our findings clearly confirm size differences between the great ape taxa in both P^3 and P^4. We were able to reproduce previous findings of 2D measurements (Hooijer, 1948; Swindler, 2002) demonstrating *Pan*’s mean sizes to be the smallest compared to *Pongo* and *Gorilla*, with the last one possessing the biggest upper premolars. Noteworthy is that size distributions of the three genera do not even touch or overlap; correct determination of the genus by size alone was possible in our studied sample (with the limitation of the *Gorilla* sample consisting of male individuals only).

Allometry plays a bigger role in great apes than in humans, especially in *Gorilla* but seems to be negligible in *Pan* (Tab. 4.4). Our data show that allometry in great apes is not only sex-dependent, with findings of strong allometry in our *Gorilla* sample which only consists of male individuals. Our results for *Gorilla* thus represent male intrasexual allometry in a species that shows high male heteromorphism related to status (Wright et al., 2018). Teeth are, however, formed long before physical maturity (Kelley & Schwartz, 2009) and before status is established (Breuer et al., 2009). This surprising result needs closer examination including both sexes and larger sample sizes. Furthermore, we cannot rule out non-size dependent differences in shape between the sexes, but this remains speculative in our study as sex is not known for more than half of our specimens. Therefore, we were not able to shed any light on sex specific differences in the three great ape taxa, unfortunately. As sex specific differences in great ape premolar 3D shape have not been studied to date they remain unknown. Future studies with larger datasets of sexed specimens might explore this unanswered question and

give more insight into and broaden the knowledge on sexual dimorphism in great ape premolars, including allometric changes and sexual dimorphism separately.

5.5 Limitations

In any study there are limiting factors. One difficulty in this study was the use of many different software programs for scanning, segmentation, data collection and analyses. The protocol included transformations of the data several times to the required formats for the different programs, making the entire process prone to mistakes; either manually produced errors or mistakes occurring due to software errors. The datasets had to be checked several times at each step to minimize the possibility of incorrect outcomes. However, the data acquisition of this study took place in an early period of developing new protocols for 3D shape analyses of teeth. Meanwhile, sharply defined sets of procedures exist which have proven to deliver accurate data efficiently (Fornai et al., 2015, Weber et al., 2016, Šimková, 2024).

Another limitation that needs to be mentioned was our dependance on the – mostly century-old – determination of the great ape (sub-)species. It is not possible to completely rule out that (sub-)species had been assessed incorrectly. For instance, specimen *Gorilla* 41460 comes to mind, which seemed to be an outlier in many analyses (see plots for instance Fig. 4.6, Fig. 4.9) and was collected in Cameroon, whereas all other *Gorilla*s were collected in the Congo area (according to the collection data). It is therefore questionable if this specimen differs due to simply belonging to a different population or was not correctly assigned and does belong to a different subspecies than all other *Gorilla* specimens in our sample. We cannot rule out this possibility but due to all specimens being labeled as the same species, and having no expertise in subspecies determination, we refrained from excluding or reassigning the specimen in question to a different subspecies.

The unbalanced subspecies ratio with unknown *Pongo* (sub-)species and – presumably – only one *Gorilla* subspecies and the unbalanced *Pan* sample (24 *Pan t. verus*, two *Pan t. troglodytes*) further limit our findings to a more general (and possibly skewed) comparison between three genera, rather than between several different species and subspecies.

However, the most limiting factors in this study is the small sample size and the unbalanced number of female and male specimens, especially in the *Gorilla* sample, which consists of only

six males and no females. Including female specimens could possibly lead to a slight overlap in size between *Pongo pygmaeus* and *Gorilla gorilla* and maybe even so in shape. This remains highly speculative, although findings in craniofacial morphology might point in that direction (Mitteröcker & Gunz, 2004). The sample size was small and unbalanced as a consequence of keeping the dataset rather small for practical reasons; time constraint (as µCT-scanning, segmentation, and reconstruction to some extent, are somewhat time consuming) was one factor. The (non-)availability of material was another and greater factor, as neither the Department of Anthropology nor the Department of Zoology at the University of Vienna were able to provide any great ape skulls with acceptable premolar conditions. Furthermore, 1/3 of the visually pre-selected material lent by the Natural History Museum of Vienna, as well as 1/3 of the visually pre-selected specimens of the *P. t. verus* collection of the Frankfurt Senckenberg Museum did not meet the criteria (heavy cracking, wear, incomplete tooth crown formation or anomalies) post-µCT-scanning to be included in this study.

Future studies with increased datasets, particularly for *Pongo* and *Gorilla*, including female *Gorillas* especially, will increase insights to our preliminary findings.

6 CONCLUSIONS

P^3 and P^4 crown shape separates the African great apes well from the Asian one. Although shape is highly variable not only between but within species, the combined landmark datasets for the whole crown morphology (occlusal EDJ morphology & cervical outline) in both P^3 and P^4 separate well between *Pan* and *Pongo*, with *Gorilla* overlapping, while the non-combined data for cervical outlines, enamel crown outlines and occlusal EDJ morphology on their own do separate the genera to a varying degree. Shape differences can be observed best between *Pan* and *Pongo* with the first having kidney-shaped, distally protruding outlines and higher horn tips and the latter having oval, distally straight outlined premolars with higher tooth crowns and lower horn tips.

Nonmetric traits vary between and within taxa. In most *Gorilla* premolars there is a sharp edged, "chipped off" structure with "crests" on the side/area of the buccal cusp, mostly visible on the EDJ, which we referred to as "side depressions". In *Pongo*, these are rounded and "softer". *Pan* and *Gorilla* both have cingulum-like structures, a rounded and soft "shelf-like" step mainly on the buccal tooth aspect, referred to as "cingula" by us. This nonmetric trait was only displayed in the African great apes (and not in *Pongo*) and might be an adaptational trait related to their diet. It might be relevant for taxonomical classification.

Occlusal tubercles were present in a few individuals in *Pan* only (mainly on P^4s), resembling real or elongated odontomes on the EDJ. These tubercles are probably not taxonomically distinct, but just a generally rare trait. Metacones and Hypocones were found in all three taxa as well as mesial and distal crests. Findings suggest possible genus-specific variation of some of the discrete traits and need to be investigated more comprehensively in the future.

Size differences were significant (Kruskal-Wallis $p<0.01$) between the great apes in both P^3 and P^4, with *Gorillas* having the biggest teeth and *Pan* having the smallest in both premolar types, which confirmed previous findings of 2D measurements. Size therefore is a good indicator to separate the three taxa and seems to play a bigger role in great apes overall. The effect of size

on shape is also much higher in *Pongo* and *Gorilla* than in humans, whereas in *Pan* it is similar to that of humans (Buchegger, 2015) and should be further investigated.

Due to the many limitations of this study we are only able to present preliminary findings that need further investigations. Nevertheless, this thesis is a first step in paving the way for the approaches and methodologies to be used for comprehensive metric and nonmetric analyses of great ape dental variation, especially upper premolars. Future studies should not continue focusing on solely molar morphology but investigate other tooth types as well, with larger sample sizes, including various species, sub-species and representation of both sexes.

ACKNOWLEDGEMENTS

In the process of working on a thesis, all kinds of obstacles appear along the way. Many people have contributed to overcoming those in many different ways; some intentionally, some unknowingly, some by simply being present.

The ones who have helped me most with working on this thesis in particular, are my supervisors Univ.-Prof. Dr. Gerhard Weber and Dr. Cinzia Fornai. I want to thank them for their support, supervision, unmatched patience, and most helpful advice.

Furthermore, I want to thank the Frankfurt Senckenberg Museum, Dr. Ottmar Kullmer, Prof. Dr. Friedemann Schrenk, Christine Hemm & the museum's staff for lending me their *Pan t. verus* collection. I also want to thank the Natural History Museum of Vienna with Priv.-Doz. Dr. Frank Emmanuel Zachos, Alexander Bibl & the museums' staff for access to their great apes' skeletal material.

My gratitude further goes to Mag. Martin Dockner for all the technical support, especially with µCT-scanning, my former colleagues Viktoria Krenn MSc and Vanda Halász MSc, for their advice and ideas, and Lisa Wurm MSc, who additionally collaborated during data acquisition. Furthermore, I want to thank Dr. Nicole Grunstra for her help with sex determination of the adult specimens of the Frankfurt Senckenberg Museums' *Pan t. verus* collection.

Additionally, I want to thank a former boss of mine who has kept my interest in bones alive, my companions, friends, and colleagues, particularly the Uhrenkinder.

All the people who have supported me – and challenged me – in the past, I want to thank the most. The last years and months were hard, long and challenging. With so many changes happening in my personal life – and more so globally – in this short period of time, I could not have made it this far without the help of so many of you. Thank you.

Finally, I want to express great gratitude towards my family; my father Johann Ernst, my mother Mitsue and my sister Anna, who have always been and always are the kindest and most inspiring people to me. Thank you all for always encouraging me to follow my passions and always supporting me in any and every way possible.

Thank you.

REFERENCES

Anemone, R. L., & Swindler, D. R. (1999): Heterochrony and sexual dimorphism in the skull of the Liberian chimpanzee (Pan troglodytes verus). International Journal of Anthropology, 14, 19-30.

Bailey, S. E. (2002): Neandertal dental morphology: implications for modern human origins. Ph.D. dissertation, Arizona State University.

Bailey, S. E. (2002): A closer look at Neanderthal postcanine dental morphology: The mandibular dentition. The Anatomical Record, 269, 148–156.

Bailey, S. E. (2008): Inter- and intra-specific variation in Pan tooth crown morphology: implications for Neandertal taxonomy. In: Irish, J. D., Nelson, G. (eds.): Technique and Application in Dental Anthropology. Cambridge University Press, Cambridge, 293-316.

Barrett, M. J. (1977): Masticatory and non-masticatory uses of teeth. Stone tools as cultural markers: change, evolution and complexity. Australian Institute of Aboriginal Studies, Canberra, 17-23.

Begg, P. R. (1954): Stone age man's dentition: With reference to anatomically correct occlusion, the etiology of malocclusion, and a technique for its treatment. Am. J. Orthod. 40 (4), 298-312.

Benazzi, S., Fornai, C., Buti, L., Toussaint, M., Mallegni, F., Ricci, S., Gruppioni, G., Weber, G. W., Condemi, S., and Ronchitelli, A. (2012): Cervical and crown outline analysis of worn neanderthal and modern human lower second deciduous molars. Am. J. Phs. Anthrop. 149, 537-546.

Benazzi, S., Nguyen, H. N., Kullmer, O., Hublin, J.-J. (2013a): Unravelling the Functional Biomechanics of Dental Features and Tooth Wear. PLoS One 8(7): e69990. Published online 2013 Jul 23. doi: 10.1371/journal.pone.0069990.

Benazzi, S., Nguyen, H. N., Schulz, D., Grosse, I. R., Gruppioni, G. et al. (2013b): The Evolutionary Paradox of Tooth Wear: Simply Destruction or Inevitable Adaptation? PLOS ONE 8: e62263. doi:10.1371/ journal.pone.0062263. PubMed: 23638020.

Benazzi, S., Panetta, D., Fornai, C., Toussaint, M., Gruppioni, G., and Hublin, J.-J. (2014): Technical Note: Guidelines for the digital computation of 2D and 3D enamel thickness in hominoid teeth: Guidelines for Digital Enamel Thickness Analysis. Am. J. Phys. Anthropol. 153, 305–313.

Berthaume, M. A. (2014): Tooth Cusp Sharpness as a Dietary Correlate in Great Apes. Am. J. Phys. Anthrop. 153, 226-235.

Buchegger, L. (2015): Variation of outer and inner crown morphology in upper premolars. Universität Wien, Masterarbeit.

Butler, P. M.: The evolution of tooth shape and tooth function in primates, In: Teaford, M. F., Smith, M. M., & Ferguson, M. W. (Eds.) (2007): Development, function and evolution of teeth. Cambridge University Press.

Bookstein, F. L. (1991): Morphometric tools of Landmark Data: Geometry and Biology; Cambridge University Press.

Bradley, B. J. (2008): Reconstructing phylogenies and phenotypes: a molecular view of human evolution. Journal of Anatomy, 212(4), 337-353.

Braga, J., Thackeray, J. F., Subsol, G., Kahn, J. K., Maret, D., Treil, J., Beck, A. (2016): The enamel-dentine junction in the postcanine dentition of *Australopithecus africanus*: intra-individual metameric and antimeric variation. J. Anatom. 216, 62-79.

Brandon-Jones, D., Groves, C. P., Jenkins, P. D. (2016): The type specimens and type localities of the orangutans, genus Pongo Lacépède, 1799 (Primates: Hominidae). Journal of Natural History, 50(33–34), 2051–2095. https://doi.org/10.1080/00222933.2016.1190414

Breuer, T., Hockemba, M. B.-N., Olejniczak, C., Parnell, R. J., Stokes, E. J. (2009): Physical maturation, life-history classes and age estimates of free-ranging western gorillas—insights from Mbeli Bai, Republic of Congo. Am. J. Primatol. 71, 106–119.

Broom, R. (1937): Discovery of a lower molar of *Australopithecus*. Nature 140, 681-682.

Carvalho, J. S., Vicente, L., Marques, T. A. (2015): Chimpanzee (*Pan troglodytes verus*) Diet Composition and Food Availability in a Human-Modified Landscape at Lagoas de Cufada Natural Park, Guinea-Bissau. Int. J. Primatol. 36, 802-822.

Constantino, P. J., Lucas, P. W., Lee, J. J.-W., Lawn, B. R. (2009): The influence of fallback foods on great ape tooth enamel. Am. J. Phys. Anthrop. 140, 653-660.

Cuozzo, F. P. The Teeth of Prosimians, Monkeys, and Apes, In: Irish, J. D., & Scott, G. R. (eds.) (2016): A Companion to Dental Anthropology. Wiley Blackwell, UK.

Delgado, R. A., Van Schaik, C.P. (2000) The behavioral ecology and conservation of the orangutan (Pongo pygmaeus): a tale of two islands. Evol. Anthropol. 9, 201–218.

Fischer A., Pollack J., Thalmann, O., Nickel B., Pääbo, S. (2006): Demographic history and genetic differentiation in apes. Curr. Biol. 16, 1133–1138.

Fornai C., Bookstein F. L., Weber G. W. (2015): Variability of Australopithecus second maxillary molars from Sterkfontein Member 4. J. Hum. Evol. 85, 181-192.

Fox, E. A., van Shaik, C. P., Sitompul, A., Wright, D. N. (2004): Intra- and Interpopulational Differences in Orangutan (*Pongo pygmaeus*) Activity and Diet: Implications for the Invention of Tool Use. Am. J. Phys. Anthrop. 125, 162-174.

Galdikas, B. M. F. (1988): Orangutan diet, range and activity at Tanjung Putting, Central Borneo. Int. J. Primatol. 9, 1-35.

Gómez-Robles, A., Martinón-Torres, M., Bermúdez de Castro, J. M., Prado-Simón, L., Arsuaga, J. L. (2011): A geometric morphometric analysis of hominin upper premolars. Shape variation and morphological integration. J. Hum. Evol. 61, 688-702.

Gonder, M. K., Disotell, T. R., Oates, J. F. (2006): New genetic evidence on the evolution of chimpanzee populations and implications for taxonomy. Int J Primatol 27, 1103–1127.

Groves, C. P. (2001): Primate taxonomy. Washington, DC, Smithsonian Institution Press.

Groves, C. P. (2002): A history of gorilla taxonomy. Gorilla biology: A multidisciplinary perspective, 15-34.

Groves, C. P. (2018): The latest thinking about the taxonomy of great apes. Int. Zoo Yb., 52, 16-24. https://doi.org/10.1111/izy.12173

Gunz, P. & Mitteroecker, P. (2013): Semilandmarks: a method for quantifying curves and surfaces. Hystrix 24, 103-109.

Guy, F., Gouvard, F., Boistel, R., Euriat, A., Lazzari, V. (2013): Prospective in (Primate) Dental Analysis through Tooth 3D Topographical Quantification. PLoS ONE 8(6): e66142. doi: 10.1371/journal.pone.0066142.

Guy, F., Lazzari, V., Gilissen, E., Thiery, G. (2015): To What Extent is Primate Second Molar Enamel Occlusal Morphology shaped by the Enamel-Dentine Junction? PLoS ONE 10(9): e0138802. doi: 10.1371/journal.pone.0138802.

Hardin, A. (2012): From the Mouths of Babes: Geographic Analysis of the Great Apes Using Non-metric Traits in the Deciduous Dentition. Anthropology Honors Projects; Paper 16.

Hardin, A. M. & Legge, S. S. (2013): Geografic Variation in Nonmetric Dental Traits of Deciduous Molars of *Pan* and *Gorilla*. Int. J. Primatol. 34, 1000-1019.

Hillson, S. (1996): Dental Anthropology. Cambridge University Press.

Hillson, S. (2005): Teeth. Cambridge university press.

Hlusko, L. J. (2004): Protostylid variation in *Australopithecus*. J. Hum. Evol. 46, 579-594.

Hooijer, D. A. (1948): Prehistoric teeth of man and the orang-utan from central Sumatra, with notes on the fossil orang-utan from Java and southern China. Zoolog-Mededelingen29, 173–301.

Irish, J. D., & Scott, G. R. (Eds.) (2016): A Companion to Dental Anthropology. Wiley Blackwell, UK.

Johanson, D. C. (1974): An odontological study of the chimpanzee with some implications for hominoid evolution. Ph.D. dissertation, University of Chicago.

Kaifu, Y. (1999): Changes in the pattern of tooth wear from prehistoric to recent periods in Japan. Am. J. Phys. Anthropol. 109, 485–499.

Kaifu, Y. (2000): Was extensive tooth wear normal in our ancestors? A preliminary examination in the genus Homo. Anthropol. Sci. 108, 371–385.

Kaifu, Y., Kasai, K., Townsend, G. C., & Richards, L. C. (2003): Tooth wear and the “design” of the human dentition: a perspective from evolutionary medicine. Am. J. Phys. Anthrop.: The Official Publication of the American Association of Physical Anthropologists, 122(S37), 47-61.

Kelley, J. & Schwartz, G. T. (2009): Dental development and life history in living African and Asian apes, Proc. Natl. Acad. Sci. U.S.A. 107 (3); 1035-1040.

Kono, R. T. (2004): Molar enamel thickness and distribution patterns in extant great apes and humans: new insights based on a 3-dimensional whole crown perspective. Anthropological Science 112, 121-146.

Martin, R. M. G., Hublin, J.-J., Gunz, P., Skinner, M. (2017): The morphology of the enamel-dentine junction in Neanderthal molars: Gross morphology, non-metric traits, and temporal trends. J. Hum. Evol.; 103, 20-44.

Mendoça, R. S., Kanamori, T., Kuze, N., Hayashi, M., Bernard, H., Matsuzawa, T. (2017): Development and behavior of wild infant-juvenile East Bornean orangutans (Pongo pygmaeus morio) in Danum Valley. Primates 58; 211-224.

Meyer-Lueckel, H. & Paris, S. (1995): Progression of artificial enamel caries lesions after infiltration with experimental light curing resins. Caries research; 42(2), 117-124.

Mitteröcker, P., & Gunz, P. (2004): Comparison of cranial ontogenetic trajectorier among great apes and humans. J. hum. Evol. 46, 679-698.

Mitteröcker, P., & Gunz, P. (2009): Advances in Geometric Morphometrics. Evol. Biol. 36, 235–247.

Molnar, S. (1971): Human tooth wear, tooth function and cultural variability. Am. J. Phys. Anthrop. 34, 175-189.

Moore, N. C., Skinner, M. M. & Hublin, J.-J. (2013): Premolar Root Morphology and Metric Variation in *Pan troglodytes verus*. Am. J. Phys. Anthrop.; 150, 632-646.

Nater, A., Mattle-Greminger, M. P., Nurcahyo, A., Nowak, M. G., de Manuel, M., Desai, T., Groves, C., Pybus, M., Sonay, T. B., Roos, C., Lameira, A. R., Wich, S. A., Askew, J., Davila-Ross, M., Fredriksson, G., de Valles, G., Casals, F., Prado-Martinez, J., Goossens, B., Verschoor, E. J., Warren, K. S., Singleton, I., Marques, D. A., Pamungkas, J., Perwitasari-Farajallah, D., Rianti, P., Tuuga, A., Gut, I. G., Gut, M., Orozco-terWengel, P., van Schaik, C. P., Bertranpetit, J., Anisimova, M., Scally, A., Marques-Bonet, T., Meijaard, E., Krützen, M. (2017): Morphometric, Behavioral, and Genomic Evidence for a New Orangutan Species. Current Biology 27, 3487-3498.

Olejniczak, A. J., Martin, L. B., Ulhaas, L. (2004): Quantification of dentine shape in anthropoid primates. Ann. Anat. 186; 479-485.

Olejniczak, A. J., Gilbert, C. G., Martin, L. B., Smith, T. M., Ulhaas, L., Grine, F. E. (2007): Morphology of the enamel-dentine junction in sections of anthropoid primate maxillary molars. J. Hum. Evol. 53, 292-301.

Oates, J. F., Groves, C. P., Jenkins, P. D. (2009): The type locality of Pan troglodytes vellerosus (Gray, 1862), and implications for the nomenclature of West African chimpanzees. Primates 50, 78- 80. https://doi.org/10.1007/s10329-008-0116-z

Ortiz, A., Skinner, M. M., Bailey, S. E., Hublin, J.-J. (2012): Carabelli's trait revisited: An examination of mesiolingual features at the enamel-dentine junction and enamel surface of *Pan* and *Homo sapiens* upper molars. J. Hum. Evol. 63, 586-596.

Perelman, P., Johnson, W. E., Roos, C., Seuánez, H. N., Horvath, J. E., Moreira, M. A. M., Kessing, B., Pontius, J., Roelke, M., Rumpler, Y., Schneider, M. P. C., Silva, A., O'Brien, S. J., and Pecon-Slattery, J. (2011): A Molecular Phylogeny of Living Primates. *PLoS Genetics* 7.3, E1001342. Web.

Pellegrini, A. (2009): Geometric morphometric craniofacial analysis of early Bronze Age Austrian populations. Universität Wien, Dissertation.

Pilbrow, V. (2006): Population systematics of chimpanzees using molar morphometrics. J. Hum. Evol. 51, 646-662.

Pilbrow, V. (2010): Dental and phylogeographic patterns of variation in gorillas. J. Hum. Evol. 59, 16-34.

Pirttiniemi, P., Alvesalo, L., Silvén, O., Heikkilä, J., Julku, J., Karjalahti, P. (1998): Asymmetry in the occlusal morphology of first permanent molars in 45,X/46,XX mosaics. Archiver of Oral Biology 43, 25-32.

Reese, A. (2017): Newly discovered orangutan species is also the most endangered. Nature 551, 151.

Robinson, J. T. (1956): The Dentition of the Australopithecinae. Transvaal Museum Memoir No. 9. The Transvaal Museum, Pretoria, South Africa.

Rogers, M. E., Maisels, F., Williamson, E. A., Fernandez, M., Tutin, C. E. (1990): Gorilla diet in the Lope Reserve, Gabon. Oecologia 84; 326-339.

Sarig, R., Fornai, C., Pokhojaev, A., May, H., Hans, M., Latimer, B., Barzilai, O., Quam, R., and Weber, G. W. (2019): The Dental Remains from the Early Upper Paleolithic of Manot Cave, Israel. Journal of Human Evolution, 102648.

Scally, A., Dutheil, J. Y., Hillier, L. W., Jordan, G. E., Goodhead, I., Herrero, J., Hobolth, A., Lappalainen, T., Mailund, T., Marques-Bonet, T., McCarthy, S., Montgomery, S. H., Schwalie, P. C., Tang, Y. A., Ward, M. C., Xue, Y., Yngvadottir, B., Alkan, C., Andersen, L. N., Ayub, Q., Ball, E. V., Beal, K., Bradley, B. J., Chen, Y., Clee, C. M., Fitzgerald, S., Graves, T. A., Gu, Y., Heath, P., Heger, A., Karakoc, E., Kolb-Kokocinski, A., Laird, G. K., Lunter, G., Meader, S., Mort, M., Mullikin, J. C., Munch, K., O'Connor, T. D., Phillips, A. D., Prado-Martinez, J., Rogers, A. S., Sajjadian, S., Schmidt, D., Shaw, K., Simpson, J. T., Stenson, P. D., Turner, D. J., Vigilant, L., Vilella, A. J., Whitener, W., Zhu, B., Cooper, D. N., de Jong, P., Dermitzakis, E. T., Eichler, E. E., Flicek, P., Goldman, N., Mundy, Nicholas I. Ning, Z., Odom, D. T., Ponting, C. P., Quail, M. A., Ryder, O. A., Searle, S. M., Warren, W. C., Wilson, R. K., Schierup, M. H., Rogers, J., Tyler-Smith, C., Durbin, R. (2012): Insights into hominid evolution from the gorilla genome sequence. Nature, 483(7388), 169-175.

Schäfer, K., Lauc, T., Mitteroecker, P., Gunz, P., Bookstein, F. L. (2006): Dental arch asymmetry in an isolated Adriatic community. Am. J. Phys. Anthrop., 129 (1), 132-142.

Scott, G. R., and Turner, C. G. (1997): The anthropology of modern human teeth: Dental morphology and its variation in recent human populations (Cambridge: Cambridge University Press).

Scott G. R., Irish J. D. (2017): Human Tooth Crown and Root Morphology: The Arizona State University Dental Anthropology System. Cambridge University Press.

Shea, B. T. (1983): Size and diet in the evolution of African ape craniodental form. Folia Primatologica 40, 32-68.

Shea, B. T. (1985): On aspects of skull form in African apes and orangutans, with implications for hominoid evolution. Am. J. Phys. Anthrop. 68, 329-42.

Šimková, P. (2024): Morphological variation and covariation in the human postcanine dentition. Universität Wien, Dissertation.

Skinner, M. M., Gunz, P., Wood, B. A., Boesch, C., Hublin, J.-J. (2009): Discrimination of Extant *Pan* Species and Subspecies Using the Enamel-Dentition Junction Morphology of Lower Molars. Am. J. Phys. Anthrop. 140, 234-243.

Skinner, M. M., Evans, A., Smith, T., Jernvall, J., Tafforeau, P., Kupczik, K., Olejniczak, A. J., Rosas, A., Radovcic, J., Thackeray, J. F., Toussaint, M., Hublin, J. J. (2010): Brief communication: Contributions of enamel-dentine junction shape and enamel deposition to primate molar crown complexity. Am. J. of Phys. Anthrop.: The Official Publication of the American Association of Physical Anthropologists, 142(1), 157-163.

Slavkin, H. C. & Diekwisch, T. G. (1997): Molecular strategies of tooth enamel formation are highly conserved during vertebrate evolution. Ciba Found Symp. 205: 73-80, 81-84.

Slice, D. E. (2005): Modern Morphometrics in Physical Anthropology; Kluwer Academic/ Plenum Publishers, New York.

Smith, T. M., Olejniczak, A. J., Reh, S., Reid, D. J. & Hublin, J.-J. (2008): Brief Communication: Enamel Thickness Trends in the Dental Arcade of Humans and Chimpanzees. Am. J. Phs. Anthrop. 136, 237-241.

Smith, T. M., Olejniczak, A. J., Reh, S., Reid, D. J., & Hublin, J. J. (2008): Brief communication: enamel thickness trends in the dental arcade of humans and chimpanzees. American Journal of Physical Anthropology: The Official Publication of the American Association of Physical Anthropologists, 136(2), 237-241.

Smith, T. M., Kupczik, K., Machanda, Z., Skinner, M. M., & Zermeno, J. P. (2012): Enamel thickness in Bornean and Sumatran orangutan dentitions. Am. J. Phys. Anthrop. 147(3), 417-426.

Spoor, C. F., Zonneveld, F. W., Macho, G. A. (1993): Linear measurements of cortical bone and dental enamel by computed tomography: applications and problems. Am. J. Phys. Anthrop. 91, 469-484.

Sugiyama, Y. & Koman, J. (1987): A preliminary list of chimpanzees' alimentation at Bossou, Guinea. Primates 28, 133-147.

Swindler, D. R. (2002): Primate dentition: An introduction to the teeth of nonhuman primates. Cambridge, U.K., Cambridge University Press.

Teaford, M. F.: Primate dental functional morphology revisited, In: Teaford, M. F., Smith, M. M., & Ferguson, M. W. (Eds.) (2007): Development, function and evolution of teeth. Cambridge University Press.

Turner, C. G. (1991): Scoring procedures for key morphological traits of the permanent dentition: the Arizona State University dental anthropology system. Advances in dental anthropology.

Uchida, A. (1998): Variation in tooth morphology of *Pongo pygmaeus.* J. Hum. Evol. 34, 71-79.

Ulhaas, L., Kullmer, O., Schrenk, F., Henke, W. (2004): A new 3-d approach to determine functional morphology of cercopithecoid molars. Annals of Anatomy Volume 186, Issues 5–6, December 2004, 487-493.

Ungar, P. S. & M'Kirera, F. (2003): A solution to the worn tooth conundrum in primate functional anatomy. PNAS 100 (7), 3874-3877; https://doi.org/10.1073/pnas.0637016100.

Van Reenen, J. F. & Reid, C. (1995): The Carabelli trait in early South African hominids: a morphological study. In: Moggi-Cecchi, J. (Ed.), Aspects of Dental Biology: Paleontology, Anthropology and Evolution. International institute for the Study of Man, Florence, 291-298.

Weber, G. W., and Bookstein, F. L., (2011): Virtual anthropology: A guide to a new interdisciplinary field. Springer, New York.

Weber, G., Fornai, C., Gopher, A., Barkai, R., Sarig, R., Hershkovitz, I. (2016): The Qesem Cave hominin material (part 1): A morphometric analysis of the mandibular premolars and molar. Quaternary International, 398; 159-174.

Williamson. E. A. (1988): Western lowland gorillas feeding in streams and savannas. Primates 19; 29-34.

Wrangham, R. W., Jones, J. H., Laden, G., Pilbeam, D., Conklin-Brittain, N. (1999): The raw and the stolen: Cooking and the ecology of human origins. Current Anthropology, 40, 567-594.

Wright, E., Galbany, J., McFarlin, S. C., Ndayishimiye, E., Stoinski, T. S., Robbins, M. M. (2019): Male body size, dominance rank and strategic use of aggression in a group-living mammal. Animal Behaviour, 151, 87-102; https://doi.org/10.1016/j.anbehav.2019.03.011.

Yamagiwa, J. & Mwanza, N. (1994): Day-journey and daily diet of solitary male gorillas in lowland and highland habitats. Int. J. Primatol. 15, 207-224.

Yamagiwa, J., & Basabose, A. K. (2009): Fallback foods and dietary partitioning among Pan and Gorilla. American Journal of Physical Anthropology: The Official Publication of the American Association of Physical Anthropologists, 140(4), 739-750.

Yamashita, N. (1998): Functional dental correlates of food properties in five Malagasy lemur species. Am. J. Phys. Anthrop. 107, 137-142.

Zhang, Y.-w., Ryder, O. A., Zhang, Y.-p. (2001): Genetic Divergenve of Orangutan Subspecies (Pongo pygmaeus). J. Mol. Evol. 52; 516-526.

Zhi, L., Karesh, W. B., Janczewski, D. N., Franzier-Taylor, H., Sajuthi, D., Gombek, F., Andau, M., Martenson, J. S., O'Brien, S. J. (1996): Genomic differntiation among natural populations of orang-utan (Pongo pygmaeus). Current Biology Vol 6, 10; 1326-1336.

LIST OF FIGURES

LIST OF TABLES